Shorter Contributions to Mineralogy and Petrology, 1979

GEOLOGICAL SURVEY PROFESSIONAL PAPER 1124-A-F

Shorter Contributions to Mineralogy and Petrology, 1979

GEOLOGICAL SURVEY PROFESSIONAL PAPER 1124-A-F

UNITED STATES GOVERNMENT PRINTING OFFICE, WASHINGTON: 1980

UNITED STATES DEPARTMENT OF THE INTERIOR

CECIL D. ANDRUS, *Secretary*

GEOLOGICAL SURVEY

H. William Menard, *Director*

Library of Congress catalog-card No. 79-600186

For sale by the Superintendent of Documents, U.S. Government Printing Office
Washington, D.C. 20402

Stock Number 024-001-03247-3

CONTENTS

[Letters designate the chapters]

CONVERSION FACTORS

Metric unit		Inch-Pound equivalent	
Length			
millimeter (mm)	=	0.03937	inch (in)
meter (m)	=	3.28	feet (ft)
kilometer (km)	=	.62	mile (mi)
Area			
square meter (m^2)	=	10.76	square feet (ft^2)
square kilometer (km^2)	=	.386	square mile (mi^2)
hectare (ha)	=	2.47	acres
Volume			
cubic centimeter (cm^3)	=	0.061	cubic inch (in^3)
liter (L)	=	61.03	cubic inches
cubic meter (m^3)	=	35.31	cubic feet (ft^3)
cubic meter	=	.00081	acre-foot (acre-ft)
cubic hectometer (hm^3)	=	810.7	acre-feet
liter	=	2.113	pints (pt)
liter	=	1.06	quarts (qt)
liter	=	.26	gallon (gal)
cubic meter	=	.00026	million gallons (Mgal or 10^6 gal)
cubic meter	=	6.290	barrels (bbl) (1 bbl=42 gal)
Weight			
gram (g)	=	0.035	ounce, avoirdupois (oz avdp)
gram	=	.0022	pound, avoirdupois (lb avdp)
metric tons (t)	=	1.102	tons, short (2,000 lb)
metric tons	=	0.9842	ton, long (2,240 lb)
Specific combinations			
kilogram per square centimeter (kg/cm^2)	=	0.96	atmosphere (atm)
kilogram per square centimeter	=	.98	bar (0.9869 atm)
cubic meter per second (m^3/s)	=	35.3	cubic feet per second (ft^3/s)
liter per second (L/s)	=	.0353	cubic foot per second
cubic meter per second per square kilometer [$(m^3/s)/km^2$]	=	91.47	cubic feet per second per square mile [$(ft^3/s)/mi^2$]
meter per day (m/d)	=	3.28	feet per day (hydraulic conductivity) (ft/d)
meter per kilometer (m/km)	=	5.28	feet per mile (ft/mi)
kilometer per hour (km/h)	=	.9113	foot per second (ft/s)
meter per second (m/s)	=	3.28	feet per second
meter squared per day (m^2/d)	=	10.764	feet squared per day (ft^2/d) (transmissivity)
cubic meter per second (m^3/s)	=	22.826	million gallons per day (Mgal/d)
cubic meter per minute (m^3/min)	=	264.2	gallons per minute (gal/min)
liter per second (L/s)	=	15.85	gallons per minute
liter per second per meter [(L/s)/m]	=	4.83	gallons per minute per foot [(gal/min)/ft]
kilometer per hour (km/h)	=	.62	mile per hour (mi/h)
meter per second (m/s)	=	2.237	miles per hour
gram per cubic centimeter (g/cm^3)	=	62.43	pounds per cubic foot (lb/ft^3)
gram per square centimeter (g/cm^2)	=	2.048	pounds per square foot (lb/ft^2)
gram per square centimeter	=	.0142	pound per square inch (lb/in^2)
Temperature			
degree Celsius (°C)	=	1.8	degrees Fahrenheit (°F)
degrees Celsius (temperature)	=	[(1.8 × °C) + 32]	degrees Fahrenheit

The Vermilion Granitic Complex—A New Name for Old Rocks in Northern Minnesota

By D. L. SOUTHWICK *and* P. K. SIMS

SHORTER CONTRIBUTIONS TO MINERALOGY AND PETROLOGY, 1979

GEOLOGICAL SURVEY PROFESSIONAL PAPER 1124-A

Prepared with the cooperation of the Minnesota Geological Survey

CONTENTS

ILLUSTRATIONS

TABLES

THE VERMILION GRANITIC COMPLEX— A NEW NAME FOR OLD ROCKS IN NORTHERN MINNESOTA

By D. L. SOUTHWICK[1] and P. K. SIMS

ABSTRACT

The name Vermilion Granitic Complex is introduced for the heterogeneous granitic and migmatitic rocks of Archean (formerly called Precambrian W) age that occur north of the Vermilion district and south of the Kabetogama peninsula in northern Minnesota. The complex consists of the following subdivisions: Lac La Croix Granite, granite-rich migmatite, schist-rich migmatite, quartz-feldspar gneiss, hornblende quartz diorite and diorite, granodiorite and trondhjemite, amphibolite and amphibolite migmatite, older migmatite, biotite schist, Burntside Gneiss, and pegmatite. Because the name Vermilion Granitic Complex is proposed as a more inclusive group term, the more restricted name Vermilion Granite (Grout, 1923) is hereby abandoned. The new name Lac La Croix Granite is proposed for the uniform, light-pink biotite granite that occurs widely in the eastern and central parts of the complex. It is defined as having less than 5 percent of schistose or gneissic inclusions and is therefore more restricted than the Vermilion Granite of Grout (1926), which included sustantial amounts of migmatitic rocks. The name Burntside Gneiss is adopted as a replacement for the older term Burntside Granite Gneiss, originally named by Grout (1926). This change is required by the conclusion that the rock is a metamorphosed dacite and not a metamorphosed granite, as formerly interpreted.

INTRODUCTION

The name Vermilion Granitic Complex is proposed for the heterogeneous granitic and migmatitic rocks of Archean (formerly called Precambrian W) age that occur north of the Vermilion district and south of the Kabetogama peninsula in northern Minnesota (fig. 1). It replaces the informal name Vermilion granite-migmatite massif assigned to these rocks by Southwick (1972). The Vermilion Granitic Complex is understood to have group status in the formal stratigraphic sense, in accordance with the proposed Article 9 (g), amended, of the Code of Stratigraphic Nomenclature (Sohl, 1977). The complex includes, but is not restricted to, the Vermilion Granite as defined by Grout 1923); it includes some rocks previously included in the abandoned terms "Vermilion series, Vermilion schist, and Vermilion group," as used by Winchell and Winchell (1887, p. 4, 192, 355, 357) and Van Hise and Clements (1901).

The greater part of the Vermilion Granitic Complex consists of pink to grayish-pink biotite granite (as classified by Streckeisen (1973) and as used by Minnesota geologists for decades), and genetically associated granite-rich migmatite. These rocks constitute the Vermilion Granite of Grout (1923). Within the area dominated by granite, lesser volumes of other igneous and metamorphic rocks are intimately involved with the granite; moreover, on the north and west the granitic terrane passes gradationally through migmatites rich in schist into nonmigmatized biotite schist. We view the minor lithologies within and the migmatite around the granitic terrane to be logically parts of a larger rock body. Accordingly, we recommend the Vermilion Granite as used by Grout (1923) be elevated in rank and broadened to the Vermilion Granitic Complex, as described below. The complex is named for the Vermilion River, along which most of its lithologic subdivisions are exposed.

The northern boundary of the Vermilion Granitic Complex is gradational and is arbitrarily placed where granitic rocks of the complex become sparse or absent from the flanking unnamed biotite schist of the Kabetogama peninsula and its eastward extension into Canada (fig. 1). The southern boundary is defined mainly by high-angle faults, which provide a sharp break between the granitic rocks and associated amphibolite-facies rocks of the complex and the greenschist-facies volcanic and sedimentary rocks of the Vermilion district (Sims, 1976). We

[1] Minnesota Geological Survey, St. Paul, Minn.

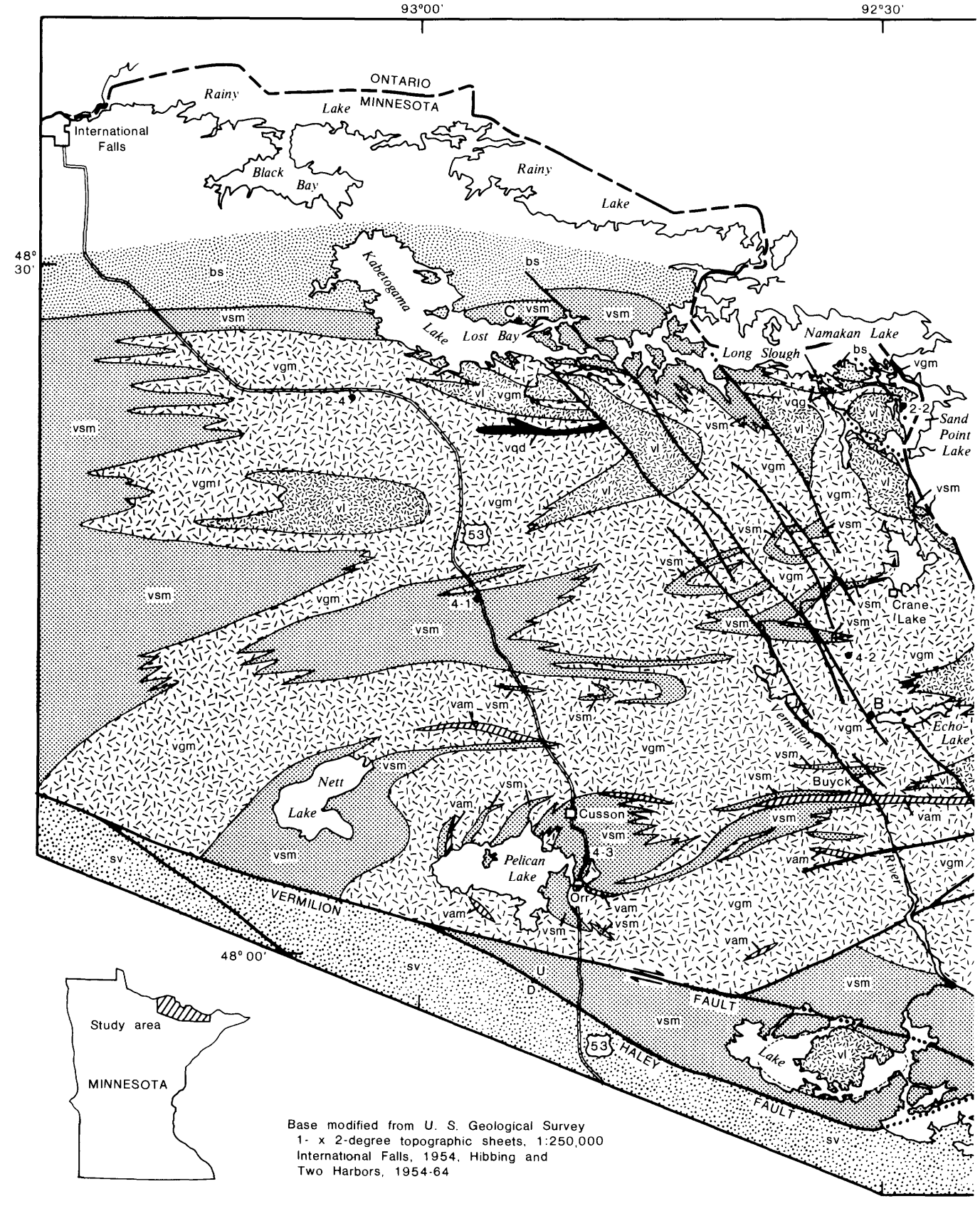

FIGURE 1.—Generalized geologic map showing Vermilion Granitic Complex. Compiled by D. L. Southwick, in 1977, from maps

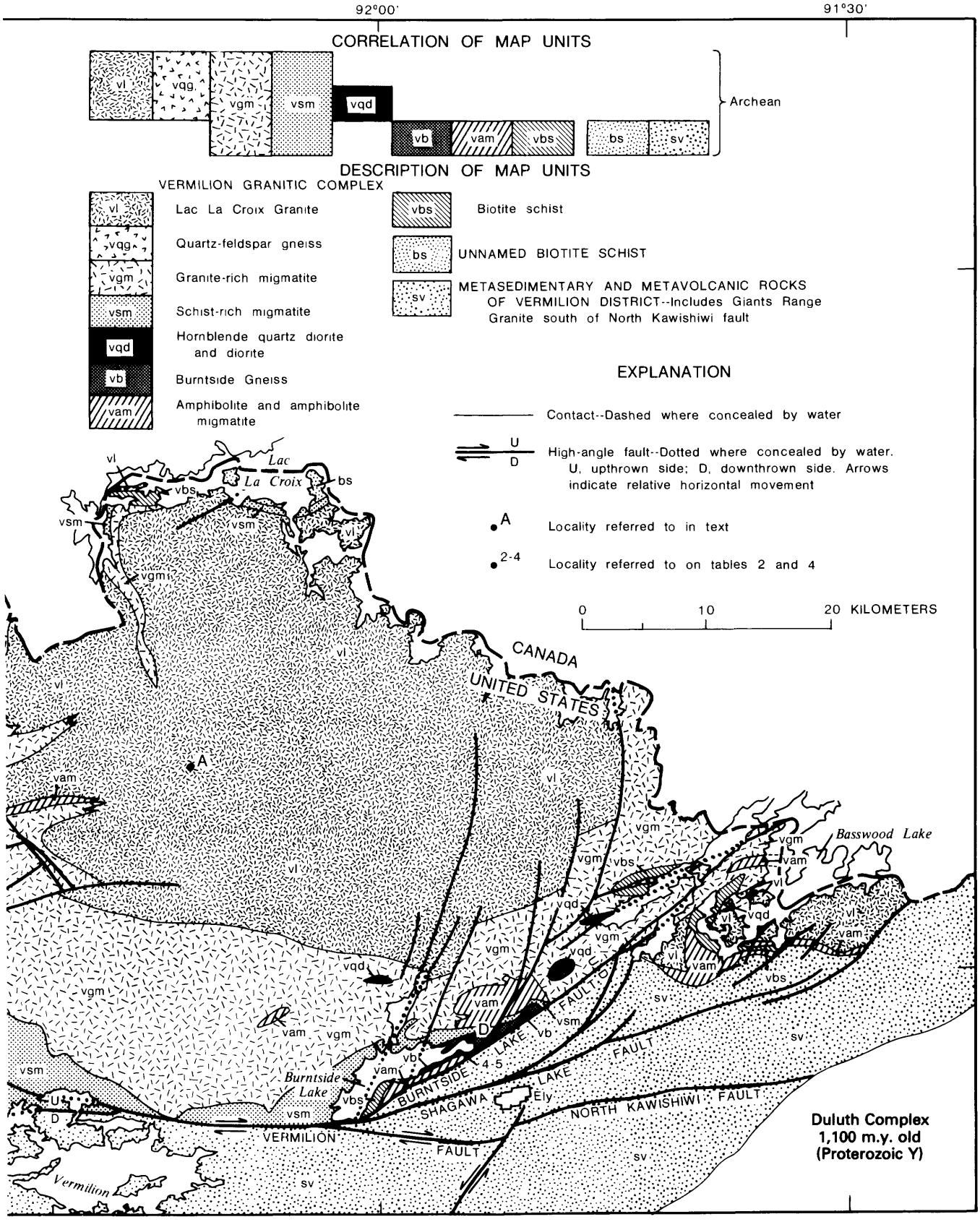

by Green (1973), Southwick and Ojakangas (1973), Sims and others (1970), Sims (1973), and Sims and Mudrey (1978).

include in the Vermilion Granitic Complex the rocks north of the Vermilion, Haley, and Shagawa Lake faults, as shown on figure 1. The limits of the complex to the west and east are impossible to define precisely with present map data. West of International Falls, Minn., the Precambrian bedrock is covered by thick glacial drift, and existing bedrock mapping is sketchy. We tentatively conclude that the complex terminates against the westward extension of the Vermilion fault (Southwick and Ojakangas, 1973). In Canada the complex merges into and appears to be virtually equivalent to the Quetico belt (Mackasey and others, 1974) and presumably continues eastward along strike for many kilometers.

SUBDIVISIONS OF THE VERMILION GRANITIC COMPLEX

On figure 1, eight subdivisions of the Vermilion Granitic Complex are delineated. In addition we recognize three other units that cannot be shown at the map scale but are probably significant to the petrogenetic history of the complex. These are (1) an early intrusive suite consisting of light-gray granodiorite, quartz diorite, and trondhjemite; (2) a migmatite that is geologically older than the early intrusive suite; and (3) late dikes of pegmatite. Relations among the subunits are shown diagrammatically in figure 2.

The east-central part of the complex (fig. 1) is a uniform, light-pink biotite granite. This remarkably homogeneous granite, together with rocks we map as granite-rich migmatite (discussed in a following section), was called the Vermilion Granite by Grout (1923). Because we propose to use Vermilion Granitic Complex as a more inclusive group term, the more restricted name Vermilion Granite is hereby abandoned. Accordingly, we propose the name Lac La Croix Granite for the distinctive, wide-

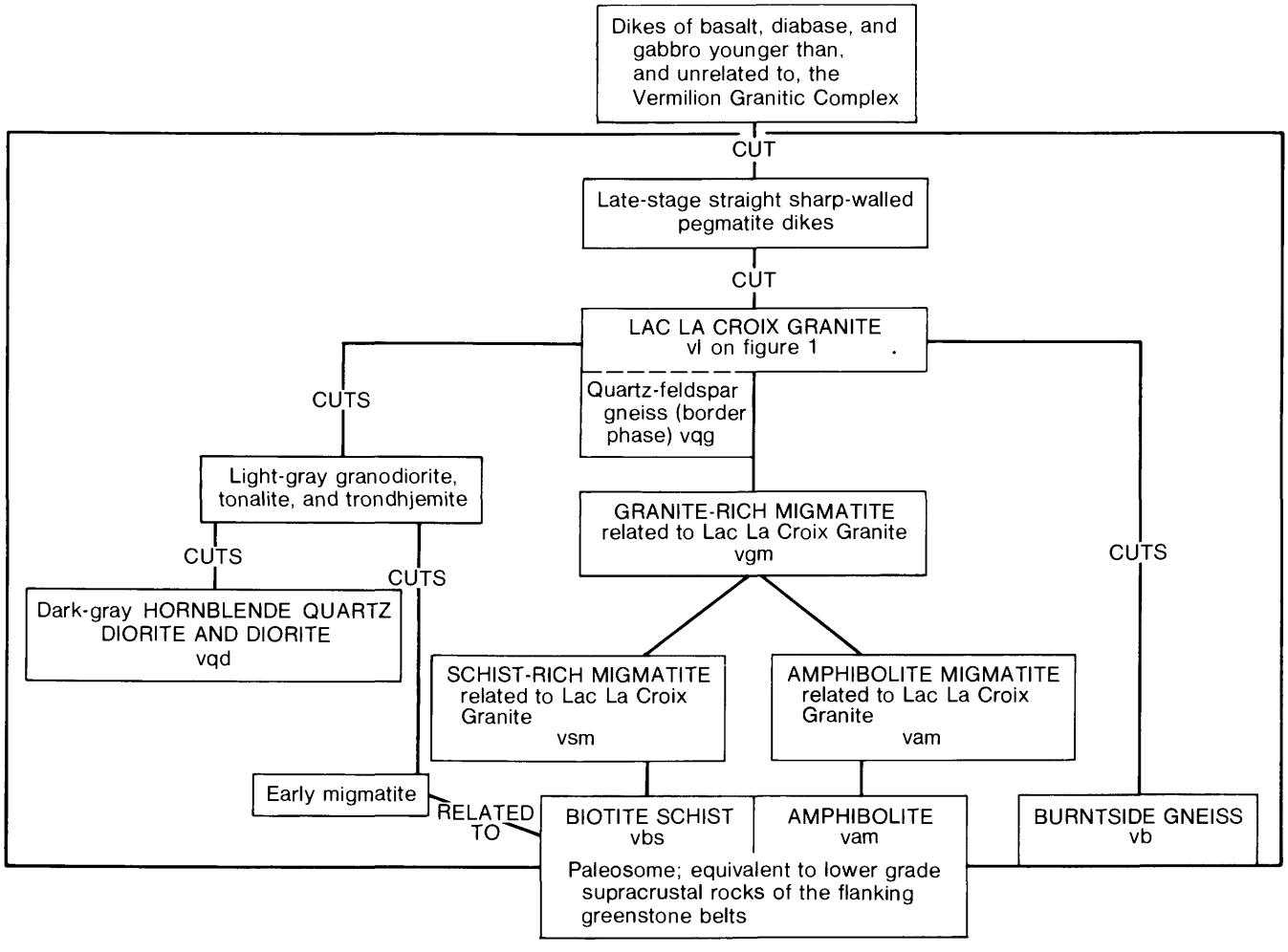

FIGURE 2.—Schematic diagram of the interrelationships among the lithologic subdivisions of the Vermilion Granitic Complex. Intrusive units are arranged with the youngest at the top of the diagram. Names spelled out in capital letters are the more abundant components of the complex.

spread, uniform, light-pink biotite granite that crops out south of Lac La Croix; these outcrops are the type area. Those granitic rocks that contain more than about 5 percent of gneissic or schistose inclusions are shown as granite-rich migmatite or schist-rich migmatite on figure 1 and are not included formally in the Lac La Croix Granite. Contacts between Lac La Croix Granite, granite-rich migmatite, and schist-rich migmatite are broadly gradational and are therefore somewhat subjectively determined in practice, especially in areas of sparse outcrop.

NOTE ON THE TERMINOLOGY OF MIGMATITES

The term "migmatite" has been used for decades by European geologists for variably gneissose rocks that consist of granite intimately mixed with nongranitic, generally dark colored metamorphic rocks. The tortuous history of the term is discussed by Mehnert (1968, p. 1–8), and his definition (p. 355) is adopted here: "Migmatite [is a] megascopically composite rock consisting of two or more petrographically different parts. One is the country rock in a more or less metamorphic stage, the other is of pegmatitic, aplitic, granitic, or generally plutonic appearance." In discussing migmatites it is convenient to have terms for the two parts; the terminology of Dietrich and Mehnert (1961) has been widely followed and is adopted here. They refer to the "older part of a composite rock (i.e., the remaining or pre-existing part)" as the paleosome, and to the "younger part of a composite rock (for example, the injected, exuded, or metasomatically introduced material)" as the neosome.

The structures and textures of migmatites are varied and complex, and inasmuch as the rocks are neither purely igneous nor purely metamorphic in origin, the descriptive structural and textural terms for igneous and metamorphic rocks are not strictly appropriate. Consequently the literature has been burdened by an excessive number of specialized terms for the structures and textures of migmatites, many of which have strong genetic connotations. Although we deplore this proliferation of jargon, we have found that some special terms illustrated and defined by Mehnert (1968, p. 8–42, especially p. 10–11) are useful in the field and are free of genetic overtones.

Many migmatites, for example, are layered, but not all layering in migmatites is the same. Migmatites with stromatic structure are layered, are chiefly paleosome, and have concordant pegmatoid neosomes that tend to pinch and swell; they are on the order of 0.1–1 m thick, and they commonly have selvages rich in biotite or hornblende. Migmatites with phlebitic structure are layered on a fine scale, highly contorted, and have neosomes that are both concordant and discordant to the foliation in the paleosome. Migmatites with schlieren structure are layered, but the proportion of granite is so high that the layering is variable to indistinct and commonly frayed or wispy in appearance. All these varieties are commonly interspersed with one another in the field, and also grade into layered migmatites having simple plane-parallel layering, for which no special term is required.

A second large class of migmatites has a blocky structure consisting of more or less equant to slab-shaped inclusions surrounded by more or less homogeneous granite. Considerable variation in the shape and degree of transformation of the included blocks occurs within this group. Specifically, migmatites with nebulitic structure have only vague, indistinct inclusions that approach the surrounding granite in modal composition. Commonly the ghostlike inclusions make up a quarter or more of the bulk rock (and rarely as much as half); the whole rock has a blotchy appearance that is aptly described as nebulous. Nebulitic migmatites are especially widespread in the granite-rich migmatite of the Vermilion Granitic Complex.

LAC LA CROIX GRANITE

The Lac La Croix Granite contains quartz, oligoclase, and perthitic microcline in subequal amounts, together with small amounts of biotite and (or) chlorite. Pegmatite dikes are sparse or absent, and, by definition, the granite contains less than about 5 percent of gneissic to schistose inclusions. Most of the granite is equant and hypidiomorphic granular, with crystals in the size range of 5–10 mm. Also common are weakly porphyritic rocks containing microcline megacrysts that are only slightly coarser than the enclosing groundmass. The average modal analysis listed in table 1 is of samples from 19 localities distributed widely over the interior of the complex. As the extremes and standard deviations show, the variation about the mean composition is remarkably slight. A chemical composition computed from the mean mode compares very well with the few available chemical analyses of the granite, as shown in table 2.

Weak deuteric and (or) hydrothermal alteration, together with slight shearing and granulation, have affected much of the granite. Typically, the plagioclase shows some sericitic alteration, biotite shows variable degrees of alteration to chlorite and Fe–Ti

TABLE 1.—*Average modal composition, in volume percent, of the Lac La Croix Granite and neosome of granite-rich migmatite, based on 19 modal analyses, 2,100 points each*

[Leaders (--) indicate not determined. Tr, trace]

	Mean	Standard deviation	Extremes
Quartz	28.3	6.7	20.7-36.4
Perthitic K-feldspar[1]	32.4	5.7	22.9-52.1
Plagioclase (An_{22})	33.3	4.9	21.5-39.0
Biotite	2.36	1.6	0.1- 5.4
Muscovite[2]	1.48	1.2	0.4- 4.5
Chlorite	1.06	.8	0.1- 2.3
Epidote and allanite	.21	.23	0.0- 2.3
Myrmekite	Tr	--	--
Opaques	.30	.22	0.1- 0.7
Carbonate	Tr	--	--
Apatite	Tr	--	--
Zircon	Tr	--	--
Sphene	Tr	--	--
Tourmaline	Tr	--	--

[1]Perthite contains 17 percent exsolved lamellae of albite.

[2]Chiefly secondary.

TABLE 2.—*Chemical analyses, in percent, of the Lac La Croix Granite (including neosome of granite-rich migmatite). See figure 1 for sample localities*

[Leaders (--) indicate not determined]

Sample Number---	2-1	2-2	2-3	2-4	2-5
SiO_2	74.0	71.73	72.06	73.8	73.2
Al_2O_3	13.8	14.76	16.00	14.6	14.8
Fe_2O_3	.36	.58	.46	.88	--
FeO	1.30	1.35	.72	--	.9
MgO	.30	.62	.97	.20	.5
CaO	.87	1.18	.86	1.40	1.6
Na_2O	3.85	3.58	4.56	4.40	3.8
K_2O	5.10	4.63	3.54	4.40	4.5
H_2O+	.25	.64	.39	--	.2
H_2O-	.03	.20	.05	.03	--
TiO_2	.13	.53	.12	.09	--
P_2O_5	.03	.14	.09	.03	--
MnO	.02	.03	.06	.01	--
CO_2	.11	--	--	--	--
Other	--	.28	.36	--	--
Total--	100.2	100.25	100.24	99.8	99.5

SAMPLE DESCRIPTIONS

2-1. Echo Trail mass, Echo Trail near crossing over Little Indian Sioux River; locality A, fig. 1 (Arth and Hanson, 1975, p. 332, col. 26).

2-2. Grassy Bay mass, Sand Point Lake (Grout, 1926, p. 48, col. 1).

2-3. Neosome of granite-rich migmatite, southeast of Pelican Lake; precise location not known (Grout, 1926, p. 48, col. 2).

2-4. Neosome of granite-rich migmatite, U.S. highway 53, 2.6 km west of St. Louis County road 122 (Arth and Hanson, 1975, p. 332, col. 25).

2-5. Analysis calculated from average mode of Lac La Croix Granite, table 1.

oxides, and quartz shows undulose extinction. Near fault zones the alteration and granulation are more severe; within 6–8 km of the Vermilion fault (Sims and others, 1968; fig. 1), the granitic rocks are extensively sheared and recrystallized to a variety of cataclastic gneisses.

Numerous exposures of the Lac La Croix Granite occur east of Echo Lake and south of Lac La Croix. The road cuts are readily accessible along the Echo Trail just south of the Little Indian Sioux River (Shell Lake 7½-minute Quadrangle) and are designated as a reference locality, shown as point A on figure 1.

A light-gray to grayish-pink granite gneiss exposed along the south shore of Namakan Lake was described by Grout (1925, p. 472–473) and has been interpreted by Southwick (1972, p. 114–116) as metasomatically replaced wall rock near the contact of the Vermilion Granite (Lac La Croix Granite as here defined). This rock is mapped on figure 1 as quartz-feldspar gneiss. It is well exposed near the mouth of Long Slough on Namakan Lake (Hale Bay 7½-minute Quadrangle), which is designated as a reference locality for quartz-feldspar gneiss border facies of the Lac La Croix.

GRANITE-RICH MIGMATITE RELATED TO THE LAC LA CROIX GRANITE

The Lac La Croix Granite grades into a rock that is mainly granite but contains 5–25 percent of paleosomatic inclusions. These inclusions range from clearly identifiable blocks of quartz diorite, biotite schist, and amphibolite to highly digested, barely discernable "ghosts." This granite-rich migmatite is the dominant rock in the west-central part of the complex. Although the granite neosome is similar to the related Lac La Croix Granite, its texture and modal composition are slightly more variable. The neosome of the granite-rich migmatite is streaky, locally pegmatoid, or weakly gneissic over substantial areas. Where gneissic, the rock is slightly richer in biotite, microcline, or both; where pegmatoid

zones are abundant, the nonpegmatoid granite matrix tends to be weakly to strongly porphyritic. Structurally the larger part of the granite-rich migmatite is nebulitic. The integrity of inclusions increases in the direction of the gradational contacts with schist-rich migmatite. The inclusions become more angular and better foliated; they gradually adopt a preferred orientation as they increase in abundance.

Numerous exposures of granite-rich migmatite occur south and southwest of Crane Lake. The road cuts are easily accessible near the junction of the Echo Trail and St. Louis County highway 23 (Kabustasa Lake 7½-minute Quadrangle) and are designated as a reference locality, shown as point B on figure 1.

SCHIST-RICH MIGMATITE RELATED TO THE LAC LA CROIX GRANITE

The schist-rich migmatite contains 25 percent or more of schistose to gneissic paleosome. Depending on the relative quantity of granite, the rock ranges from an assemblage of discrete inclusions engulfed in granite to a more or less uniform schist shot through with thin sheets and dikes of granite. The commonest paleosome is dark-gray biotite schist composed of biotite, quartz, and sodic plagioclase. Garnet, chlorite, and muscovite occur in uncommonly aluminous layers. Amphibolitic rocks make up no more than 5 percent of the paleosome in the northwest part of the complex, but they increase in abundance toward the south and east. Typically the amphibolite contains blue-green hornblende, andesine, epidote, and variable but small amounts of quartz. The schist-rich migmatite masses southwest of Crane Lake and west of Buyck contain abundant schist with subequal amounts of biotite and hornblende, as well as the more common hornblende-free variety of schist. Megacrysts of microcline have grown in some schist that has been intimately permeated by thin stringers of granite, but these megacrysts are not ubiquitous. Some of the schistose rocks in schist-rich migmatite are identical to metagraywacke outside the Vermilion Granitic Complex and almost certainly were derived from it. Others are largely replaced or veined by granitic material and cannot be linked directly to known wall-rock types.

The granitic fraction of schist-rich migmatite is white to light-pink coarse-grained leucogranite. The ratio of perthitic microcline to quartz and plagioclase is variable in stringers thinner than 20 or 30 mm, but the composition of thicker layers is quite constant and averages near the granite minimum. The texture is generally coarse but highly variable. Vague zones and clots of very coarse quartz and feldspar occur within somewhat finer grained rock, and subhedral to anhedral megacrysts of perthitic microcline are locally abundant. Some very thin neosomatic stringers contain microcline megacrysts that are larger than the width of the stringer; these crystals invade the schist on both sides without disturbing its foliation, indicating that they grew by replacement. Commonly the contacts between paleosome and neosome in thinly layered migmatite are wavy and marked by a zone a few millimeters thick that is anomalously rich in biotite. Such rocks typically have a braided appearance because of intertwined mafic and feldspathic wisps.

The schist-rich migmatite typically is layered. Rocks with plane-parallel layering are less common than rocks with stromatic, phlebitic, or schlieren structure; however, all the layering variants commonly occur close together. Layering is more or less continuous and coherent in migmatites that are less than about half granite; the granite in these rocks has a strong tendency to occur as conformable sheets. Migmatites that are more than half granite commonly exhibit some degree of discordance between granite contacts and foliation in the paleosome, and the overall structure grades into an assemblage of blocky inclusions surrounded by more or less uniform granite. Little rotation of blocks occurs until the granite fraction reaches about 75 percent, however, and it is possible to map regional structures from planar elements in even the most granitic of the schist-rich migmatites.

Good exposures of schist-rich migmatite occur along the shores of Kabetogama and Namakan Lakes. Particularly good exposures occur on the north side of Kabetogama Lake near the mouth of Lost Bay (Daley Bay 7½-minute Quadrangle), which is designated as a reference locality and is shown as point C on figure 1.

AMPHIBOLITE AND AMPHIBOLITE MIGMATITE

Amphibolitic rocks are moderately abundant at and near the southeast margin of the complex. Where amphibolite is intruded by many dikelets of granite, the resulting mixed rock is termed amphibolite migmatite. Most amphibolite migmatite is blocky in structure, and these amphibolite blocks are no different from unmigmatized amphibolite in texture and mineralogy. Locally, however, as in the area east of Pelican Lake, the amphibolite migmatite

displays stromatic layering or schlieren structure. The amphibolite in the southeast part of the complex is composed of both layered and massive varieties. The layered varieties are layered on a scale of a few millimeters or centimeters; the layering is given by color contrasts that reflect different proportions of hornblende, oligoclase-andesine, quartz, and biotite. The massive variety contains variable amounts of hornblende and plagioclase and lesser amounts of quartz and biotite. Associated with the massive varieties are numerous small bodies of metagabbro. The massive amphibolite is interpreted to be a metamorphosed basalt; the associated metagabbro is probably a subvolcanic equivalent of the basalt (Sims and Mudrey, 1978).

With increasing granite the amphibolite grades along and across strike into blocky amphibolite migmatite, which grades into granite. These relationships can be seen at several localities in the Shagawa Lake 7½-minute Quadrangle (Sims and Mudrey, 1978), about 1 km north of Burnside Lake. The granitic fraction of the amphibolite migmatite is dominantly pink leucogranite, virtually identical with the Lac La Croix Granite at its reference localities.

INTRUSIVE ROCKS THAT ARE GEOLOGICALLY OLDER THAN THE LAC LA CROIX GRANITE

Several kinds of plutonic igneous rocks that have little or no potassium feldspar are sharply crosscut by dikes or irregular masses of pink biotite granite related to the Lac La Croix Granite. These older plutonic rocks make up only a small fraction of the total exposed area of the complex. They tend to be small, irregular bodies in complicated migmatites, and except for the bodies of hornblende diorite and quartz diorite shown on figure 1, can be delineated only on detailed geologic maps.

The oldest intrusive rocks are hornblende diorite and dark-gray biotite-hornblende quartz diorite that in turn are intruded by light-gray granodiorite, tonalite, and trondhjemite. The hornblende diorite and quartz diorite are exposed near the Ash River and at a few localities near the south edge of the complex; only the larger masses appear on figure 1. Younger biotite granodiorite and trondhjemite are more widespread but occur in smaller bodies. Irregular dikes, sills, and plugs of granodiorite and trondhjemite are especially common in the schist-rich migmatite belt between Cusson and Buyck (fig. 1) and in the migmatite bodies at the west end of Namakan Lake. These light-gray, medium- to coarse-grained rocks typically vary considerably in texture within distances of a few meters. Average mode, modal range, and chemical compositions are listed in tables 3 and 4.

TABLE 3.—*Average modal composition, in volume percent, of gray granodiorite, tonalite, and trondhjemite, based on 14 modal analyses, 2,100 points each*

[Leaders (--) indicate not determined. Tr, trace]

	Mean	Standard deviation	Extremes
Quartz	24.7	5.47	9.8-32.3
Microcline	9.4	8.23	0.6-26.9
Plagioclase	56.0	8.50	40.3-65.9
Biotite	7.06	2.92	2.0-11.9
Muscovite	1.44	1.23	0.1- 4.8
Chlorite	.22	.25	0.1- 0.5
Epidote and allanite	.51	.80	0.1- 2.1
Myrmekite	Tr	--	--
Opaques	.10	--	0.1- 0.5
Carbonate	.10	--	0.1- 0.6
Apatite	.10	--	0.1- 0.6
Zircon	Tr	--	--
Sphene	.20	--	0.1- 1.8
Tourmaline	Tr	--	--

MIGMATITE GEOLOGICALLY OLDER THAN THE GRAY GRANODIORITE

Complex, highly contorted schist-rich migmatite that is intruded by gray granodiorite is exposed near Buyck and Cusson. This migmatite is composed of compact garnet-biotite-quartz-plagioclase schist and granofels, biotite-poor quartz-plagioclase granofels, and minor amphibolite that are complexly interlayered with pegmatoid leucogranite. Structurally the rock has all variants of migmatite layering within short distances, and the neosome has been intensely boudined. Numerous thin stringers of gray granodiorite are concordant with the layering of the migmatite, but cross-cutting relations are common also. Both the migmatite and gray granodiorite are invaded on all scales by pink granite. This older magmatite is spatially associated with younger schist-rich migmatite and appears to represent a phase of migmatite generation that affected the paleosome of that rock. In general it cannot be delineated as a separate unit except on very detailed geologic maps.

BURNTSIDE GNEISS

Grout (1926, p. 29) named the Burntside Granite Gneiss for exposures around Burntside Lake, northwest of Ely. He mapped the lakeshore exposures in some detail and interpreted the gneiss to be an early phase of the Vermilion Granite (Grout, 1926, p. 30).

TABLE 4.—*Chemical analyses, in percent, of gray granodiorite and trondhjemite, including the Burntside Gneiss*

[Leaders (--) indicate not determined]

Sample Number---	4-1	4-2	4-3	4-4	4-5	4-6
SiO_2-----	67.70	68.25	65.70	67.2	68.54	69.3
Al_2O_3----	15.86	16.94	17.27	18.4	17.89	16.5
Fe_2O_3----	.71	.70	.77	--	1.77	--
FeO------	2.45	1.92	2.56	1.57	.52	1.6
MgO------	1.02	.75	1.42	.67	1.22	.9
CaO------	3.79	2.92	3.39	3.89	4.02	2.7
Na_2O-----	4.91	5.52	5.05	6.32	5.14	5.4
K_2O------	1.16	1.17	1.62	.92	1.05	1.8
H_2O+ ----	--	--	--	--	.46	.3
H_2O- ----	.91	.81	.90	.03	.18	--
TiO_2-----	.33	.28	.47	.23	.20	--
P_2O_5-----	.17	.10	.17	.12	Tr[1]	--
MnO------	.03	.04	.06	.03	--	--
CO_2------	1.08	.44	.31	--	--	--
Other----	--	--	--	--	.06	--
Total--	100.12	99.84	99.69	99.4	101.05	98.5

[1]Tr, trace

SAMPLE DESCRIPTIONS

4-1. Biotite trondhjemite (1.5 percent K-feldspar), Duluth, Winnipeg, and Pacific Railroad, 5 km north of Ash Lake, Ash River SW 7½-minute quadrangle.
4-2. Biotite trondhjemite (0.6 percent K-feldspar), U.S. Forest Service Vermilion River road at Camp 40 Creek, Kabustasa Lake 7½-minute quadrangle.
4-3. Light-gray biotite granodiorite (6.6 percent K-feldspar), U.S. highway 53 at Moose Lake Road, 1.6 km north of Orr, Orr 7½-minute quadrangle.
4-4. Burntside Gneiss, Echo Trail just north of beach on east side of Burntside Lake; locality D, fig. 1 (Arth and Hanson, 1975, p. 332, col. 17).
4-5. Burntside Gneiss, portage between Burntside and Little Long Lakes (Grout, 1926, p. 29).
4-6. Analysis calculated from average mode of gray granodiorite and related rocks, table 3.

Later, Goldich and others (1961, p. 58–59) suggested that the gneiss might be older than the Ely Greenstone and therefore substantially older than the Vermilion Granite of Grout (1926), which intrudes the Ely and interstratified metasedimentary rocks in the Vermilion district. Mapping by Sims and Mudrey (1972) confirmed Grout's original conclusion as to relative age. They interpreted the gneiss to be a cataclastically foliated leucocratic tonalite (trondhjemite) that intrudes amphibolite and schist correlative with Ely Greenstone and related rocks; the gneiss is in turn cut by apophyses of pink biotite granite related to the Lac La Croix Granite, as herein defined. From more detailed subsequent studies, Sims has concluded that the Burntside Granite Gneiss of Grout (1926) is metamorphosed dacite. During the metamorphism, which was associated with the emplacement of the major granitic components of the Vermilion Granitic Complex, the dacite was partially remelted and intruded into adjacent amphibolite and biotite schist. Because of its trondhjemitic composition and its apparent metavolcanic origin, we propose that Burntside Granite Gneiss be renamed Burntside Gneiss. The best exposures of the gneiss are on islands in and along the shores of Burntside Lake; the reference locality at the east end of the lake is designated D on figure 1.

The Burntside Gneiss is a light-gray gneiss having a moderate or strong cataclastic foliation. It contains conspicuous quartz eyes of light-blue color in a medium-grained matrix of oligoclase, quartz, lesser K-feldspar, and biotite. The biotite is strongly chloritized. Two chemical analyses of the gneiss are listed in table 4; representative modes were published previously (Sims and Mudrey, 1972, p. 100).

BIOTITE SCHIST

Several small areas of biotite schist are mapped within the boundaries of the Vermilion Granitic Complex northeast of Burntside Lake (fig. 1). The schist is typically dark gray on fresh surfaces but brown where weathered, fine to medium grained, and well foliated. Bedding is prominent locally. The commonest rock is composed of biotite, quartz, and sodic plagioclase; aluminous layers contain sparse garnet and muscovite as well. The schist is equivalent to somewhat less metamorphosed metasedimentary rocks (chiefly volcanogenic metagraywackes) that are abundant south of the Burntside Lake fault. It also is identical with the paleosome of adjacent schist-rich migmatite, into which it grades as granitic wisps and stringers oriented parallel to the foliation become more abundant.

PEGMATITE

Two distinct types of pegmatite occur in the Vermilion Granitic Complex. Irregular patches and indistinct, gradationally bounded dikes of simple quartz-alkali feldspar pegmatite are abundant in the granite-rich migmatite. These masses range in size from a few tens of millimeters to several tens of meters; typically the texture at the contact grades from granitoid to pegmatitic over distances of a few tens of millimeters to perhaps half a meter. The second type of pegmatite occurs in sharp-walled, straight dikes that postdate all other rocks of the complex. These pegmatite dikes commonly contain

traces of muscovite and garnet where they traverse aluminous schistose wall rocks. Northwest of Echo Lake (fig. 1) some of the pegmatite bodies contain as much as 5–10 percent of primary magnetite (Grout, 1923, 1926); these pegmatites were explored in the early 1920's as possible iron-ore deposits.

AGE OF THE COMPLEX

The first systematic radiometric age study of the Vermilion Granitic Complex was by Goldich and others (1961), who reported K-Ar mineral ages on biotite from seven samples and a Rb-Sr mineral age on K-feldspar from one. All reported ages were between 2,390 and 2,620 m.y. (million years), with the mean about 2,550 m.y. (Goldich and others, 1961, table 14, p. 53; samples 47B, 46B, 239B, 249B, 250B, 94B, and 4B). The samples used were from older migmatite, younger migmatite related to the Lac La Croix Granite, and the Lac La Croix Granite as herein defined; the several subunits of the complex were indistinguishable on the basis of radiometric age. Later, Peterman and others (1972) reported a Rb-Sr whole rock-isochron age of $2,680 \pm 95$ m.y. for the Vermilion Granite, with an initial Sr^{87}/Sr^{86} of 0.7005 ± 0.0012. The isochron was based on three samples studied earlier by Goldich and others (1961) and on eight new samples collected from the Lac La Croix Granite and its associated migmatites as here defined. A refined Rb-Sr whole rock-isochron age of $2,700 \pm 50$ m.y. has been reported for the complex by Jahn and Murthy (1975). They used eight data points from Peterman and others (1972) and three new analyses to define the isochron. Their initial Sr^{87}/Sr^{86} ratio of 0.7004 ± 0.0003 is less uncertain than that reported by Peterman and others (1972), because two of the three new samples are relatively nonradiogenic mafic migmatite paleosomes. The Rb-Sr ages were calculated usng a decay constant for Rb^{87} of 1.39×10^{-11} yr^{-1}.

The Rb-Sr whole-rock age of 2,700 m.y. agrees well with a U-Pb zircon age of 2,710 m.y. for geologically similar granite complexes in the Rainy Lake area (Peterman and others, 1972, p. 200–201), and it is accepted as the age of emplacement for the major Lac La Croix Granite phase of the Vermilion Granitic Complex. However, the ages of the rocks within the complex that are geologically older than the Lac La Croix Granite, as indicated by cross-cutting relationships, have not been determined. By analogy with determined radiometric ages of the greenstone-granite complexes in the broad region along and adjacent to the Minnesota–Ontario border (Goldich, 1972, p. 34), however, it is probable that most of the older rocks in the complex are in the range of 2,700–2,750 m.y. old.

REFERENCES CITED

Arth, J. G., Jr., and Hanson, G. N., 1975, Geochemistry and origin of the early Precambrian crust in northeastern Minnesota: Geochimica et Cosmochimica Acta, v. 39, no. 3, p. 325–362.

Dietrich, R. V., and Mehnert, K. R., 1961, Proposal for the nomenclature of migmatites and associated rocks: International Geological Congress, 21st, Copenhagen, Report, pt. 26 (Supplementary vol.), p. 56–57, 73–76.

Goldich, S. S., 1972, Geochronology in Minnesota, *in* Sims, P. K., and Morey, G. B., eds., Geology of Minnesota—A centennial volume in honor of George M. Schwartz: Minnesota Geological Survey, p. 27–37.

Goldich, S. S., Nier, A. O., Baadsgaard, Halfdan, Hoffman, J. H., and Krueger, H. W., 1961, The Precambrian geology and geochronology of Minnesota: Minnesota Geological Survey Bulletin 41, 193 p.

Green, J. C., 1973, Geologic map of Minnesota, Two Harbors sheet: Minnesota Geological Survey Open-File Map, scale 1:250,000.

Grout, F. F., 1923, The magnetite pegmatites of northern Minnesota: Economic Geology, v. 18, no. 3, p. 253–269.

———1925, The Vermilion batholith of Minnesota: Journal of Geology, v. 33, no. 5, p. 467–487.

———1926, The geology and magnetite deposits of northern St. Louis County, Minnesota: Minnesota Geological Survey Bulletin 21, 330 p.

Jahn, Bor-Ming, and Murthy, V. R., 1975, Rb-Sr ages of the Archean rocks from the Vermilion district, northeastern Minnesota: Geochimica et Cosmochimica Acta, v. 39, p. 1679–1689.

Mackasey, W. O., Blackburn, C. E., and Trowell, N. F., 1974, A regional approach to the Wabigoon-Quetico belts and its bearing on exploration in northwestern Ontario: Ontario Division of Mines Miscellaneous Paper 58, 29 p.

Mehnert, K. R., 1968, Migmatites and the origin of granitic rocks: Amsterdam, Elsevier, 393 p.

Peterman, Z. E., Goldich, S. S., Hedge, C. E., and Yardley, D. H., 1972, Geochronology of the Rainy Lake region, Minnesota—Ontario, *in* Doe, B. R., and Smith, D. K., eds., Studies in mineralogy and Precambrian geology, a volume in honor of John W. Gruner: Geological Society of America Memoir 135, p. 193–215.

Sims, P. K., 1973, Geologic map of western part of Vermilion district, northeastern Minnesota: Minnesota Geological Survey Miscellaneous Map Series No. 13, scale 1:48,000.

———1976, Early Precambrian tectonic-igneous evolution in the Vermilion district, northeastern Minnesota: Geological Society of America Bulletin, v. 87, no. 3, p. 379–389.

Sims, P. K., Morey, G. B., Ojakangas, R. W., and Griffin, W. L., 1968, Preliminary geologic map of the Vermilion district and adjacent areas, northern Minnesota: Minnesota Geological Survey Miscellaneous Map Series, M–5, scale 1:125,000.

Sims, P. K., Morey, G. B., Ojakangas, R. W., and Viswanathan, S., 1970, Geologic map of Minnesota, Hibbing sheet: Minnesota Geological Survey, scale 1:250,000.

Sims, P. K., and Mudrey, M. G., Jr., 1972, Burntside Granite Gneiss, Vermilion district, *in* Sims, P. K., and Morey, G. B., eds., Geology of Minnesota—A centennial volume in honor of George M. Schwartz: Minnesota Geological Survey, p. 98–101.

Sims, P. K., and Mudrey, M. G., Jr., 1978, Geologic map of the Shagawa Lake quadrangle, St. Louis County, Minnesota: U.S. Geological Survey Geologic Quadrangle Map GQ–1423, scale 1:24,000.

Sohl, N. F., 1977, Stratigraphic Commission, Note 45–Application for amendment concerning terminology for igneous and high-grade metamorphic rocks: American Association of Petroleum Geologists Bulletin, v. 61, no. 2, p. 248–252.

Southwick, D. L., 1972, Vermilion granite-migmatite massif, *in* Sims, P. K., and Morey, G. B., eds., Geology of Minnesota—A centennial volume in honor of George M. Schwartz: Minnesota Geological Survey, p. 108–119.

Southwick, D. L., and Ojakangas, R. W., 1973, Geologic map of Minnesota, International Falls sheet: Minnesota Geological Survey Open-File Map, scale 1:250,000.

Streckeisen, A. L., chairman, 1973, Plutonic rocks—classification and nomenclature recommended by the IUGS Subcommission on the Systematics of Igneous Rocks: Geotimes, v. 18, no. 10, p. 26–30.

Van Hise, C. R., and Clements, J. M., 1901, The Vermilion iron-bearing district: U.S. Geological Survey 21st Annual Report, pt. 3, p. 401–409.

Winchell, N. H., and Winchell, Alexander, 1887, The Geological and Natural History Survey of Minnesota: Minnesota Geological and Natural History Survey 15th Annual Report, 496 p.

Potassium-Argon Ages from the Mount Taylor Volcanic Field, New Mexico

By PETER W. LIPMAN *and* HARALD H. MEHNERT

SHORTER CONTRIBUTIONS TO MINERALOGY AND PETROLOGY, 1979

GEOLOGICAL SURVEY PROFESSIONAL PAPER 1124-B

Most volcanic activity occurred between 4.3 and 1.5 million years ago

CONTENTS

ILLUSTRATIONS

TABLE

POTASSIUM-ARGON AGES FROM THE MOUNT TAYLOR VOLCANIC FIELD, NEW MEXICO

By PETER W. LIPMAN and HARALD H. MEHNERT

ABSTRACT

Fourteen new K-Ar dates for volcanic rocks of the Mount Taylor field, New Mexico, indicate that most activity occurred between 4.3 and 1.5 m.y. (million years) ago. Peak activity was at about 3.0–2.5 m.y., both on the central andesite-rhyolite shield volcano and on the surrounding alkali basalt-trachyte volcanic plateau, and occurred concurrently with an episode of NNE-trending basin-range faulting. The K-Ar dates also indicate that the regional Ortiz pediment surface, graded to the ancestral Rio Grande, existed in the Mount Taylor area as recently as 3 m.y. ago and that 250–400 m of erosional downcutting has occurred in subsequent time. Growth of the Mount Taylor field was also concurrent with peak volcanic activity along the northeast-trending Springerville–Raton zone, a major late Cenozoic volcanic belt that is considered to reflect the presence of a regional structural discontinuity of Precambrian age in the North American craton.

INTRODUCTION

The general sequence of volcanic events in the Mount Taylor area of north-central New Mexico, well established from the reconnaissance work of Hunt (1938), has recently been the subject of detailed mapping and petrologic studies (Baker and Ridley, 1970; Lipman and Moench, 1972; Crumpler, 1977). None of these studies has provided close chronologic control on the volcanic events, however, and accordingly we here report and interpret 14 new K-Ar dates on rocks of late Cenozoic age of the Mount Taylor field. These dates were determined in conjunction with mapping of the Mount Taylor 7½-minute quadrangle (Lipman and others, 1979); the interested reader may wish to consult this map. The new dates demonstrate that virtually all volcanic activity in the field occurred during a 2 m.y. (million year) span between about 4.3 and 1.5 m.y. ago, and peak activity was about 3.0–2.5 m.y. Flanking basaltic rocks were erupted before, during, and after growth of the central Mount Taylor cone.

ACKNOWLEDGMENTS

We thank John Pallister for assistance in collecting samples and making mineral separations. Discussions with Robert Moench and George Bachman of the U.S. Geological Survey have contributed to our understanding the volcanic history of the Mount Taylor field and its geologic setting. Larry Crumpler, while a graduate student at the University of New Mexico, made available some preliminary results of his field and petrologic study on central Mesa Chivato.

VOLCANIC HISTORY

Upper Cenozoic volcanic rocks of the Mount Taylor field presently cover an area of about 1,000 km^2 in north-central New Mexico, near the southeast edge of the Colorado Plateau (fig. 1*A*). Mount Taylor is a central stratovolcano consisting of rocks ranging in composition from alkali andesite to rhyolite (Baker and Ridley, 1970); the central cone is surrounded by an eroded basalt-capped plateau consisting of flows erupted before, during, and after the growth of the central cone (fig. 1*B*). Many of these flows are silicic alkalic basalt (hawaiite), but flows are present in a nearly continuous range from basanite to trachyte (Lipman and Moench, 1972; Crumpler, 1977).

The Mount Taylor cone has been deeply eroded, and prevolcanic sedimentary rocks of Cretaceous age are exposed in its core (Hunt, 1938; figs. 1, 2). The earliest volcanic unit exposed in this area is a trachyte lava dome (Lipman and others, 1979), which has yielded a K-Ar age of 4.37±0.27 m.y. (table 1, loc. no. 1). This is the oldest seemingly reliable radiometric age thus far determined for any rock in the volcanic field, and it thus provides a

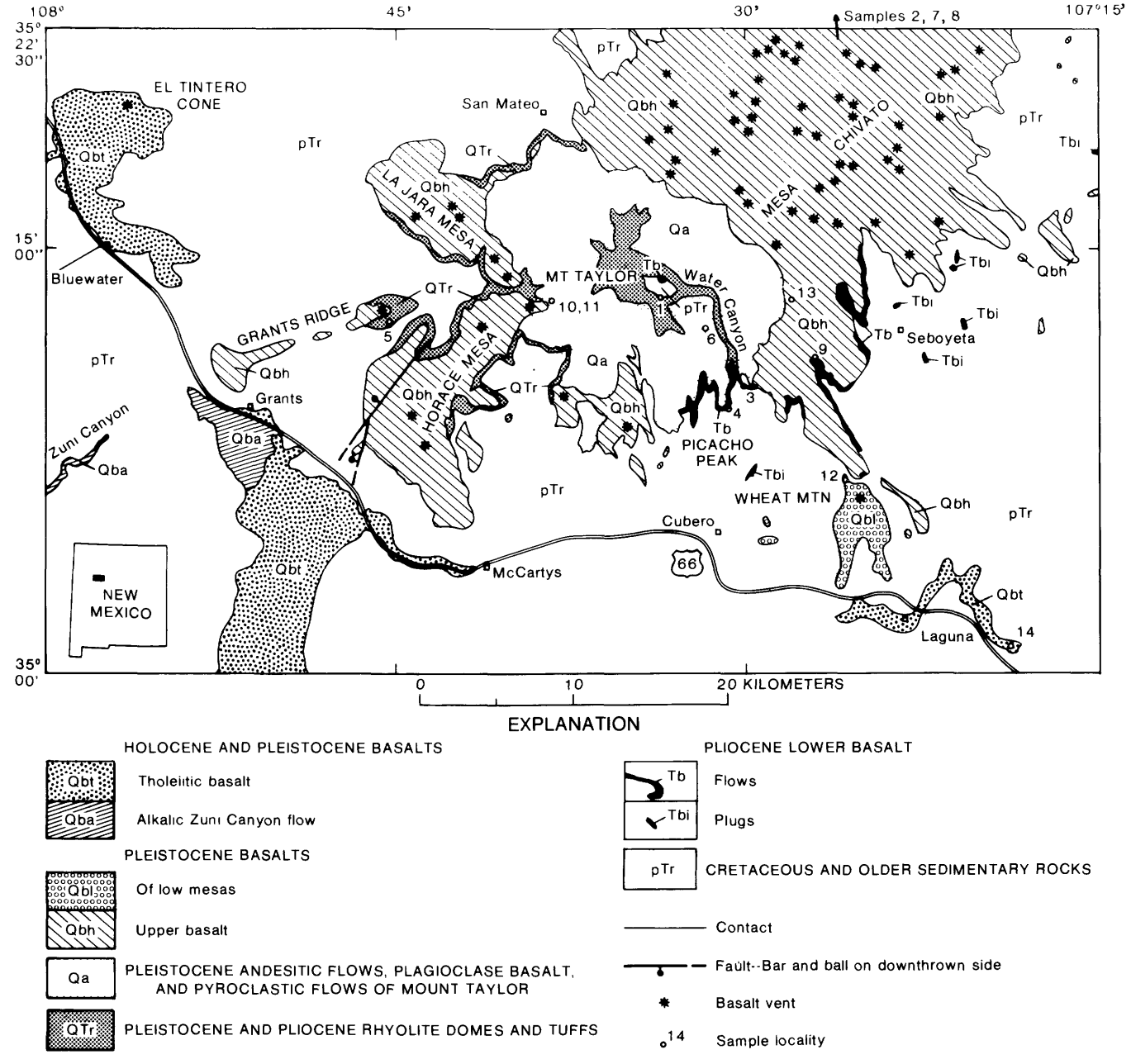

FIGURE 1.—*A*, Generalized geologic map of volcanic rocks in the Mount Taylor area, New Mexico, showing localities of dated samples.

lower limit for the beginning of the growth of the Mount Taylor cone.

Another trachyte occurs as a large dome-flow complex on Mesa Chivato, the volcanic plateau north of Mount Taylor (fig. 1). This trachyte has yielded a somewhat younger age of 3.30 ± 0.20 m.y. (table 1, no. 2). Subsequent to determination of this age, several basaltic units were mapped underlying this trachyte by Crumpler (1977), so rocks may exist on the northern plateau as old as or older than the trachyte in the core of the Mount Taylor volcano. The dated trachyte on the northern plateau is also significant because it predates a 12-km-wide zone of normal faulting of basin-range type that trends

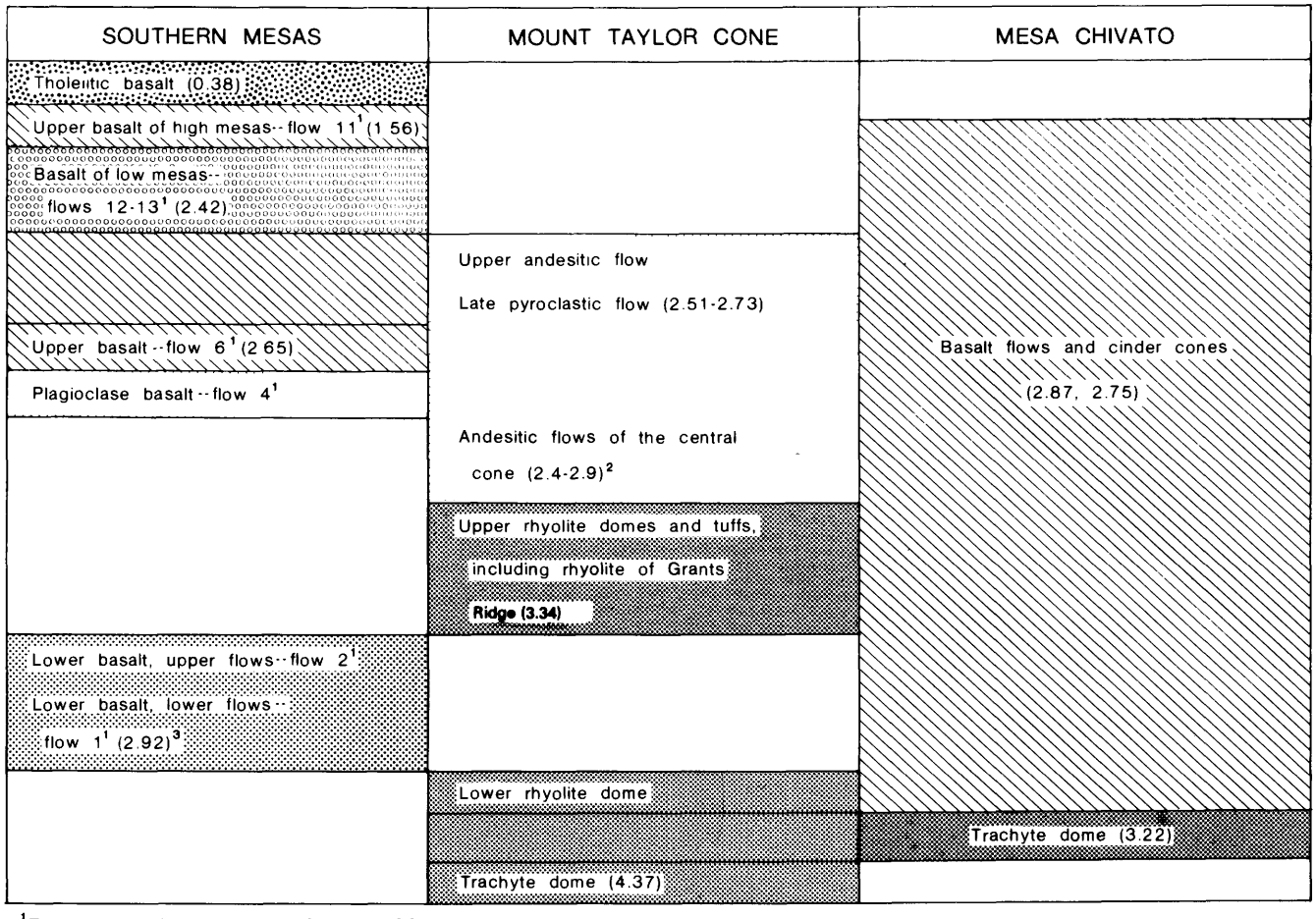

[1]Terminology of Moench and Schlee (1967).

[2]Dates from Bassett and others (1963)

[3]Most reasonable of two determinations.

FIGURE 1.—*B*, Generalized stratigraphic correlations in the Mount Taylor volcanic field (modified from Lipman and others, 1979). K-Ar ages, in millions of years, given in parentheses. Patterns correspond to those used in *A*.

north-northeast across the mesa; the age of this trachyte accordingly provides a lower limit on the age of this faulting.

In the erosional basin within Mount Taylor and on the south flank of the volcano (figs. 1, 2), the trachyte dated at 4.37 m.y. is overlain by rhyolitic ash-fall tuffs related to upper rhyolite lava domes and by distinctive basanite basalt flows (lower basalt, upper flows) that, when traced to the southeast, are underlain by one or two silicic basalt flows (lower basalt, lower flows). The upper flows are everywhere conformable with the lower flows and lack intervening sedimentary deposits; They appear closely related in age; accordingly, both are probably younger than the 4.37-m.y. trachyte. Two radiometric ages determined from lower flows of the lower basalt are 9.87 ± 1.52 and 2.97 ± 0.86 m.y. (table 1, nos. 3–4). The older age, although analytically reproducible, is considered to be of doubtful geologic significance for the reasons cited above, although such an age for one of the lower flows cannot rigorously be excluded on stratigraphic evidence. These flows tend to be weakly deuterically altered (Lipman and Moench, 1972); the alteration may in some way be related to the apparently anomalous date. The relatively low radiogenic argon contents of both samples (9.2 and 13.5 percent) also suggest the possibility of unreliable ages.

The lower basalts are overlain both within the Mount Taylor cone and around its south flank by rhyolite lava domes and associated pyroclastic ash-flow and ash-fall tuffs of the upper rhyolite (fig. 1*B*). Two rhyolitic vent areas have been mapped: one within the core of the Mount Taylor cone and the other on Grants Ridge to the west (fig. 1). Pyroclastic rocks from both vent areas merge at a common

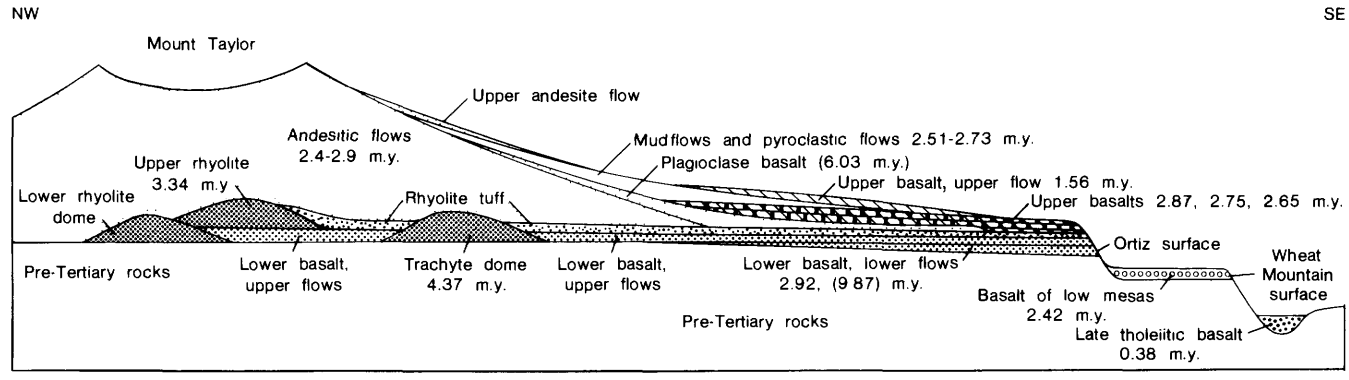

FIGURE 2.—Diagrammatic cross section, showing stratigraphic relations between dated volcanic units on south side of Mount Taylor and adjacent mesas. Dates are K-Ar ages; seemingly unreliable ages in parentheses.

TABLE 1.—K-Ar *ages from volcanic rocks from the Mount Taylor area, New Mexico*

[$K^{40}\lambda_\varepsilon = 0.581\times10^{-10}$/yr; $\lambda_\beta = 4.962\times10^{-10}$/yr; atomic abundance $K^{40}/K = 1.167\times10^{-4}$]

Sample locality Number	Unit	Field Number	Location (lat N., long W.)		Rock type or mineral	Na_2O (percent)	K_2O (percent)	$*Ar^{40}$ (10^{-10} moles/gram)	$*Ar^{40}$ (percent)	Age m.y. ±2σ
14	Tholeiitic basalt, Laguna.	68L-218	35°02',	107°19'	basalt	2.65, 2.56	0.60, 0.59	0.003	3.2	0.38±0.25
13	Upper basalt, flow 11.	68L-201B	35°12',	107°28'	--do	3.69, 3.69	1.74, 1.75 1.73, 1.72	.039	18.8	1.56±0.17
12	Basalt of low mesas, flow 13.	68L-216B	35°07',	107°26'	--do	3.98, 3.92	1.46, 1.46	.051	29.9	2.42±0.18
11	Late pyroclastic flow, Mount Taylor.	74L-134B	35°13',	107°39'	biotite	.80, .83	7.84, 7.95	.311	36.1	2.73±0.16
10	----do	74L-134B	35°13'	107°39'	plagioclase-	7.50, 7.43	1.02, 1.02	.037	23.8	2.51±0.25
9	Upper basalt, flow 6.	68L-200C	35°10',	107°27'	basalt	3.72, 3.71	1.50, 1.51 1.50, 1.49	.057	46.6	2.65±0.15
8	Basalt cinder cone, Cerros de Guadaloupe.	74L-117	35°28',	107°22'	--do	3.70, 3.70	1.56, 1.56	.062	19.3	2.75±0.30
7	Basal basalt, north end Mesa Chivato.	74L-16	35°34',	107°16'	--do	4.87, 4.85	2.01, 1.99	.084	40.7	2.87±0.20
6	Plagioclase basalt, Mount Taylor.	74L-118B	35°11',	107°31'	plagioclase-	5.51, 5.48	.63, .62	.054	31.1	[1]6.03±0.60
5	Rhyolite of Grants Ridge.	68L-204B	35°13',	107°45'	glass	4.92, 4.77	4.23, 4.23	.203	69.9	3.34±0.16
4	Lower basalt, lower flows.	68L-202A	35°10'30",	107°29'30"	basalt	3.14, 3.13	1.39, 1.37	.058	9.2	2.92±0.86
3	----do	74L-104A	35°11',	107°31'	--do	3.16, 3.17	1.50, 1.51	.214	13.5	[1]9.87±1.52
2	Trachyte dome, Cerros de Guadaloupe.	74L-113	35°25',	107°23'	sanidine	6.91, 6.86	4.01, 4.00	.191	42.3	3.30±0.20
1	Trachyte dome, Mount Taylor.	74L-111	35°13',	107°33'	--do	6.53, 6.49	3.71, 3.69	.233	39.0	4.37±0.27

[1]Geologically inconsistent date.

stratigraphic horizon between the lower and the upper basalts. A whole-rock obsidian date for the rhyolite on Grants Ridge is 3.34±0.16 m.y. (table 1, no. 5), which is only slightly older and not analytically discordant with the preferred date of 2.92± 0.86 for the underlying lower basalt flow that occurs below this rhyolite horizon to the east.

The thick cone-forming sequence of porphyritic andesite flows on the Mount Taylor volcano was not dated by us, but an early published date of relatively low analytical precision for a sample of this unit is 2.4–2.9 m.y. (Basset and others, 1963, table 1, no. 8). This date is in reasonable agreement with limiting ages determined by us for underlying and overlying units (fig. 1*B*).

A thick sequence of basaltic flows that were erupted following growth of the main Mount Taylor cone includes (1) distinctive, coarsely porphyritic plagioclase basalt flows erupted from high on the Taylor cone late in its growth, (2) sequences of as many as eight silicic alkalic basalt flows preserved on mesas around the east, south, and west sides of Mount Taylor (upper basalt, table 1), and (3) complexly interfingering sequences of basalts and more silicic alkalic flows on Mesa Chivato to the north (Crumpler, 1977).

An attempt to date the plagioclase basalt was unsuccessful: a date of 6.03±0.60 m.y. (table 1, no. 6) would seem too old by about 3 m.y., as indicated by the inconsistency with dated underlying units, in-

cluding the cone andesites, the upper rhyolite, the lower basalt, and the trachyte (fig. 1*B*; table 1). We have no direct explanation for this inconsistent date, but some dates from volcanic plagioclase phenocrysts have been interpreted as being anomalously old owing to excess argon (Damon and others, 1967).

A flow of upper basalt that directly overlies the plagioclase basalt southeast of Mount Taylor yielded an age of 2.65±0.15 m.y. (table 1, no. 9). This sample helps bracket the age of the main Mount Taylor cone to between about 3.0 and 2.5 m.y., in reasonable agreement with the older published age of 2.3–2.8 m.y. (Basset and others, 1963).

Two basalt samples from Mesa Chivato to the north yielded roughly similar ages of 2.87±0.20 and 2.75±0.30 m.y. (table 1, nos. 7–8). The younger date is from a spatter cone in Cerros de Guadaloupe that rests on the trachyte from the same locality dated at 3.30±0.20 m.y. (table 1, no. 2). This basalt cone is alined along a major north-northeast-trending fault that displaces the trachyte at least 20–30 m, but the cone and its related flow are displaced by the fault at most about 2 m. These relations indicate significant fault movement during a relatively restricted time interval about 3 m.y. ago, concurrent with peak activity in the Mount Taylor volcanic field. The older date, from the lowest flow at the northern end of Mesa Chivato (Bachman and Mehnert, 1978), indicates that all basaltic activity this far north was as young as or younger than the main cone-building stage of Mount Taylor to the south.

An intermediate-composition pyroclastic flow on the southwest flank of Mount Taylor, which postdates the main cone-building phase and overlies the capping basalts of Horace Mesa (fig. 1), yielded K-Ar ages of 2.73±0.16 and 2.51±0.25 m.y. for biotite and plagioclase phenocrysts (table 1, nos. 10–11). These dates provide further confirmation that growth of the main cone was essentially complete by about 2.5 m.y. ago. The capping basalt flows on Horace Mesa, which underlie the dated pyroclastic flow and wedge out against the Mount Taylor cone, are also accordingly bracketed as having been erupted within a geologically brief time about 2.5 m.y. ago, preceding emplacement of the pyroclastic flow. Widespread pyroclastic deposits—mainly mudflow breccias and conglomerates—and a single late flow of porphyritic andesite from the central cone underlie and interfinger with the upper basalts on the mesas east of Mount Taylor (fig. 2; Lipman and others, 1979); these also would appear to have been emplaced mainly about 2.5 m.y. ago, as indicated by ages on underlying and overlying basalt flows (fig. 1*B*).

On the southeast side of Mount Taylor, two basalt flows occur as mesa-capping remnants of a pediment surface about 50 m lower than the high mesas (the Wheat Mountain surface of Moench and Schlee, 1967). The upper of these two flows yielded a K-Ar date of 2.42±0.18 m.y. (table 1, no. 12), indicating that significant erosion had occurred around the margins of the volcanic plateau by this time.

The highest mapped flow of upper basalt, on the mesa southeast of Mount Taylor (flow 11 of Moench and Schlee, 1967), yielded a relatively young age of 1.56±0.17 m.y. (table 1, no. 13). This flow overlies all the mudflow conglomerates derived from the Mount Taylor cone and does not extend to the mesa rim. If this K-Ar date is taken at face value (and we see no obvious reason to reject it), it would indicate that basaltic activity continued in central parts of the volcanic plateau while margins of the mesas were being eroded. Some younger basalt units mapped farther north on Mesa Chivato by Crumpler (1977) overlie the dated 2.75 m.y. flow there (table 1, no. 8) and may also be relatively young. Such late high-mesa basalts would seem relatively uncommon, however, as is indicated by the general absence of observable channel-and-fill relations or plasters across erosional scarps at mesa rims.

The youngest dated basalt flows in the region occur around the south and southwest side of the Mount Taylor field, to within a few meters above present drainage levels. Of this group, a distinctive tholeiitic basalt near Laguna (fig. 1) yielded a K-Ar age of 0.38±0.25 m.y. This flow, derived from an unidentified vent further west, is probably genetically related to a complex basalt field centered in the Zuni Mountains that includes the McCartys, Zuni Canyon, and Bluewater flows (fig. 1; Lipman and Moench, 1972; Laughlin and others, 1972).

DISCUSSION

The new K-Ar dates, while not completely resolving all details of the volcanic history of the Mount Taylor field, demonstrate that the bulk of volcanic activity in this area occurred within a geologically brief interval between about 4.3 and 1.5 m.y. ago. A voluminous alkali basalt-trachyte sequence was erupted over a large region to form a volcanic plateau, with concurrent eruption of rocks ranging from alkali andesite to rhyolite, to form the central Mount Taylor cone. Peak volcanic activity both on the cone and on the surrounding plateau was be-

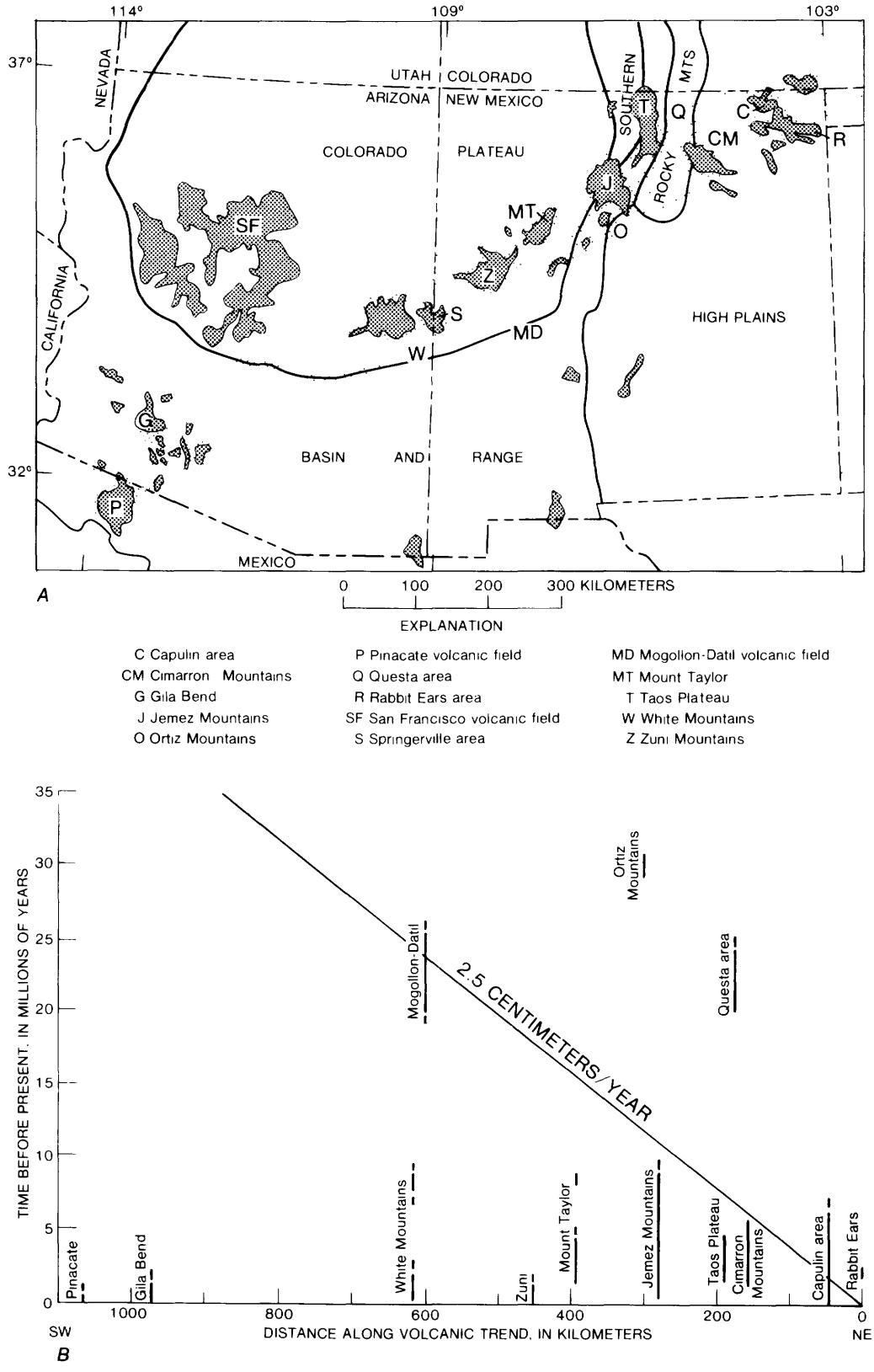

FIGURE 3.—Space-time relations of Cenozoic volcanism along the Springerville–Raton zone (shaded). *A*, Distribution of Pliocene-Pleistocene volcanic fields along the Springerville–Raton zone (modified from U.S. Geological Survey, 1965). *B*, Plot of age of volcanic activity versus distance along the Springerville–Raton zone (ages from Doell and others, 1968; Elston and others, 1975; Merrill, 1974; P. W. Lipman and H. H. Mehnert, unpub. data; and this report). Sloping line indicates the observed migration rate for inception of silicic volcanism along the eastern Snake River–Yellowstone zone. No similar age-distance trend is evident for the Springerville–Raton zone.

tween about 3.0 and 2.5 m.y. ago, concurrent with a significant episode of north-northeast-trending basin-range faulting in the same area.

The oldest volcanic rocks of the Mount Taylor field were deposited on a broad surface of low relief that probably constitutes part of the regional Ortiz surface (Bryan, 1938; Bachman and Mehnert, 1978), a regional, widespread pediment in central New Mexico graded to the ancestral Rio Grande. The new dates indicate that this surface existed as recently as about 3 m.y. ago, and that drainage levels adjacent to the Mount Taylor field have been lowered approximately 250–300 m in areas adjacent to the Mount Taylor field since that time.

Major activity in the Mount Taylor area also coincides with the time of a widespread volcanism in New Mexico and Arizona along a northeast-trending belt (fig. 3)—the Springerville–Raton zone, or the Jemez zone of Mayo (1958). Volcanic activity of roughly similar age occurred to the northeast in the Jemez Mountains, on the Taos Plateau, and on several parts of the High Plains of New Mexico and to the southwest in the Zuni Mountains, in the White Mountains, in the Springerville area, near Gila Bend, and as far as the Pinacate volcanic field in northernmost Mexico. These alined volcanic fields have recently been interpreted by Suppe, Powell, and Berry (1975, p. 512–513) as marking the trace of a mantle plume, but the lack of any consistent age progression of volcanism along the belt (fig. 3*B*) makes this hypothesis improbable. More likely, the volcanic belt follows an old zone of weakness in the lithosphere (Mayo, 1958; Laughlin, 1976) that parallels the northeast-trending Precambrian structures, which are dominant in the southwest (Shoemaker and others, 1974), and coincides closely with a boundary between major Precambrian age provinces (L. T. Silver, unpub. data, cited in Cordell, 1978).

REFERENCES CITED

Bachman, G. O., and Mehnert, H. H., 1978, New K-Ar dates and the late Pliocene to Holocene geomorphic history of the central Rio Grande region, New Mexico: Geological Society of America Bulletin, v. 89, no. 2, p. 283–292.

Baker, I., and Ridley, W. I., 1970, Field evidence and K, Rb, Sr data bearing on the origin of the Mt. Taylor volcanic field, New Mexico, U.S.A.: Earth and Planetary Science Letters, v. 10, no. 1, p. 106–114.

Bassett, W. A., Kerr, P. F., Schaeffer, O. A., and Stoenner, R. W., 1963, Potassium-argon ages of volcanic rocks near Grants, New Mexico: Geological Society of America Bulletin, v. 74, no. 2, p. 221–226.

Bryan, Kirk, 1938, Geology and ground-water conditions of the Rio Grande depression in Colorado and New Mexico, *in* U.S. National Resource Planning Board, The Rio Grande Joint Investigation in the upper Rio Grande basin: Washington, U.S. Government Printing Office, v. 1, no. 2, p. 197–225.

Cordell, L., 1978, Regional geophysical setting of the Rio Grande rift: Geological Society of America Bulletin, v. 89, no. 7, p. 1073–1090.

Crumpler, L. S., 1977, Alkali basalt-trachyte suite and volcanism, northern part of the Mount Taylor volcanic field, New Mexico: Albuquerque, University of New Mexico M.S. thesis, 131 p.

Damon, P. E., Laughlin, A. W., and Percious, J. K., 1967, Problems of excess argon-40 in volcanic rocks, *in* Radioactive dating and methods of low-level counting, IAEA–ICSU Symposium, Monaco, 1967, Proceedings: Vienna, International Atomic Energy Agency, p. 463–482.

Doell, R. R., Dalrymple, G. B., Smith, R. L., and Bailey, R. A., 1968, Paleomagnetism, potassium argon ages, and geology of rhyolites and associated rocks of the Valles Caldera, New Mexico: Geological Society of America Memoir 116, p. 211–248.

Elston, W. E., Damon, P. E., Coney, P. J., Rhodes, R. C., Smith, E. I., and Bikerman, M., 1973, Tertiary volcanic rocks, Mogollon-Datil province, New Mexico, and surrounding region—K-Ar dates, Patterns of Eruption, and Periods of Mineralization: Geological Society of America Bulletin, v. 84, no. 7, p. 2259–2273.

Hunt, C. B., 1938, Igneous geology and structure of the Mount Taylor volcanic field, New Mexico: U.S. Geological Survey Professional Paper 189–B, p. 51–80.

Laughlin, A. W., 1976, Late-Cenozoic basaltic volcanism along the Jemez zone of New Mexico and Arizona: Geological Society of America Abstracts with Programs, v. 8, no. 5, p. 598.

Laughlin, A. W., Brookins, D. G., and Causey, J. D., 1972, Late Cenozoic Basalts from the Bandera Lava Field, Valencia County, New Mexico: Geological Society of America Bulletin, v. 83, no. 5, p. 1543–1551.

Lipman, P. W., Pallister, J. S., and Sargent, K .A., 1979, Geologic map of the Mount Taylor quadrangle, Valencia County, New Mexico: U.S. Geological Survey Geological Quadrangle Map GQ–1523, scale 1:24,000.

Lipman, P. W., and Moench, R. H., 1972, Basalts of the Mount Taylor Volcanic Field, New Mexico: Geological Society of America Bulletin, v. 83, no. 5, p. 1335–1343.

Mayo, E. B., 1958, Lineament tectonics and some ore districts of the Southwest: Mining Engineering, v. 10, no. 11, p. 1169–1175.

Merrill, R. K., 1974, The late Cenozoic geology of the White Mountains, Apache County, Arizona: Tempe, Arizona State University Ph. D. thesis, 202 p.

Moench, R. H., and Schlee, J. S., 1967, Geology and uranium deposits of the Laguna district, New Mexico: U.S. Geological Survey Professional Paper 519, 117 p.

Shoemaker, E. M., Squires, R. L., and Abrams, M. J., 1974, The Bright Angel and Mesa Butte fault systems of northern Arizona, *in* Karlstrom, T. N. V., Swann, G. A., and Eastwood, R. L., eds., Geology of Northern Arizona, Part 1, Regional studies: Published for Geological Society of America Rocky Mountain Section Meeting, Flagstaff,

Arizona p. 355–392. [Available from Northern Arizona University Bookstore, Flagstaff, Arizona.]

Suppe, J., Powell, C., and Berry, R., 1975, Regional topography, seismicity, Quaternary volcanism and the present-day tectonics of the western United States: American Journal of Science, v. 275–A, p. 397–436.

U.S. Geological Survey, 1965, Geologic map of North America: U.S. Geological Survey, 2 sheets, scale 1:5,000,000.

Crystals of Coexisting Alunite and Jarosite, Goldfield, Nevada

By WILLIAM J. KEITH, LEWIS CALK, *and* R. P. ASHLEY

SHORTER CONTRIBUTIONS TO MINERALOGY AND PETROLOGY, 1979

GEOLOGICAL SURVEY PROFESSIONAL PAPER 1124-C

CONTENTS

ILLUSTRATIONS

TABLE

CRYSTALS OF COEXISTING ALUNITE AND JAROSITE, GOLDFIELD, NEVADA

By WILLIAM J. KEITH, LEWIS CALK, and R. P. ASHLEY

ABSTRACT

Alunite ($KAl_3(SO_4)_2(OH)_6$) and jarosite ($KFe_3(SO_4)_2(OH)_6$) coexist in optically continuous crystals in a sample from the Goldfield mining district, Esmeralda County, Nev. Beam scans with an electron microprobe indicate that no intermediate minerals of the solid-solution series alunite-jarosite occur in these crystals. An Eh-pH diagram demonstrating the equilibrium relations between alunite, jarosite, and geothite suggests the crystals most likely developed by a rise in Eh, which oxidized ferrous to ferric iron, thus allowing jarosite to precipitate.

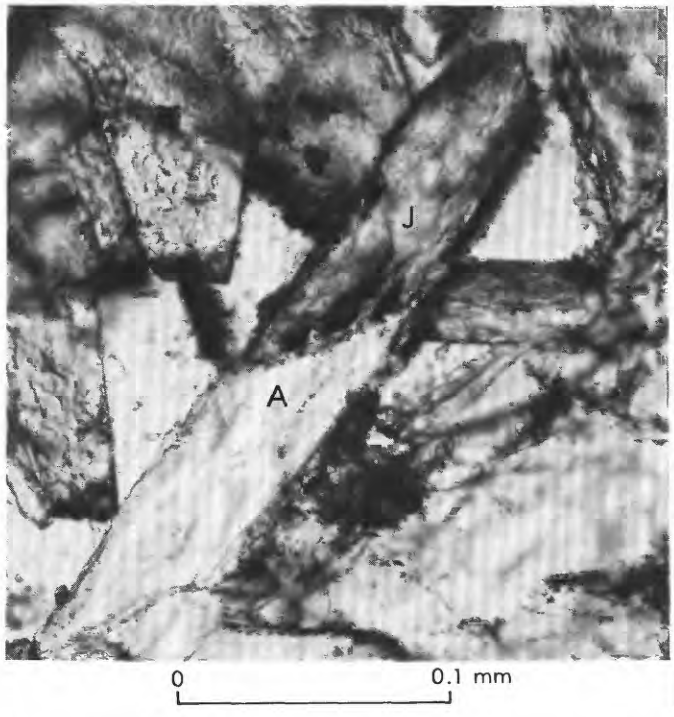

FIGURE 1.—Optically continuous single crystal composed of alunite (A) and jarosite (J) that projects into a vug. Plane-polarized light.

INTRODUCTION

Alunite and jarosite coexist in the same optically continuous crystal (fig. 1) in a hand specimen from the Goldfield mining district (fig. 2), Esmeralda County, Nev. Brophy, Scott, and Snellgrove (1962) have shown that, although the intermediate minerals are rare, a solid solution exists between these two minerals in nature. The purpose of this study is to determine whether any intermediate varieties are present in the Goldfield sample and to propose a model explaining how these two-phase crystals might have formed.

GEOLOGIC SETTING

The epithermal precious-metal deposits of the Goldfield mining district produced over 130,000 kg of gold between 1903 and 1961. The district is part of a Tertiary volcanic center in which the rocks range from andesite to rhyolite. The ore bodies occur within a hydrothermally altered area (fig. 2) that covers approximately 39 km^2 (Ashley and Albers, 1975, p. A3). The sample described in this report is from Preble Mountain, in the southern part of the area (fig. 2). Preble Mountain is composed largely of trachyandesite and rhyodacite flows and tuffs (Ashley, 1975) that have been argillized and silicified (Ashley and Keith, 1976).

OCCURRENCE AND PROPERTIES

Alunite and jarosite are relatively common sulfate minerals of the alunite group and are frequently associated with hydrothermal mineral deposits, although they are by no means limited to them. The

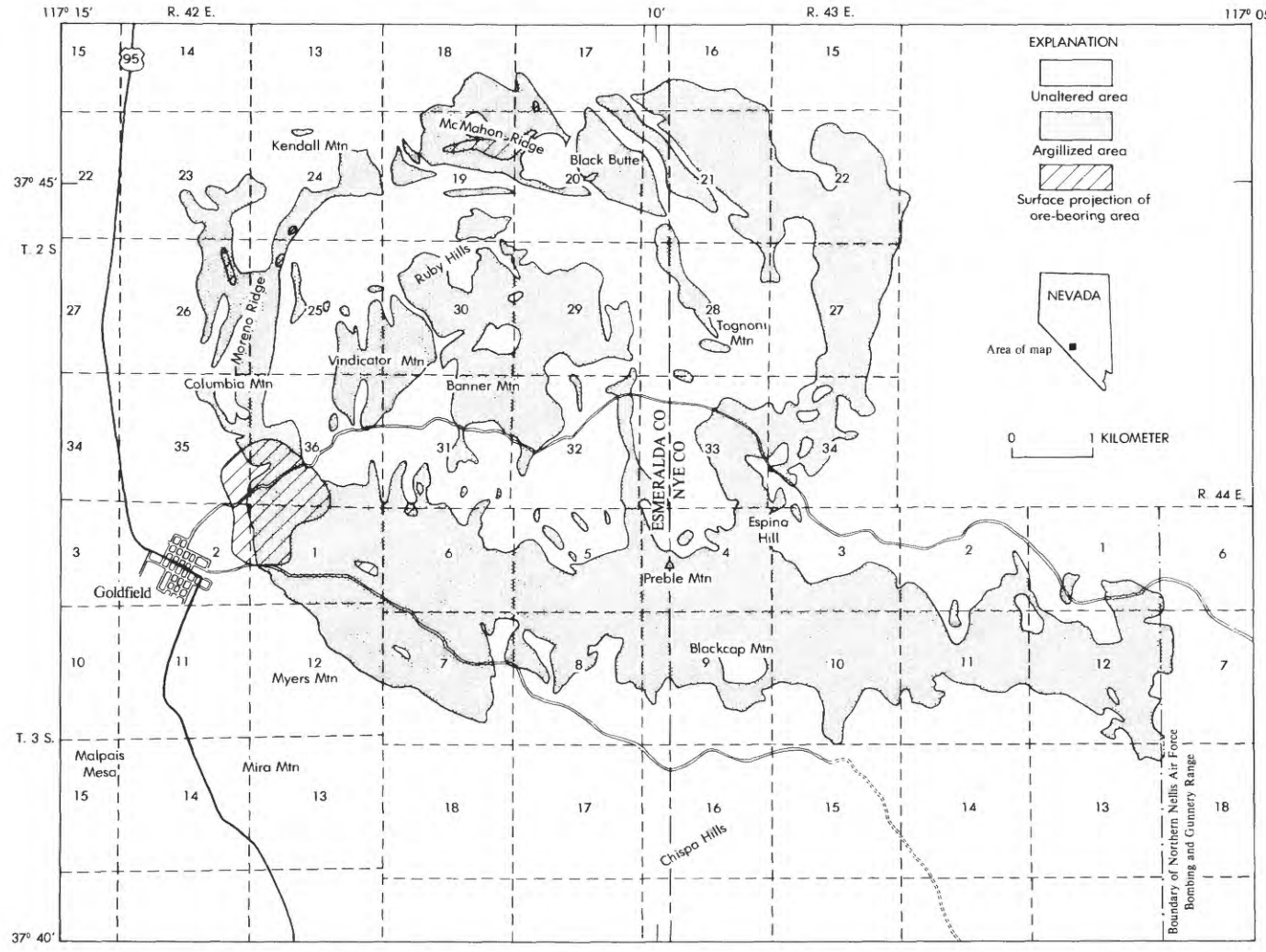

FIGURE 2.—Map of Goldfield, Nev., and vicinity showing areas of hydrothermal alteration and ore deposits.

general formula for the group is $AB_3(SO_4)_2(OH)_6$, where "A" represents potassium and "B" represents aluminum in alunite and ferric iron in jarosite. Sodium ions, and occasionally others, may substitute for potassium in varying amounts. Where the sodium-potassium ratio exceeds 1, the mineral is called natroalunite or natrojarosite. Alunite and jarosite both belong to the space group $R3m$ and, therefore, have the same crystal symmetry. The alunite and jarosite in this study have developed perpendicular to the c crystallographic axis.

Alunite and jarosite in the Preble Mountain area are thought to be of hypogene origin because a sample of coarse-grained alunite intergrown with jarosite gave a K-Ar age of 20 ± 0.4 million years, which is concordant with the age of mineralization determined by dating post- and premineralization rocks (Ashley and Silberman, 1976). The normal sequence of crystallization is alunite followed by jarosite (Ashley and Keith, 1976, p. B10; Ashley and Silberman, 1976). Initially, alunite formed comblike growths surrounding silicified rock breccia fragments (fig. 3) and extending into fractures and vugs. Then both alunite and jarosite formed crystal aggregate linings in vugs. Small vugs were completely filled in places by a cream to yellow-brown aggregate of the two minerals. The alunite crystals found in these aggregates are typically larger than the jarosite and commonly appear to be surrounded by fine-grained jarosite. In the final stage, jarosite alone encrusted remaining vein walls, covering alunite-jarosite aggregates where they were present. Where the aggregates were absent, jarosite filled open spaces among alunite crystals and formed termina-

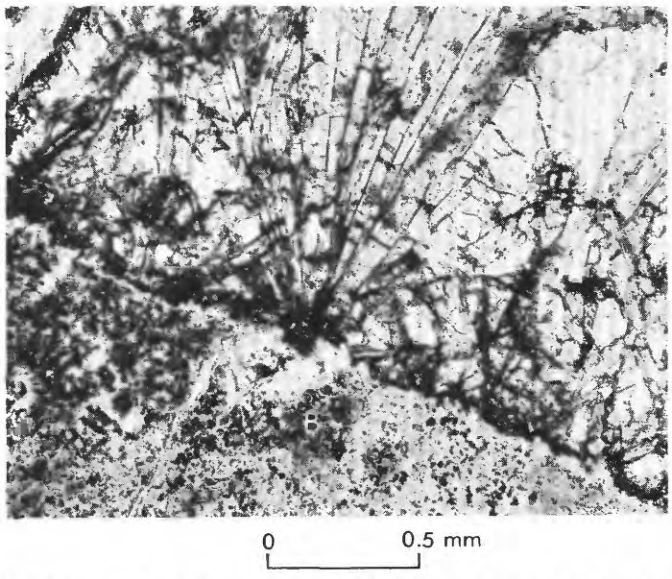

FIGURE 3.—Comblike growth of alunite (A) forming around silicified breccia fragment (B). Plane-polarized light.

tions on some (fig. 1). Fracture fillings of coexisting alunite and jarosite have been seen at more than 60 localities in a 3-km^2 area at Preble Mountain, but notably coarse-grained alunite or jarosite or both occur at only a few of these localities.

Where jarosite forms optically continuous terminations on alunite crystals, the planar boundary between the two phases is quite sharp and appears to parallel the terminating faces (fig. 1). The boundaries do not show embayments or other irregularities typical of replacement of one mineral by another.

ELECTRON MICROPROBE DATA

An Applied Research Laboratories EMX–SM[1] electron microprobe was used to examine compositional changes across two of the two-phase crystals. Step scans were performed across the phase boundaries of the crystals (fig. 4) using 3-μm intervals and a counting period of 10 sec. The crystals were analyzed for potassium, aluminum, and iron.

The data from the microprobe scans (fig. 5) show that iron and aluminum are relatively homogeneous in both phases although they change in quantity from one phase to the other. Iron does not increase in alunite as the phase boundary is approached, and, conversely, aluminum does not increase in jarosite. The potassium is relatively constant throughout, changing little from one phase to the other. Alunite is much less stable than jarosite under the electron beam (fig. 4). The beam craters are much more pronounced in alunite, suggesting that potassium may be more abundant in alunite than we determined. Nonetheless, the stable quantities of iron or aluminum indicate that intermediate species between alunite and jarosite do not exist in these crystals.

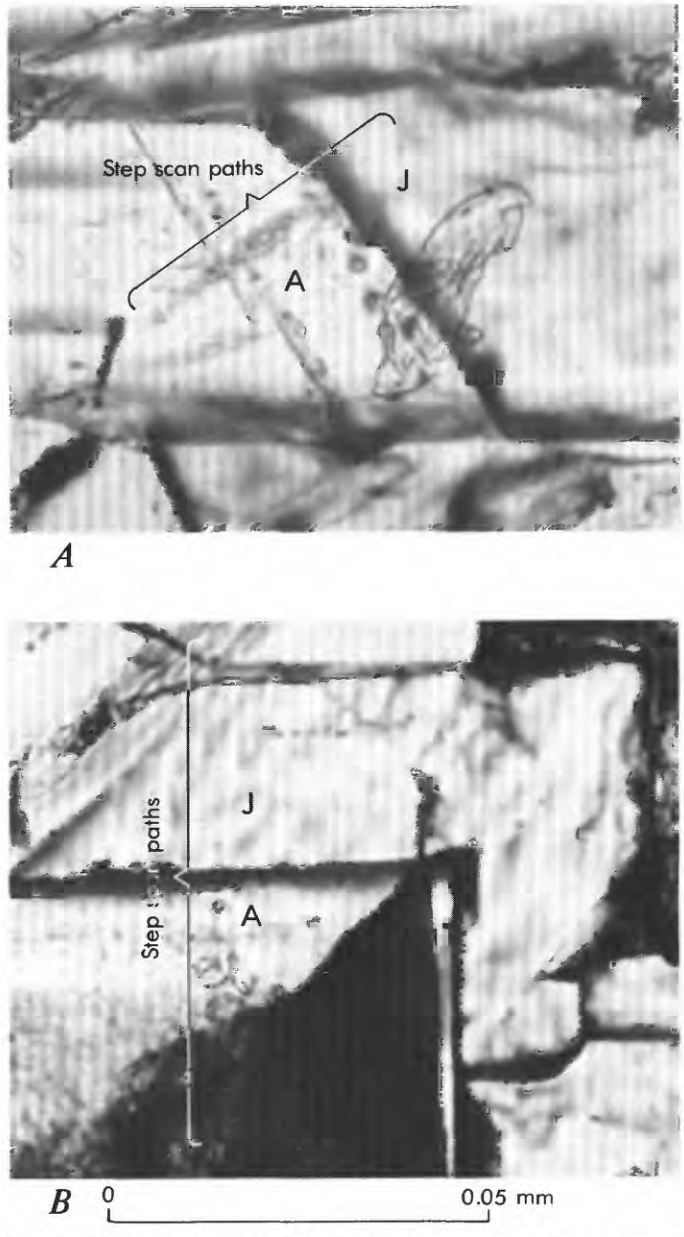

FIGURE 4.—Two crystals of alunite (A) capped by jarosite (J) showing step scan paths across contact. Plane-polarized light. For data on *A* and *B* refer to figure 5*A* and *B*, respectively.

[1] The use of trade names and trademarks in this publication is for descriptive purposes only and does not constitute endorsement by the U.S. Geological Survey.

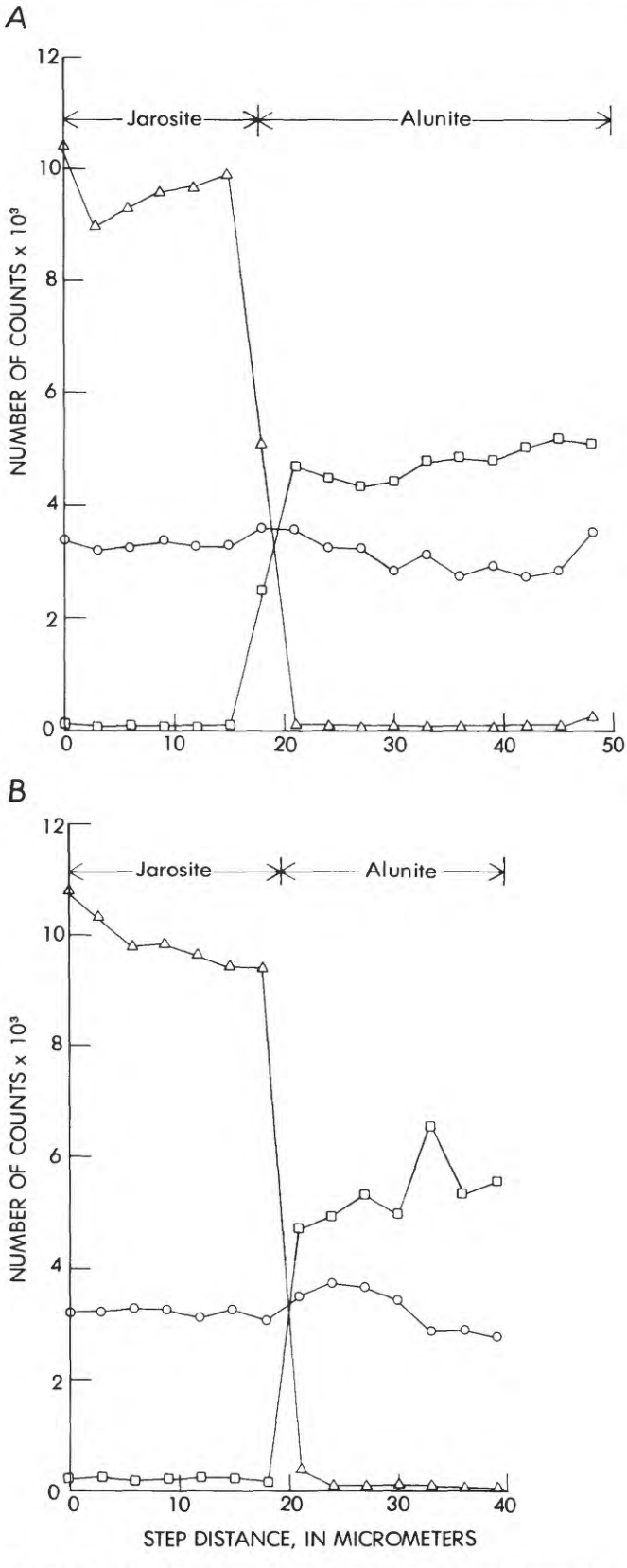

FIGURE 5.—Distribution of aluminum (squares), iron (triangles), and potassium (circles) across alunite-jarosite boundary in two crystals: *A* (shown in fig. 4*A*) and *B* (shown in fig. 4*B*).

DISCUSSION

The two-phase crystals were probably formed in one of two ways:

1. All of the Preble Mountain localities were deficient in iron and then were flooded with iron-rich solutions.
2. The late-stage hydrothermal fluids presumed to have formed these minerals underwent a change in Eh and pH, thus oxidizing existing iron to the Fe^{3+} state and causing the precipitation of jarosite.

The possibility of flooding with iron-rich solutions cannot be ruled out although it is unlikely that iron was totally absent during the formation of alunite. The sequence of deposition from one locality to another in the Preble Mountain area is generally consistent, although one or two stages may be absent. This consistency suggests that alunite and jarosite formed sequentially from solutions that had similar compositions at all of the localities. There is no independent evidence in the Preble Mountain area that would support the hypothesis of sudden flooding with iron-rich solutions. Thus, the hypothesis of changing Eh and pH seems more plausible.

A generalized Eh-pH diagram (fig. 6) showing the approximate stability fields for alunite and jarosite was constructed for 25° C at 101.3 kPa using the procedure outlined by Garrels and Christ (1965). Free-energy data used in the calculations for figure 6 are listed in table 1. The activities were derived from data modified from Brown (1971) and were chosen because they have been shown to occur in nature and also because the concentrations exceed the solubilities of alunite and jarosite. An increase in iron would expand the jarosite stability field and also lower the minimum Eh.

Three hypothetical paths are shown in figure 6 that would produce the two-phase crystals of this study. In an unbuffered solution, a rise in Eh should also lead to a decrease in pH and produce crystallization sequences similar to ones indicated by the diagram. On all three paths (A–A′, B–B′, C–C′), a rapid increase in Eh or decrease in pH would produce the two-phase crystals because the solutions would not remain outside the alunite or jarosite field long enough to precipitate anything else. Path A–A′ is self-explanatory, and the crystals observed could have been produced in this manner. The same crystals could also have been formed following path B–B′ because there is nothing to precipitate between alunite and jarosite. Path C–C′ should produce crystals including a third phase, which has been observed. A few of the crystals show a thin red film of

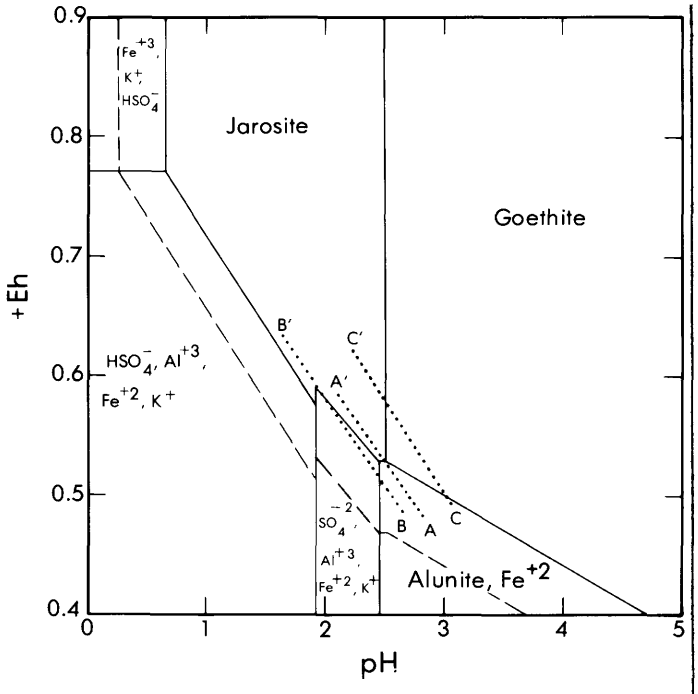

FIGURE 6.—Generalized Eh-pH diagram showing relative stability fields for alunite and jarosite. Activity of species used in calculations are as follows: $(a_{\Sigma S})=10^{-2}$m; $(a_{\Sigma Fe^{2+},\ Fe^{3+}})=10^{-1}$m; $(a_{Al^{3+}})=10^{-3}$m; $(a_{K^+})=10^{-3}$m. Dashed lines represents $(a_{\Sigma Fe^{2+},\ Fe^{3+}})=10^{-3}$m. Dotted lines represent hypothetical crystallization paths. (See text for explanation.)

TABLE 1.—*Free energy data used in calculations of generalized Eh-pH diagram for alunite and jarosite*

Species	$\Delta G_f°$ kcal/mol at 25°C, 101.3 kPa	Reference
$KAl_3(SO_4)_2(OH)_6$ (alunite).	-1113.600	Hemley, Hostetler, Gude, and Mountjoy (1960).
FeOOH (goethite)---	-116.878	Berner (1969).
H_2O (water)--------	-56.690	Robie and Waldbaum (1968).
$KFe_3(SO_4)_2(OH)_6$ (jarosite).	-794.00	Brown (1971).
Al^{3+}----------	-116.000	Robie and Waldbaum (1968).
Fe^{2+}----------	-20.300	Do.
Fe^{3+}----------	-2.520	Do.
K^+----------	-67.700	Do.
S^{2-}----------	+20.500	Do.
SO_4^{2-}----------	-177.970	Do.
HSO_4^-----------	-179.94	Weast (1969).

hematite or goethite between the alunite and jarosite; the film does not appear to be an exsolution phenomenon.

A rise in Eh or a decrease in pH could be accomplished in the Preble Mountain area by the entry of downward moving, deeply circulating meteoric waters as the rocks cooled during the later part of hypogene alteration. Alunite and jarosite typically formed in voids produced by local shattering of the silicified rocks after silicification was complete. These voids would greatly facilitate permeation by descending water.

REFERENCES CITED

Ashley, R. P., 1975, Preliminary geologic map of the Goldfield mining district, Nevada: U.S. Geol. Survey Misc. Field Studies Map MF–682, scale 1:24,000.

Ashley, R. P., and Albers, J. P., 1975, Distribution of gold and other ore-related elements near ore bodies in the oxidized zone at Goldfield, Nevada: U.S. Geol. Survey Prof. Paper 843–A, p. A1–A48.

Ashley, R. P., and Keith, W. J., 1976, Distribution of gold and other metals in silicified rocks of the Goldfield mining district, Nevada: U.S. Geol. Survey Prof. Paper 843–B, p. B1–B17.

Ashley, R. P., and Silberman, M. L., 1976, Direct dating on mineralization at Goldfield, Nevada, by potassium-argon and fission-track methods: Econ. Geol., v. 71, p. 904–924.

Berner, R. A., 1969, Goethite stability and the origin of red beds: Geochim. et Cosmochim. Acta 33, p. 267–273.

Brophy, G. P., Scott, E. S., and Snellgrove, R. A., 1962, Sulfate studies II—Solid solution between alunite and jarosite: Am. Mineralogist, v. 47, p. 112–126.

Brown, J. B., 1971, Jarosite-goethite stabilities at 25°C, 1 atm: Mineralium Deposita, v. 6, p. 245–252.

Garrels, R. M., and Christ, C. L., 1965, Solutions minerals, and equilibria: New York, Harper and Row, 450 p.

Hemley, J. J., Hostetler, P. B., Gude, A. J., and Mountjoy, W. T., 1960, Some stability relations of alunite: Econ. Geology, v. 64, no. 6, p. 599–612.

Robie, R. A., and Waldbaum, D. R., 1968, Thermodynamic properties of minerals and related substances at 298.15°K and 1 atm pressure and at higher temperatures: U.S. Geol. Survey Bull. 1259, 256 p.

Weast, R. C., ed., 1969, General Chemical, section D, *of* Handbook of chemistry and physics—A ready-reference of chemical and physical data: Cleveland, The Chemical Rubber Co., p. D1–D218.

Zeolitization of Tertiary Tuffs in Lacustrine and Alluvial Deposits in the Ray–San Manuel Area, Pinal and Gila Counties, Arizona

By MEDORA H. KRIEGER

SHORTER CONTRIBUTIONS TO MINERALOGY AND PETROLOGY, 1979

GEOLOGICAL SURVEY PROFESSIONAL PAPER 1124–D

Tuff beds were studied to determine the approximate mineralogic composition and type of alteration. Thicker beds containing at least 80 percent zeolite are potentially minable

CONTENTS

ILLUSTRATIONS

TABLES

ZEOLITIZATION OF TERTIARY TUFFS IN LACUSTRINE AND ALLUVIAL DEPOSITS IN THE RAY–SAN MANUEL AREA, PINAL AND GILA COUNTIES, ARIZONA

By MEDORA H. KRIEGER

ABSTRACT

Specimens of tuff in the Ray–San Manuel area, southeastern Arizona, have been X-rayed to determine the present approximate mineralogic composition and the type and degree of alteration of the tuffs. Some of the tuffs consist largely of glass or have been partly or completely altered to calcium montmorillonite; many of them have been almost completely zeolitized or contain a zeolite and some clay. Only three zeolitized specimens contain a little glass. With four exceptions, the zeolitie is clinoptilolite; the exceptions are one altered to chabazite, one to mordenite, one to erionite, and one to erionite, clinoptilolite, and chabazite. The tuffs are mostly of airfall origin and of rhyolitic or probable rhyolitic composition and generally contain negligible percentages of crystal and lithic fragments. Two specimens are tuffaceous sedimentary rocks, and two are ash-flow tuffs. The tuffs range in age from early Pliocene or late Miocene to Oligocene. Some were deposited in lacustrine or playa environments; others were deposited in freshwater alluvial environments. All the beds examined in the lower Miocene and older formations have been zeolitized. Zeolitization of beds in younger formations depends on the environment of deposition. Zeolitized tuffs that contain at least 80 percent zeolite and are in beds more than one-third meter thick are considered potentially minable.

INTRODUCTION

Tuffs of Teritiary age in the Ray–San Manuel area, Pinal and Gila Counties, southeastern Arizona are interbedded in the Quiburis Formation, unnamed deposits in Dripping Spring Valley, Big Dome Formation, San Manuel Formation, the Araviapa Member of the Galiuro Volcanics, and the Whitetail Conglomerate. The formations range in age from early Pliocene or late Miocene to early Oligocene and were deposited in lacustrine, playa, and alluvial environments. The distribution and age of the formations and locations of specimens studied are shown in figure 1.

More than 60 specimens of tuff were X-rayed (tables 1, 2). The study was undertaken originally as an aid in separating the San Manuel Formation from the overlying Big Dome Formation in the Crozier Peak (Krieger, 1974d) and the Kearny and Grayback (Cornwall and Krieger, 1975a, b) Quadrangles. Preliminary X-ray studies showed that the tuffs in the Big Dome Formation in the Kearny Quadrangle had remained vitric or had partly altered to calcium montmorillonite, whereas those in the San Manuel Formation in the Crozier Peak Quadrangle had been largely replaced by zeolite. It was hoped that X-ray analyses of tuffs would be an effective way of separating the two formations in areas where they are conformable and nearly identical in composition and appearance.

Additional studies, however, did not bear out the early indications that zeolitization occurred only in tuffs in the older formation. Tuffs in the Big Dome Formation in the Crozier Peak Quadrangle, some in the Hayden (Banks and Krieger, 1977) and Kearny Quadrangles, and some in the younger deposits within Dripping Spring Valley and in the Quiburis Formation have also been zeolitized. Studies by Hay (1966), Sheppard and Gude (1964, 1965, 1968, 1969, 1973), and Sheppard, Gude, and Munson (1965) of zeolitization of tuffs in sedimentary deposits have shown that silicic glass generally is not altered to a zeolite if it is deposited in fresh water, has not been affected by moderately alkaline or moderately saline ground water, and has not been deeply buried. Age is also a factor, as few deposits older than the Cenozoic contain relic glass. Age and depth of burial have had little effect on the amount of zeolitization

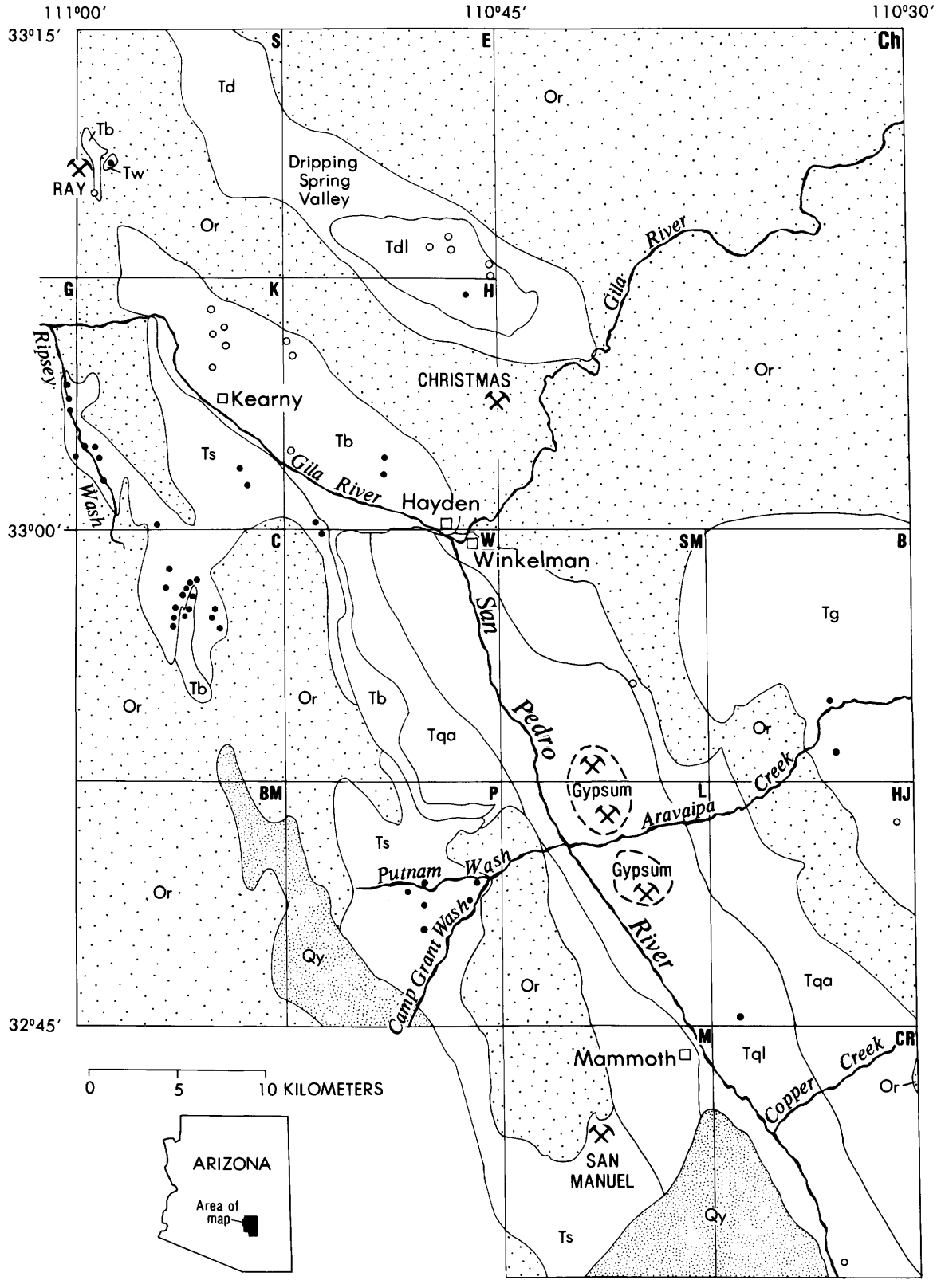

FIGURE 1.—The distribution of formations and sample

EXPLANATION

Qy YOUNGER ROCKS

QUIBURIS FORMATION (Early Pliocene or late Miocene)—Hemphillian age vertebrate fossils (Krieger, 1974c)

Tqa Alluvial facies

Tql Lakebed facies—Tuff beds, Q-1 to Q-3, table 1. Gypsum deposit shown by dashed boundary

DEPOSITS IN DRIPPING SPRING VALLEY—May correlate in age with Big Dome Formation or possibly with Quiburis Formation (Cornwall and Krieger, 1977)

Td Alluvial facies

Tdl Lakebed facies—Tuff beds, D-1 to D-6, table 1

Tb BIG DOME FORMATION (Middle or early Miocene)—Tuff beds, B-1 to B-11, table 1. Mostly alluvial deposits. B-6A gave K—Ar age of 17 m.y. (hornblende), 14 m.y. (biotite) (Cornwall and others, 1971; Banks and others,1972)

Ts SAN MANUEL FORMATION (Early Miocene or late Oligocene)—Tuff beds, S-1 to S-30, table 2. Alluvial and playa deposits. S-2 gave K—Ar age of 17.1±1 m.y. (biotite) (Cornwall and Krieger, 1975a). S-10 gave 18.0±0.5 m.y. (biotite), 24.1±0.7 m.y. (sanidine), (Krieger, 1974a)

Tg GALIURO VOLCANICS, ARAVAIPA MEMBER (Late Oligocene to early Miocene)—Ash-flow tuff, G-1 to G-3, table 2. Unaltered part gave K—Ar age of 25.7±0.8 m.y. (sanidine) 22.9±0.8 m.y. (biotite)(Creasy and Krieger, 1977)

Tw WHITETAIL CONGLOMERATE (Early Oligocene)—Tuff bed, W-1, table 2. W-1 gave K—Ar age of 32 m.y. (biotite)(Cornwall and others, 1971; Banks and others, 1972)

Or OLDER ROCKS

—— Contact

⚒ Mine or quarry

○ Nonzeolitized tuff—Glass and (or) clay

● Zeolitized tuff—Zeolite is clinoptilolite, except for chabazite in D-6, erionite in S-21, erionite with chabazite and clinoptilolite in S-30, and mordenite in G-2A

Quadrangle names and sources of data:

- **B** Brandenburg Mountain (Krieger, 1968a)
- **BM** Black Mountain (Krieger, 1974b)
- **C** Crozier Peak (Krieger, 1974d)
- **Ch** Christmas 15-minute (Willden,1964)
- **CR** Clark Ranch (Creasy, 1967)
- **E** El Capitan (Cornwall and Krieger, 1977)
- **G** Grayback (Cornwall and Krieger, 1975b)
- **H** Hayden (Banks and Krieger, 1977)
- **HJ** Holy Joe Peak (Krieger, 1968b)
- **K** Kearny (Cornwall and Krieger, 1975a)
- **L** Lookout Mountain (Krieger, 1968c)
- **M** Mammoth (Creasy, 1965, 1967)
- **P** Putnam Wash (Krieger, 1974e)
- **S** Sonora (Cornwall and others, 1971)
- **SM** Saddle Mountain (Krieger, 1968d)
- **W** Winkelman (Krieger, 1974c)

locations of zeolitized and nonzeolitized tuffs.

TABLE 1.—*Present mineralogical composition of specimens of tuff from the Quiburis Formation, deposits in Dripping Spring Valley, and the Big Dome Formation*

[Estimated from X-ray diffractometer patterns of bulk samples: •, abundant, more than 50 percent; o, 10-50 percent; x, trace to 10 percent; -, looked for but not found. Arranged in approximate order of increasing age. See figure 1 for distribution of formations and location and name of quadrangles]

Quad.	Lat.	Long.	Spec. No.	Field No.	Glass	Clay	Zeolite[1]	Quartz	Feldspar	Biotite[2]	
							Quiburis Formation				
SM	32°55'	110°40'	Q-1	H-24	•	o	-	x	x	-	Rhyolite tuff, 0.3- to 0.6-m-thick beds, unmapped, vitric shards, altered matrix
HJ	45'	36'	Q-2	H-366	-	-	o	o	o	-	Tuffaceous sandstone, unmapped. Contains hornblende and calcite
CR	38'	32'	Q-3	M-2	•	o	-	x	x	-	Rhyolite tuff bed, unmapped, associated with diatomite. Shard structure preserved
							Deposits in Dripping Spring Valley				
H	33°8'	47'	D-1	EC-1	•	o	-	-	-	-	Rhyolite tuff composed largely of shards
E	9'	47'	D-2	254-55	•	o	-	-	-	x	Rhyolite tuff composed of shards. Same bed as D-1
E	8'	45'	D-3	275-16	o	o	-	x	x	x	Rhyolite tuff bed, unmapped
E	7'	45'	D-4	276-10	•	o	-	x	-	x	Rhyolite tuff, unmapped. Identical to D-2. Finer grained beds contain more clay
E	8'	47'	D-5	253-2	•	x	-	x	x	x	Rhyolite tuff, 0.3- to 0.6-m bed, unmapped. Shard structure
H	7'	46'	D-6	253-1	-	x	•	x	x	-	Rhyolite tuff[3], 0.3 m thick, unmapped. Zeolite is chabazite. Shard structure preserved
							Big Dome Formation, lapilli tuff				
K	5'	54'	B-1	43-17A	•	o	-	x	x	-	Rhyolite tuff interbedded in lapilli tuff
K	7'	55'	B-2	43-17W	o	•	-	x	-	-	White structureless pumice lapilli. Gray lapilli with tube structure has same composition
K	6'	55'	B-3A	45-21A	•	-	-	x	-	x	Unaltered pumice lapilli; n. 1.496
K	6'	55'	B-3B	45-21B	o	•	-	x	x	-	White matrix is largely Ca-montmorillonite. Unaltered pumice lapilli has n. 1.498
K	6'	55'	B-4	45-3	•	o	-	x	x	-	Lapilli tuff
K	6'	52'	B-5	198-1	o	o	-	x	x	x	Do.
							Big Dome Formation, ash-flow tuff unit				
K	5'	55'	B-6A	43-13A	•	o	-	x	x	x	Upper pink part. Chemical analysis[3] of specimen 75/80/1 from same area
K	5'	55'	B-6B	43-13B	•	o	-	x	x	x	Lower white part. Contains more clay than overlying pink part
H	2'	52'	B-7A	Ha-4	•	-	-	x	x	x	Upper pink part. Contains hornblende
H	2'	52'	B-7B	Ha-4a	o	•	-	x	-	x	White area surrounding lithophysae
H	5'	52'	B-8	DH-1	-	•	-	x	x	x	From drill hole in mineralized area. Glass and much of feldspar altered to Ca-montmorillonite. Contains hornblende and calcite. Sample submitted by Neil Cambell, Ray Mines Division, Kennecott Copper Corp.
							Big Dome Formation, relations unknown				
H	2'	48'	B-9	240-5	-	x	•	x	x	x	Rhyolite tuff, 15 cm thick, unmapped
H	2'	48'	B-10	240-6	-	x	•	x	x	-	Massive rhyolite tuff bed, 0.3 m thick, unmapped
S	11'	59'	B-11	79/78/1	•	o	x	x	x	x	Air-fall tuff[3]
C	32°58'	56'	B-12	3	-	x	•	o	o	-	Rhyolite tuff, unmapped. Contains hornblende
C	58'	56'	B-13	4	-	x	•	x	x	x	Do.
C	58'	56'	B-14	8	-	-	•	x	x	x	Do.

[1]Zeolite is clinoptilolite, except for chabazite in D-6.
[2]Some X-rays show hornblende, see description.
[3]See table 3 for chemical analysis.

that has occurred in tuff beds in the Ray–San Manuel area.

Diffractograms of whole-rock tuffs (fig. 2) illustrate the resolution of individual minerals and mineral aggregates. Phenocrystic quartz, biotite, and unaltered feldspar can be distinguished in glassy, zeolitized, and argillized tuffs. Quantitative determination of the amounts of zeolites in altered tuffs is difficult, because of preferred orientations of minerals in the X-ray mounts, different degrees of crystallinity, and masking by amorphous matrix material. The X-ray diffraction of the whole-rock tuffs, however, clearly shows the relative abundance of the alteration products, and many alteration mineral identifications were relatively easy owing to the nearly monomineralogic composition of some samples. Sheppard and Gude (1964) by using X-ray diffraction were able to recognize zeolite concentrations as low as 10 percent in some altered rocks.

RESULTS OF STUDIES OF TUFFS IN RAY–SAN MANUEL AREA

TUFFS IN THE QUIBURIS FORMATION

The Quiburis Formation, of which about 200 m is exposed (Heindl, 1963 Krieger, 1968a–d, 1974c; Creasey, 1965, 1967), was deposited in a long, narrow, closed basin that extended for many kilometers southeast of the area mapped on figure 1. The formation consists of an alluvial and a lakebed facies separated by a narrow transition zone. The alluvial facies occurs around the margin of the basin and consists of sandy pebble conglomerate and some interbedded sandy and silty beds. The lakebed facies occupies the center of the basin and consists of thin, evenly bedded clay, silt, marl, and very fine grained sandstone. Thick deposits of gypsum occur in the lakebed facies north and south of present-day Aravaipa Canyon (fig. 1). Their occurrence indicates that Aravaipa Creek and Putnam Wash, west of the

TABLE 2.—*Present mineralogical composition of specimens of tuff from the San Manuel Formation, Aravaipa Member of the Galiuro Volcanics, and the Whitetail Conglomerate*

[Estimated from X-ray diffractometer patterns of bulk samples: •, abundant, more than 50 percent; o, 10-50 percent; x, trace to 10 percent; -, looked for but not found. Arranged in approximate order of increasing age. See figure 1 for distribution of formations and location and name of quadrangles]

Quad.	Lat.	Long.	Spec. No.	Field No.	Glass	Clay	Zeolite[1]	Quartz	Feldspar	Biotite[2]	Description
							San Manuel Formation				
K	33°2'	110°59'	S-1	12-105	-	x	•	x	x	x	Rhyolite tuff in lower part of upper granitic conglomerate. Contains hornblende
K	2'	59'	S-2	12-100	-	x	•	x	x	x	Rhyolite tuff[3] from top of tuffaceous sandstone and conglomerate unit. Contains hornblende
K	2'	59'	S-3	13-40B	-	x	•	x	x	x	Rhyolite tuff near base of tuffaceous sandstone and conglomerate unit in this area
G	5'	111°1'	S-4	14-67	-	o	•	o	o	x	Rhyolite tuff at base of tuffaceous sandstone and conglomerate unit in this area. S-4 to S-7 are from different parts of the same lapilli tuff unit, not the same bed as S-3
K	1'	110°59'	S-5A	12-79C	o	o	o	x	x	x	Rhyolite tuff near middle of 1.2-m-thick bed of lapilli tuff. Glass probably is in pumice
K	1'	59'	S-5B	12-79B	x	x	x	-	-	-	Large (3.5 cm) pumice lapillus near base of lapilli tuff. Largely replaced by calcite. Shard structure preserved
G	3'	111°1'	S-6	12-106	-	x	•	x	x	x	Lapilli tuff in tuffaceous sandstone and conglomerate unit
G	4'	1'	S-7	176-45	-	o	•	x	x	x	Lapilli tuff at base of tuffaceous sandstone and conglomerate unit. Tube structure preserved
G	2'	0'	S-8	174-45	-	o	o	x	o	x	Rhyolite tuff near base of lower granitic conglomerate, unmapped. Contains hornblende
C	32°58'	110°57'	S-9	W-143B	-	o	•	x	x	-	Thin bed of rhyolite tuff, unmapped
C	59'	57'	S-10	W-158	-	o	•	x	x	x	Thin bed of rhyolite tuff, unmapped[3]
C	57'	55'	S-11A	W-136	-	o	•	o	x	x	Tuffaceous sandstone unmapped, with pumice lapilli as much as 2 cm long
C	57'	55'	S-11B	10	-	x	•	x	x	x	Tuffaceous sandstone with pumice lapilli, unmapped
C	58'	55'	S-12	11	-	-	•	x	x	-	Rhyolite tuff, unmapped. Contains hornblende
C	57'	55'	S-13	W-138	-	-	•	x	o	x	Thin bed of lapilli tuff, unmapped
C	58'	56'	S-14	1	-	x	•	o	x	x	Thin rhyolite tuff bed, unmapped
C	58'	56'	S-15	2	-	o	•	x	x	x	Do.
C	58'	56'	S-16	5	-	x	o	o	x	x	Rhyolite tuff with lapilli, unmapped
C	58'	56'	S-17	6	-	x	•	x	x	x	Tuffaceous sandstone, unmapped. Contains hornblende
C	58'	56'	S-18	7	-	o	o	x	x	x	Do.
C	58'	56'	S-19	9	-	x	•	o	o	x	Tuffaceous sandstone, unmapped. Contains calcite and hornblende
K	33°0'	57'	S-20	37-59	-	o	•	x	x	-	Concretionary tuff, unmapped
K	1'	54'	S-21	67-24	-	x	•	-	-	-	Rhyolite tuff, 5-6 cm thick, unmapped, in dark playa deposits. Zeolite is erionite
K	2'	54'	S-22	41-37	-	o	•	x	x	-	Rhyolite tuff, 0.3 m thick, unmapped, in dark conglomerate
H	0'	51'	S-23	Ha-3	-	x	•	x	x	x	Rhyolite tuff in dark conglomerate. Contains hornblende
W	0'	59'	S-24	W-71	-	x	•	x	x	-	Rhyolite tuff 0.6 m thick, unmapped. Good shard structure. Contains hornblende
P	32°49'	46'	S-25	W-12B	-	o	•	x	x	x	Rhyolite tuff, unmapped, in alluvial conglomerate. Pumice lapilli. Shard structure preserved
P	49'	46'	S-26	W-14	-	o	o	o	o	x	Rhyolite tuff, unmapped, in alluvial conglomerate. Contains hornblende
P	49'	48'	S-27	W-16A	-	x	•	x	x	-	Pumice lapilli in tuffaceous sandstone, unmapped, in granitic playa deposits. Contains three parts calcite
P	49'	48'	S-28	W-394	-	x	•	x	x	-	Rhyolite tuff, unmapped, in granitic playa deposits. Composed almost entirely of shards
P	48'	48'	S-29	W-52	-	x	•	o	x	x	Concretionary tuff in alluvial conglomerate
P	48'	48'	S-30	W-395A	-	-	•	x	x	-	Large pumice lapillus[3] in tuffaceous sandstone, unmapped. Contains erionite and some chabazite and clinoptilolite
							Aravaipa Member, Galiuro Volcanics				
HJ	51'	31'	G-1	H-202L			Devitrified zone[4]				Welded tuff, Aravaipa Member
B	53'	33'	G-2	A-4	-	-	•	x	x	x	Distal end of Aravaipa Member[5] (ash-flow tuff). Zeolite is clinoptilolite
B	55'	33'	G-3A	H-343M	-	-	•	x	x	x	Distal end of Aravaipa Member[5] (north of Aravaipa Canyon). Below columnar-jointed unit zeolite is entirely mordenite
B	55'	33'	G-3B	H-343A	-	-	•	-	x	x	Distal end of Aravaipa Member, above columnar-jointed unit. Zeolite is entirely of clinoptilolite
							Whitetail Conglomerate				
S	33°12'	59'	W-1	79/78/2	-	x	•	x	x	-	Rhyolite tuff[3], unmapped, near top of Whitetail Conglomerate

[1]Zeolite is clinoptilolite except of erionite in S-21, mordenite in G-2 and erionite, chabazite, and clinoptilolite in S-30.
[2]Some X-rays show hornblende, see description.
[3]See table 3 for chemical analysis.
[4]Composed of cristobalite, feldspar, quartz and a little clay and biotite. See table 4 for chemical analysis.
[5]See table 4 for chemical analysis.

San Pedro River, probably did not exist when the gypsum was forming or did not supply much fresh water to the lake. The sulfur to form the gypsum may have been supplied through erosion of the San Manuel and Copper Creek ore deposits.

Only three specimens of tuff from the Quiburis Formation were X-rayed. Two of them had remained vitric; the other contains some clinoptilolite. The vitric character of one of the specimens (Q–1, table 1) from the alluvial margin of the basin and the zeolitized character of the altered specimen (Q–2) from the central lakebed are as to be expected (Shepard and Gude, 1968). The third specimen (Q–3), from a thick section of rhyolite tuff and diatomite was collected about equidistant from the eastern and western margins of the lakebed facies.

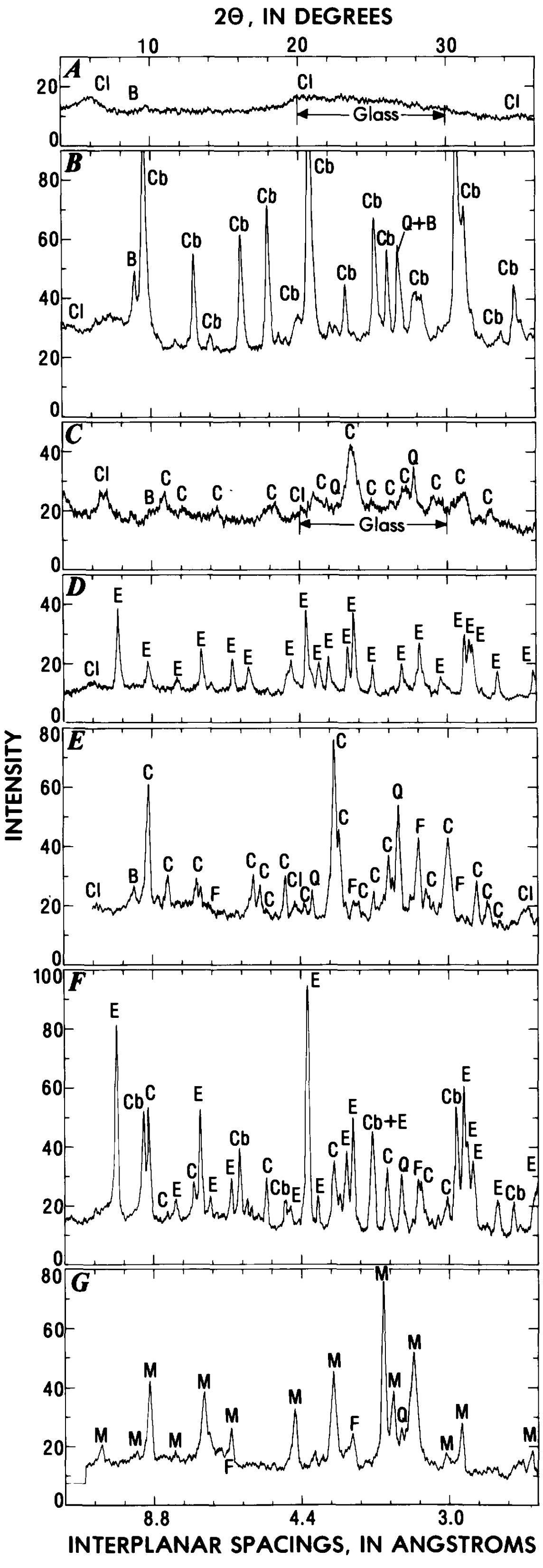

FIGURE 2.—X-ray diffractograms of selected specimens of tuff, showing type of peak heights involved in the estimation of composition. Cu/Ni radiation, λCuKα=1.5418Å. Scan from 4° 2Θ at 1° 2Θ/minute. *A*, Dripping Spring Valley, D–1; glass and clay. *B*, Dripping Spring Valley, D–6; altered to chabazite. *C*, San Manuel Formation, S–5A; glass, clay, and clinoptilolite. *D*, San Manuel Formation, S–21; altered to erionite. *E*, San Manuel Formation, S–29; altered to clinoptilolite. *F*, San Manuel Formation, S–30; altered to erionite, chabazite, and clinoptilolite. *G*, Aravaipa Member, Galiuro Volcanics, G–3A; altered to mordenite. (B, biotite; Cl, clay; C, clinoptilolite; Cb, chabazite; E, erionite; F, feldspar; M, mordenite; Q, quartz)

The presence of the diatomite and the vitric character of the tuff suggest that the lake water here must have been fresh at the time the tuff was deposited and remained so since. This area was probably near the intake end of the lake.

TUFFS IN DEPOSITS IN DRIPPING SPRING VALLEY

Sedimentary deposits, which are at least 450 m thick, in Dripping Spring Valley (Banks and Krieger, 1977; Cornwall and Krieger, 1977; Cornwall and others, 1971; and Willden, 1964) accumulated in a closed basin as did the Quiburis Formation; the deposits are a coarse alluvial conglomerate around the margins and a fine-grained material, mostly clay containing some silt and fine sand, in the center (fig. 1). The two facies are separated by a narrow transition zone on the southwest side of the basin and by a wide transition zone on the northeast side of the basin. The wide transition zone is included in the lakebed facies mapped on figure 1 because of the abundance of freshwater limestone, much of which is coarsely conglomeratic. The limestone was formed probably when calcium-bearing fresh water was brought by streams from surrounding Paleozoic limestone; the calcium was precipitated as calcite when it came in contact with the alkaline and possibly saline waters of the lake (Sheppard and Gude, 1968). All specimens of tuff X-rayed from this transition zone (D–1 through D–5, table 1) are vitric (fig. 2*A*); two have undergone some clay alteration. Freshwater in the pores and the freshness of the ground water to which the tuff was subsequently exposed, prevented zeolitization of the tuff beds. One specimen of tuff (D–6) from a 0.3-m-thick white tuff bed exposed in a roadcut in the lakebed facies is composed almost entirely of chabazite (fig. 2*B*). The presence in this area of thick deposits of montmorillonitic clay, in which gypsum fills little fractures, suggests that the tuff bed was deposited in an alkaline or saline environment.

TUFFS IN THE BIG DOME FORMATION

The Big Dome Formation, which is about 600 m thick (Krieger and others, 1974; Cornwall and Krieger, 1975a; Banks and Krieger, 1977; Krieger, 1974a, c–e), is an alluvial deposit comprising several lithologic units, including two mappable tuff units. The upper one, about 12 m thick is a lapilli tuff and interbedded rhyolite tuff, tuffaceous sandstone, and conglomerate. It is extensively exposed in the northeastern part of the Kearny Quadrangle; its easternmost exposure is northeast of Kearny near the west edge of the Hayden Quadrangle. The lower unit, about 6 m thick, is a nonwelded quartz-latite ash-flow tuff that crops out intermittently from about 3.2 km northwest of Kearny to the west edge of the Hayden Quadrangle just north of the Gila River. The tuff was also found in a drill hole in a mineralized area of the western part of the Hayden Quadrangle a short distance southeast of the easternmost exposure of the lapilli tuff. Other tuffs studied in the Big Dome Formation are in the south-central part of the Hayden Quadrangle and north-central part of the Crozier Peak Quadrangle; all are thin, unmapped beds. A more extensive tuff bed is northeast of Ray. The relations of these tuff beds to the lapilli tuff and ash-flow tuff are unknown.

None of the X-rayed specimens of the lapilli tuff (B–1 through B–5, table 1) contains any zeolite. They are largely vitric or contain generally minor amounts of calcium montmorillonite; locally, matrix or lapilli have been largely altered to clay. Ash-flow tuff specimens (B–6 through B–8) also contain no zeolite. B–6 and B–7 are vitric but have been somewhat altered to calcium montmorillonite; the clay is locally more abundant in the lower part of the ash flow or surrounding the lithophysae. X-ray and thin-section studies show that glass and much of the feldspar in the specimen obtained from the drill hole (B–8) has been altered to calcium montmorillonite; biotite and hornblende, however, are unaltered. The tuff bed near Ray (B–11) is largely vitric but contains some clay and traces of clinoptilolite. It is one of the few tuffs studied that contains both glass and a zeolite in a single sample; all the other tuff beds from the Big Dome Formation have been almost completely altered to clinoptilolite. These beds in the Hayden Quadrangle (B–9 through B–10) may have been zeolitized because ground water became more alkaline as it circulated through the enclosing conglomerate, which is composed largely of andesitic volcanic clasts. Zeolitization of the tuff beds in the Crozier Peak Quadrangle (B–12 through B–14) may be related to whatever conditions zeolitized the tuff beds in the underlying San Manuel Formation.

TUFFS IN THE SAN MANUEL FORMATION

The San Manuel Formation, which is at least 3,000 m thick (Heindl, 1963; Krieger, 1974a, c–e; Krieger and others, 1974; Cornwall and Krieger, 1975a, b; Banks and Krieger, 1977), consists of alluvial and playa deposits that have been separated into more than nine members. Numerous curled mud chips in playa sandstone and mud cracks in conglomerate beds attest to the alternate wet and dry condtions. Many of the tuff beds studied are enclosed in granitic alluvial deposits. The associated fine-grained granitic sandstone and conglomerate may have been deposited in a playa environment. A few of the tuffs are associated with dark nongranitic alluvial or playa deposits.

The most abundant tuffaceous material, and probably the youngest part of the formation, is in the downfaulted graben along Ripsey Wash in the Grayback and Kearny Quadrangles (fig. 1; S–1 to S–8, table 2). Here the granitic tuffaceous sandstone and conglomerate and the overlying and underlying granitic conglomerate contain many relatively pure tuff beds (0.3–3 m), several of which have been traced from 0.2 to more than 3 km. One lapilli tuff unit was traced for about 8 km. Except for two thin tuff beds (S–22 and S–24) that were traced for short distances, all the other specimens of tuff studied are from thin unmapped beds.

All the tuffs studied from the San Manuel have been zeolitized (table 2); most contain a little clay, and four (S–5, S–8, S–18, S–26) contain nearly as much clay as zeolite. Only two (S–5A, S–5B) contain some vitric material, which is believed to be concentrated in large pumice lapilli. A large pumice lapillus (S–5B) has been largely replaced by calcite. The zeolite is clinoptilolite in all except two tuffs X-rayed; in one the zeolite was erionite (S–21), and in the other it was an assemblage of erionite (the most abundant), chabazite, and clinoptilolite (S–30).

The reason for zeolitization of the tuffs in the San Manuel Formation is uncertain. Some of the tuffs may have been deposited in a playa environment in which the water was sufficiently alkaline or saline to cause zeolitization. Those that were deposited apparently in an alluvial freshwater environment must have been zeolitized by later changes in ground water.

ARAVAIPA MEMBER OF THE GALIURO VOLCANICS

The Aravaipa Member, whose thickness is 60–90 m except for 15–30 m at the distal margin (Krieger, 1968a, b; 1979; Creasey and Krieger, 1977; Simons, 1964), is an ash-flow tuff of rhyolite composition; it has a well-formed zonal pattern that indicates that it was a simple cooling unit and probably a single ash flow. Horizontal and vertical zonations are completely exposed in canyon walls. Dense welding, characteristic of the lower part of the interior of the ash flow, decreases vertically as well as horizontally away from the interior of the sheet. Near the member's distal margin, south of Aravaipa Canyon, slightly welded columnar-joined tuff pinches out and is replaced and surrounded by nonwelded tuff (about 20 m thick). In the only section of nonwelded tuff studied north of the canyon, about 25 m of welded tuff separates about 25 m of nonwelded tuff below from 5 m of nonwelded tuff above.

No zeolite is present in any of the welded part of the ash flow (G1, table 2). Except for the basal vitrophyre all of the welded part has been devitrified. The nonwelded part of the ash flow has been completely zeolitized except for tiny unaltered crystal fragments. South of Aravaipa Canyon the zeolite is clinoptilolite (G–2). North of the canyon it is clinoptilolite above the columnar-jointed tuff (G–3B) but is mordenite below it (G–3A). X-ray studies of many specimens (Krieger, 1979) show that all the nonwelded tuff south of the canyon has been altered to clinoptilolite.

Zeolitization of the nonwelded parts of the Aravaipa Member must have been caused by later changes in ground water, as the formation appears to have been deposited in an alluvial environment.

TUFF IN THE WHITETAIL CONGLOMERATE

One specimen of an unmapped tuff was collected from the Whitetail Conglomerate (Cornwall and others, 1971). It has been altered to clinoptilolite and traces of clay and unaltered crystal fragments (W–1, table 2).

ORIGINAL COMPOSITION OF THE TUFFS AND CHANGES DUE TO ZEOLITIZATION

The tuffs in the general area mapped on figure 1 are chiefly rhyolites or tuffs of probable rhyolite composition. On the basis that rhyolitic glass has a refractive index of less than 1.500 (George, 1924), tuffs from the Quiburis Formation (Q1, Q3, table 1), from basin deposits in Dripping Spring Valley (D–1 through D–5), and from the Big Dome Formation (B–3A, B–3B) are considered to be rhyolite. The ash-flow tuff in the Big Dome Formation is a quartz latite based on its chemical analysis (B–6, table 3).

Table 3 contains chemical analyses of seven tuffs; five are strongly zeolitized, and two are largely vitric but three have undergone some clay alteration. Table 4 shows chemical analyses of three specimens

TABLE 3.—*Chemical composition of selected tuffs, Ray–San Manuel area, Arizona*

[Major oxide analyses, weight percent, under direction of L. Shapiro; by methods described by Shapiro and Brannock (1962), supplemented by atomic absorpiton, except no. D-6, by methods described by Shapiro (1967)]

Location No.	D-6	B-6	B-11	S-2	S-10	S-30	W-1
Field No.	253-1	75/80/1	79/78/1	12-100	W-158	W-395A	79/78/2
Laboratory No.	M122781W	M105898W	M105895W	M113934W	M104768W	M107983W	M105896W
SiO_2	53.2	67.7	68.7	59.8	59.4	56.2	64.5
Al_2O_3	14.8	14.5	13.2	14.2	15.8	14.4	12.4
Fe_2O_3	1.6	2.3	1.7	1.4	2.2	.81	1.5
FeO	.16	.26	.18	.88	1.7	0	.06
MgO	2.8	1.2	.91	1.4	2.0	1.4	2.1
CaO	2.1	1.7	1.8	5.9	3.7	4.2	3.3
Na_2O	4.4	3.0	2.6	2.5	2.6	2.5	.55
K_2O	1.2	3.4	3.8	1.4	1.3	1.4	1.5
H_2O+	9.4	1.6	4.5	7.4	5.6	11.3	4.8
H_2O-	9.6	3.6	2.1	3.0	4.6	7.4	8.8
TiO_2	.06	.44	.25	.31	.64	.10	.24
P_2O_5	.08	.12	.05	.10	.17	.00	.06
MnO	.03	.08	.07	.04	.12	.15	.05
CO_2	.07	.05	.05	1.6	<.05	.20	.08
Total	100	100	100	100	100	100	100

Sample description:
- D-6 - Air-fall tuff composed largely of chabazite
- B-6 - Quartz-latite ash-flow tuff, some clay alteration
- B-11 - Air-fall tuff, some clay alteration
- S-2 - Air-fall tuff, largely altered to clinoptilolite
- S-10 - Air-fall tuff, largely altered to clinoptilolite
- S-30 - Pumice lapilli, composed of about equal parts of erionite, chabazite, and clinoptilolite
- W-1 - Air-fall tuff, altered to clinoptilolite

TABLE 4.—*Chemical analyses and comparisons of unaltered and altered specimens of the Aravaipa Member, Galiuro Volcanics*

[See table 5 for minor-element analyses. Major-oxide analyses (weight percent), no. 1 by P. Elmore, S. Botts, and G. Chloe; by rapid methods described by Shapiro and Brannock (1962); nos. 2, 3 by H. Smith by methods described by Shapiro (1967)]

	Original analyses			Recalculated without H_2O and CO_2		
	1	2	3	1	2	3
SiO_2	73.4	67.0	63.6	74.6	75.2	74.4
Al_2O_3	13.6	12.5	12.1	13.8	14.0	14.1
Fe_2O_3	1.2	1.2	1.0	1.2	1.4	1.2
FeO	.08	.12	.08	.08	.13	.09
MgO	.47	1.0	.40	.48	1.1	.47
CaO	.44	2.6	3.0	.45	2.9	3.5
Na_2O	3.6	.78	1.9	3.7	.88	2.2
K_2O	5.2	3.5	3.0	5.3	3.9	3.5
H_2O	.93	7.6	7.9	--	--	--
H_2O	.93	4.0	5.6	--	--	--
TiO_2	.24	.16	.12	.24	.18	.14
P_2O_5	.06	.15	.04	.06	.06	.05
MnO	.08	.07	.06	.08	.08	.07
CO_2	<.05	.22	.06	--	--	--
Total	100	100	99	99.99	99.83	99.72

Sample description
1. G-1. Devitrified tuff, H202L, Lab 159531
2. G-2. Tuff altered to clinoptilolite, A-4, Lab M126691W
3. G-3A. Tuff altered to mordenite, H343M, Lab M126692W

TABLE 5.—*Semiquantitative spectrographic analyses of minor elements in specimens of tuffs, Ray–San Manuel area, Arizona*

[Minor-element analyses in parts per million by semiquantitative spectrographic methods by R. E. Mays (D-6, B-6, B-11, S-2, W-1); by C. R. Heropoulos (S-10, S-30, G-2, G-3A): and I. H. Barlow (G-1). Results are to be identified with geometric brackets whose boundaries are 1.2, 0.83, 0.56, 0.38, 0.26, 0.18, 0.12, and so forth, but are reported arbitrarily as midpoints of these brackets, 1, 0.7, 0.5, 0.3, 0.2, 0.15, 0.1, and so forth. The precision of a reported value is approximately plus or minus one bracket at 68-percent confidence, or two brackets at 95-percent confidence. N, not detected, --, not looked for; <, less than. Looked for but not found: As, Au, Bi, Cd, Eu, Ge, He, In, Li, Pd, Re, Sb, Sm, Ta, Te, Th, Tl, U, W]

Location No.---	D-6	B-6	B-11	S-2	S-10	S-30	G-1	G-2	G-3A	W-1
Field No.------	253-1	75/80/1	79/78/1	12-100	W-158	W-395A	H-202L	A-4	H-343M	79/78/2
Laboratory No.-	M122718W	M105898W	M105895W	M113934W	M104768W	M107983W	159531	M126691W	M126692W	M105896W
Ag	1	N	N	N	N	N	<.7	N	N	N
B	30	20	N	N	N	N	<30	7	10	N
Ba	200	700	300	700	1000	150	500	200	200	1000
Be	N	3	2	N	3	5	5	7	7	2
Ce	N	N	N	N	150	N	100	--	--	N
Co	N	N	N	N	70	N	N	N	N	N
Cr	7	N	15	50	7	3	<3	1.5	3	10
Cu	20	10	15	10	20	20	3	5	7	30
Ga	10	20	15	15	15	15	20	--	--	10
Gd	--	--	--	--	--	--	N	--	--	--
La	N	N	N	N	50	N	50	50	100	N
Mo	N	N	N	N	N	N	<3	N	N	N
Nb	N	N	N	N	30	50	20	30	50	N
Nd	--	--	--	--	N	--	N	--	--	--
Ni	7	N	3	5	3	7	10	.7	.7	N
Pb	N	20	20	10	30	30	30	30	30	30
Sc	N	5	N	3	15	3	3	5	7	N
Sn	--	N	N	N	N	N	N	N	N	N
Sr	500	300	200	700	5000	500	70	100	200	1000
V	20	20	15	30	50	N	10	7	20	20
Y	N	30	20	15	30	N	30	30	30	20
Yb	N	3	2	1.5	3	1.5	3	--	--	2
Zn	N	N	N	N	N	N	N	30	30	N
Zr	70	150	70	100	300	70	200	300	300	100

Sample description:
- D-6 - Air-fall tuff composed largely of chabazite
- B-6 - Quartz-latite ash-flow tuff, some clay alteration
- B-11 - Air-fall tuff, some clay alteration
- S-2 - Air-fall tuff, largely altered to clinoptilolite
- S-10 - Air-fall tuff, largely altered to clinoptilolite
- S-30 - Pumice lapilli, composed of erionite, chabazite, and clinoptilolite
- G-1 - Unaltered Aravaipa Member, devitrified zone, probably close to original composition of magma
- G-2 - Aravaipa Member, altered to clinoptilolite
- G-3A - Aravaipa Member, altered to mordenite
- W-1 - Air-fall tuff, altered to clinoptilolite

(two altered and one unaltered) from the Aravaipa Member. Table 5 gives spectrographic analyses of all ten specimens. The chemical compositions of the fresh equivalents of the five zeolitized tuffs (D–6, S–2, S–10, S–30, and W–1, table 3) are unknown, although they were probably rhyolites.[1] In comparison with tuff samples slightly altered to clay (B–6A, B–11), the zeolitized samples have lost SiO_2 and K_2O and gained H_2O, CaO, and MgO. Na_2O is unchanged, except in D–6 (altered to chabazite), in which it shows a gain. The change in SiO_2 and Na_2O in the zeolitized tuffs, however, may have been greater than that shown in table 3, as some SiO_2 and Na_2O may have been lost in B–6A and B–11 by groundwater leaching, which is most advanced in porous glassy tuffs including nonwelded ash-flow tuffs (Lipman, 1965).

More specific information on the composition of fresh and altered tuffs from the Aravaipa Member of the Galiuro Volcanics is available from analyses of G–1 (unaltered, but devitrified), G–2 (altered to clinoptilolite), and G–3A (altered to mordenite) (table 4). The major change has been a large increase in H_2O. To more readily compare the nonvolatile constitutents, the analyses have been recalculated on a water-free basis. In addition to H_2O, the major changes during alteration to both clinoptilolite and mordenite have been an increase in CaO (greater when altered to mordenite) and losses in Na_2O (greater when altered to clinoptilolite) and

[1] Specimen S–2 is probably also a rhyolite, although it was called rhyodacite (Cornwall and Krieger, 1975a) because of its chemical composition, which is due to zeolitization.

K_2O (greater when altered to mordenite). Clinoptilolite shows a small increase in MgO and SiO_2, whereas mordenite show little change.

ECONOMIC IMPORTANCE OF THE ZEOLITES

Nearly monomineralic zeolitized tuffs are common in Cenozoic rocks. Those that contain at least 80 percent zeolite and are more than 0.3 m thick are considered potentially minable (Sheppard, 1971; see also Hawkins and Mumpton, 1976). Many of the tuff beds examined are very thin, or their thickness and extent were not determined because of poor exposures.

Only one tuff (D–6) in the Dripping Spring Valley is zeolitized (to chabazite), and it is exposed only in a roadcut; it might be of considerable extent. Numerous thin unmapped zeolitized tuff beds are in the San Manuel Formation (S–14 to S–19) and the overlying Big Dome Formation (B–12 to B–14) in the Crozier Peak Quadrangle. Some of the beds are composed largely of clinoptilolite. The zeolite here may be present in economic amounts. The greatest concentration of zeolite in the San Manuel Formation is along Ripsey Wash (S–1 to S–8), where thin beds of nearly pure clinoptilolite have been mapped and are associated with numerous unmapped zeolitized tuffaceous sedimentary rocks. The Aravaipa Member of the Galiuro Volcanics contains the greatest known amount of zeolite in the Ray–San Manuel area. South of Aravaipa Canyon the nonwelded zeolitized tuff covers an area of nearly 2 km^2. A nearly horizontal section, about 0.8 km long and nearly 20 m thick, appears to be composed almost entirely of clinoptilolite. The known amount of mordenite is confined to a vertical section north of the canyon and is nearly 20 m thick. The rest of the nonwelded tuff north of Aravaipa Canyon has been altered to clinoptilolite (Krieger and others, 1979).

REFERENCES CITED

Banks, N. G., Cornwall, H. R., Silberman, M. L., Creasey, S. C., and Marvin, R. F., 1972, Chronology of intrusion and ore deposition at Ray, Arizona—Part 1, K-Ar ages: Economic Geology, v. 67, no. 7, p. 864–878.

Banks, N. G., and Krieger, M. H., 1977 [1978], Geologic map of the Hayden Quadrangle, Pinal and Gila Counties, Arizona: U.S. Geological Survey Geologic Quadrangle Map GQ–1391, scale 1:24,000.

Cornwall, H. R., Banks, N. G., and Phillips, C. H., 1971, Geologic map of the Sonora Quadrangle, Pinal and Gila Counties, Arizona: U.S. Geological Survey Geologic Quadrangle Map GQ–1021, scale 1:24,000.

Cornwall, H. R., and Krieger, M. H., 1975a, Geologic map of the Kearny Quadrangle, Pinal County, Arizona: U.S. Geological Survey Geologic Quadrangle Map GQ–1188, scale 1:24,000.

——— 1975b, Geologic map of the Grayback Mountain Quadrangle, Pinal County, Arizona: U.S. Geological Survey Geologic Quadrangle Map GQ–1206, scale 1:24,000.

——— 1977 [1978], Geologic map of the El Capitan Mountain Quadrangle, Gila and Pinal Counties, Arizona: U.S. Geological Survey Geologic Quadrangle Map GQ–1442, scale 1:24,000.

Creasey, S. C., 1965, Geology of the San Manuel area, Pinal County, Arizona: U.S. Geological Survey Professional Paper 471, 64 p.

——— 1967, General geology of the Mammoth Quadrangle, Pinal County, Arizona: U.S. Geological Survey Bulletin 1218, 94 p.

Creasey, S. C., and Krieger, M. H., 1977 [1978], The Galiuro Volcanics in southeastern Arizona: U.S. Geological Survey Journal of Research, v. 6, no. 1, p. 115–131.

George, W. O., 1924, The relation of the physical properties of natural glasses to their chemical composition: Journal of Geology, v. 32, no. 5, p. 353–372.

Hawkins, D. B., and Mumpton, F. A., 1976, The world of zeolites, report on international conference on natural zeolites: Geotimes, v. 21, no. 12, p. 25–27.

Hay, R. L., 1966, Zeolites and zeolitic reactions in sedimentary rocks: Geological Society of America Special Paper 85, 130 p.

Heindl, L. A., 1963, Cenozoic geology in the Mammoth area, Pinal County, Arizona: U.S. Geological Survey Bulletin 1141–E, 41 p.

Krieger, M. H., 1968a, Geologic map of the Brandenburg Mountain Quadrangle, Pinal County, Arizona: U.S. Geological Survey Geologic Quadrangle Map GQ–668, scale 1:24,000.

——— 1968b, Geologic map of the Holy Joe Peak Quadrangle, Pinal County, Arizona: U.S. Geological Survey Geologic Quadrangle Map GQ–669, scale 1:24,000.

——— 1968c, Geologic map of the Lookout Mountain Quadrangle, Pinal County, Arizona: U.S. Geological Survey Geologic Quadrangle Map GQ–670, scale 1:24,000.

——— 1968d, Geologic map of the Saddle Mountain Quadrangle, Pinal County, Arizona: U.S. Geological Survey Geologic Quadrangle Map GQ–671, scale 1:24,000.

——— 1974a, Generalized geology and structure of the Winkelman 15-minute quadrangle and vicinity, Pinal and Gila Counties, Arizona: U.S. Geological Survey Journal of Research, v. 2, no. 3, p. 311–321.

——— 1974b, Geologic map of the Black Mountain Quadrangle, Pinal County, Arizona: U.S. Geological Survey Geologic Quadrangle Map GQ–1108, scale 1:24,000.

——— 1974c [1975], Geologic map of the Winkelman Quadrangle, Pinal and Gila Counties, Arizona: U.S. Geological Survey Geologic Quadrangle Map GQ–1106, scale 1:24,000.

——— 1974d [1975], Geologic map of the Crozier Peak Quadrangle, Pinal County, Arizona: U.S. Geological Survey Geologic Quadrangle Map GQ–1107, scale 1:24,000.

——— 1974e [1975], Geologic map of the Putnam Wash Quadrangle, Pinal County, Arizona: U.S. Geological Survey Geologic Quadrangle Map GQ–1109, scale 1:24,000.

———1979, Ash-flow tuffs of the Galiuro Volcanic in northern Galiuro Mountains, Pinal County, Arizona: U.S. Geological Survey Professional Paper 1104.

Krieger, M. H., Cornwall, H. R., and Banks, N. G., 1974, The Big Dome Formation and revised Tertiary stratigraphy in the Ray–San Manuel area, Arizona: U.S. Geological Survey Bulletin 1394–A, p. A54–A62.

Krieger, M. H., Johnson, M. G., and Bigsby, P. R., 1979, Mineral resources of the Aravaipa Canyon Instant Study Area, Pinal and Graham Counties, Arizona: U.S. Geological Survey Open-File Report 79–291, 183 p.

Lipman, P. W., 1965, Chemical comparison of glassy and crystallized volcanic rocks: U.S. Geological Survey Bulletin 1201–D, p. D1–D24.

Shapiro, Leonard, 1967, Rapid analysis of rocks and minerals by a single-solution method, *in* Geological Survey Research 1967: U.S. Geological Survey Professional Paper 575–B, p. B187–B191.

Shapiro, Leonard, and Brannock, W. W., 1962, Rapid analysis of silicate, carbonate, and phosphate rocks: U.S. Geological Survey Bulletin 1144–A, p. A1–A56.

Sheppard, R. A., 1971, Clinoptilolite of possible economic value in sedimentary deposits of the conterminous United States: U.S. Geological Survey Bulletin 1332–B, p. B1–B15.

Sheppard, R. A., and Gude, A. J., 3d, 1964, Reconnaissance of zeolite deposits in tuffaceous rocks of the western Mohave Desert and vicinit, Caligornia, *in* Geological Survey Research 1964: U.S. Geological Survey Professional Paper 501–C, p. C114–C116.

——— 1965, Zeolitic authigenesis of tuffs in the Ricardo Formation, Kern County, California, *in* Geological Survey Research 1965: U.S. Geological Survey Professional Paper 525–D, p. D44–D47.

——— 1968, Distribution and genesis of authigenic silicate minerals in tuffs of Pleistocene Lake Tecopa, Inyo County, California: U.S. Geological Survey Professional Paper 597, p. 1–36.

——— 1969, Diagenesis of tuffs in the Barstow Formation, Mud Hills, San Bernardino County, California: U.S. Geological Survey Professional Paper 597, p. 1–34.

——— 1973, Zeolites and associated authigenic silicate minerals in tuffaceous rocks of the Big Sandy Formation, Mohave County, Arizona: U.S. Geological Survey Professional Paper 830, 36 p.

Sheppard, R. A., Gude, A. J., 3d, and Munson, E. L., 1965, Chemical composition of diagenetic zeolites from tuffaceous rocks of the Mojave Desert and vicinity, California: American Mineralogist, v. 50, nos. 1–2, p. 244–249.

Simons, F. S., 1964, Geology of the Klondyke Quadrangle, Graham and Pinal Counties, Arizona: U.S. Geological Survey Professional Paper 461, 173 p.

Willden, Ronald, 1964, Geology of the Christmas Quadrangle, Gila and Pinal Counties, Arizona: U.S. Geological Survey Bulletin 1161–E, p. E1–E64.

Drake Peak—
A Structurally Complex Rhyolite Center in Southeastern Oregon

By RAY E. WELLS

SHORTER CONTRIBUTIONS TO MINERALOGY AND PETROLOGY, 1979

GEOLOGICAL SURVEY PROFESSIONAL PAPER 1124-E

CONTENTS

ILLUSTRATIONS

TABLES

DRAKE PEAK—A STRUCTURALLY COMPLEX RHYOLITE CENTER IN SOUTHEASTERN OREGON

By RAY E. WELLS

ABSTRACT

The Drake Peak volcanic center of middle Miocene age, located about 25 km northeast of Lakeview, Oreg., is a structurally complex eruptive center that resulted from several episodes of intrusion and extrusion of rhyolite. Two thousand meters of andesite and basalt flows, lahars, and volcaniclastic rocks of late Eocene age, and of basaltic andesite, tuff, and flood basalts of Eocene to middle Miocene age were structurally domed by the piston-like intrusion of a large body of rhyolite. The eruption of rhyolite flows at 14.3±2 million years followed the structural doming, and upper Miocene tuffs and basalt flows lapped against the dome and the rhyolite. A felsitic rhyolite ring intrusion 3 km in diameter, emplaced during the doming, is now exposed in the deeply eroded core of the dome. The rhyolites range in SiO_2 content from 69 to 76 percent and are peraluminous. The nonporphyritic ring intrusion is more silicic than the flows erupted later, which contain up to 23 percent phenocrysts of plagioclase, hypersthene, biotite, clinopyroxene, and quartz. The progressive depletion of Mg, Ca, Sr, Fe, Ti, and Al and the enrichmnet in silicon and rubidium are compatible with the generation of the observed rhyolite types by tapping a compositionally zoned magma chamber.

INTRODUCTION

More than 150 centers of Cenozoic silicic volcanism are indicated on reconnaissance maps of southeastern Oregon (Walker, 1963, 1973; Walker and Repenning, 1965, 1966; Walker and others, 1967; Greene and others, 1972), and the ages of many are reported by MacLeod, Walker, and McKee (1975). The geology and petrology of individual centers, however, are not well known. Many appear to be relatively simple groups of cumulodomes and flows, but a few have more complicated histories involving several episodes of volcanism and large-scale deformation of the underlying volcanic rocks. One of the more complex silicic vents is centered near Drake Peak about 30 km northeast of Lakeview, Oreg. (fig. 1). There, rhyolite of variable composition has been erupted, and several structural domes and a variety of silicic intrusions, including a ring dike 3 km in diameter, are exposed beneath a carapace of rhyolite flows. This report briefly describes the geologic setting, petrography, petrochemistry, structure, and eruptive history of this vent area, which is informally referred to as the Drake Peak volcanic center.

ACKNOWLEDGMENTS

This work was funded in part by Geological Society of America Penrose Grant 1858–74 and by University of Oregon student research grants. The potassium-argon age determinations were made by E. H. McKee as part of an investigation of the geothermal potential of Oregon. N. S. MacLeod and B. H. Baker made helpful comments on earlier versions of the manuscript.

REGIONAL SETTING

The Oregon Basin and Range covers 57 000 km^2 of southeastern Oregon and consists almost entirely of volcanic rocks of Eocene [1] to Holocene age. Post-middle Miocene basalt and rhyolite in a bimodal association cover much of the area. Older Tertiary volcanic rocks consisting of andesite, dacite, and rhyolite are locally exposed beneath the voluminous basalt-rhyolite sequence. Middle Miocene to Holocene normal faulting has created several north-trending grabens where facing escarpments expose up to 2200 m of Tertiary volcanic rocks. Pre-Tertiary rock is exposed in two small areas in the Pueblo and the Trout Creek Mountains near the Nevada border.

Miocene and younger rhyolite domes form two west-northwest-trending belts across southeastern Oregon (Walker, 1973). Domes younger than 10

[1] Ages of epochs used in this report are from Berggren (1972). They are younger than those traditionally used in reports on eastern Oregon, which are based on radiometric ages of mammalian stages (Evernden and others, 1964).

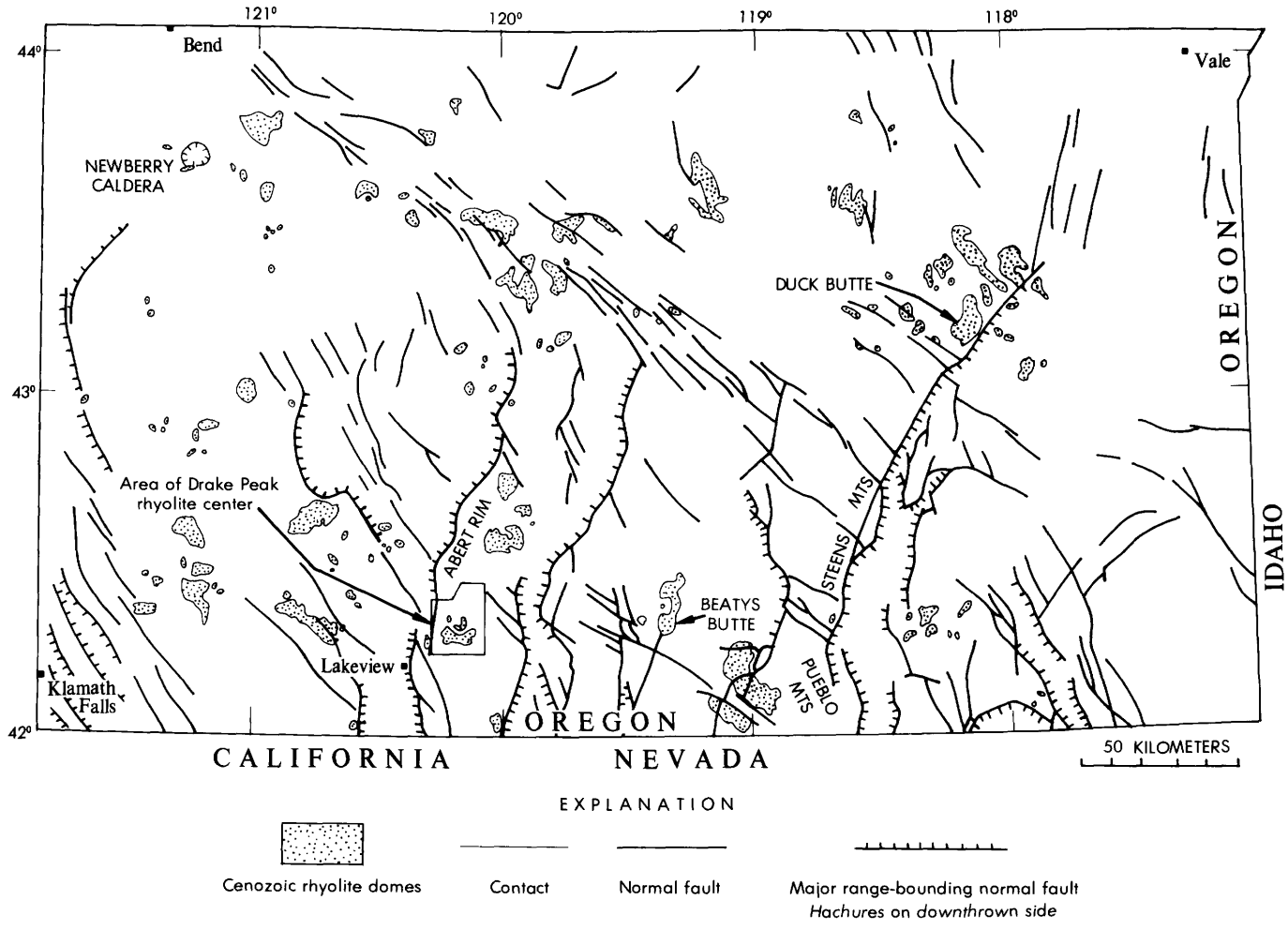

FIGURE 1.—Location map of southeastern Oregon showing area of investigation. Cenozoic silicic domes and faults from Walker and King (1969), Walker (1973), and MacLeod, Walker, and McKee (1975).

m.y. (million years) show a well-defined southeast-to-northwest age progression from approximately 10 m.y. at Duck Butte and Beatys Butte to less than 1 m.y. at Newberry caldera (fig. 1); older domes, mostly about 15 m.y. old, are widespread but are fewer in number than the younger domes and show no age progression. The Drake Peak volcanic center is in the southern belt of domes, and radiometric ages presented here indicate that it belongs to the older group.

The volcanic center is situated near the western escarpment of the north Warner Mountains block and lies southeast of Abert Rim, one of the largest fault scarps in southeastern Oregon. It forms a striking circular group of peaks clustered around the headwaters of Twelvemile and McDowell Creeks. The peaks form two concentric rings 2100–2400 m in elevation separated by a 300- to 600-m-deep circular valley. The outer ring, about 8 km in diameter, consists of fault blocks that dip radially outward. The inner ring, about 3.2 km in diameter, is composed of intrusive rhyolite (fig. 2).

OLDER TERTIARY VOLCANIC ROCKS

Middle Miocene and older volcanic rocks form the structural foundation for the later silicic flows and intrusions of the Drake Peak volcanic center. Miocene structural doming and later erosion have exposed a 2100-m sequence of basaltic and andesitic lava, volcanic breccia, ash-flow tuff, sedimentary tuff, and flood basalt in its core (fig. 3). The three oldest units, informally termed the lower andesitic sequence, the basaltic andesite of Twelvemile Peak, and basalt and andesite of Crook Peak, are exposed only in the strongly uplifted blocks of the structural domes. Oligocene or Miocene tuff and Miocene flood basalt that form the upper part of the foundation volcanic sequence are widely exposed throughout the Abert Rim area.

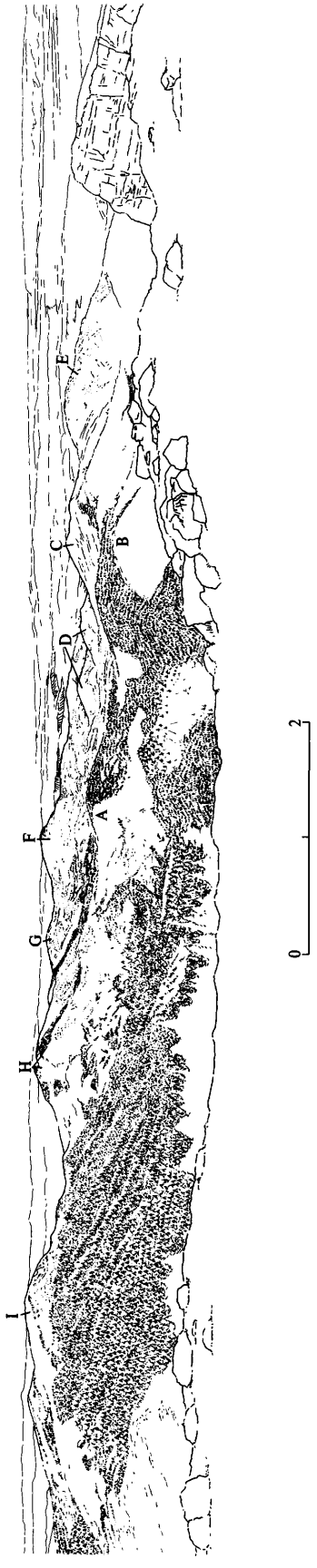

FIGURE 2.—View looking north across Drake Peak volcanic center from summit of Drake Peak. A, B, C, and D represent a rhyolite ring intrusion; E, F, G, H, and I (east flank, Crook, McDowell, Twelvemile, and Light Peaks, respectively) represent outward-dipping blocks of older volcanic rocks that are remnants of a deeply eroded structural dome. Twelvemile (H) and Light Peaks (I) are capped by rhyolite flows erupted after doming.

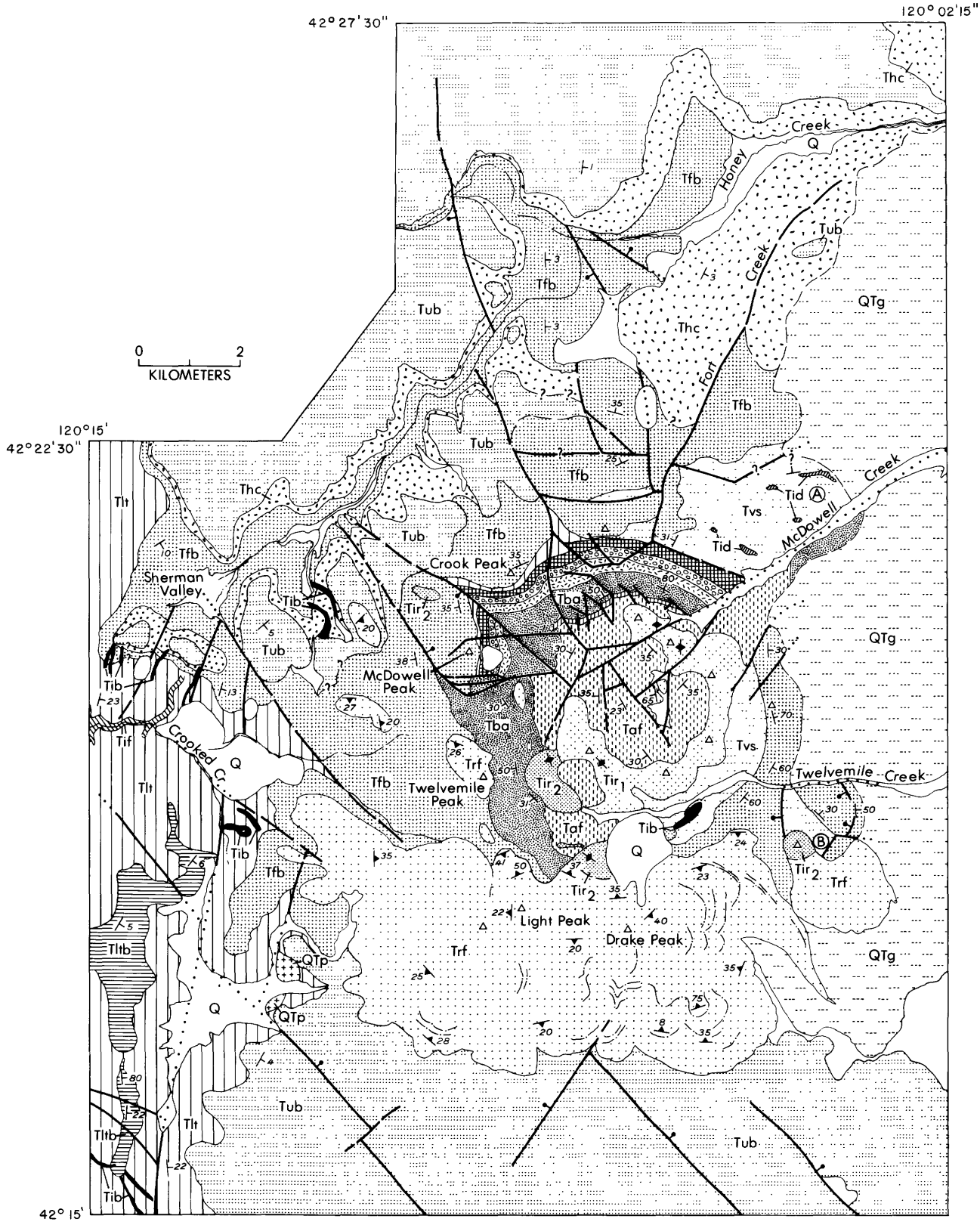

FIGURE 3.—Geologic map of Drake Peak area.

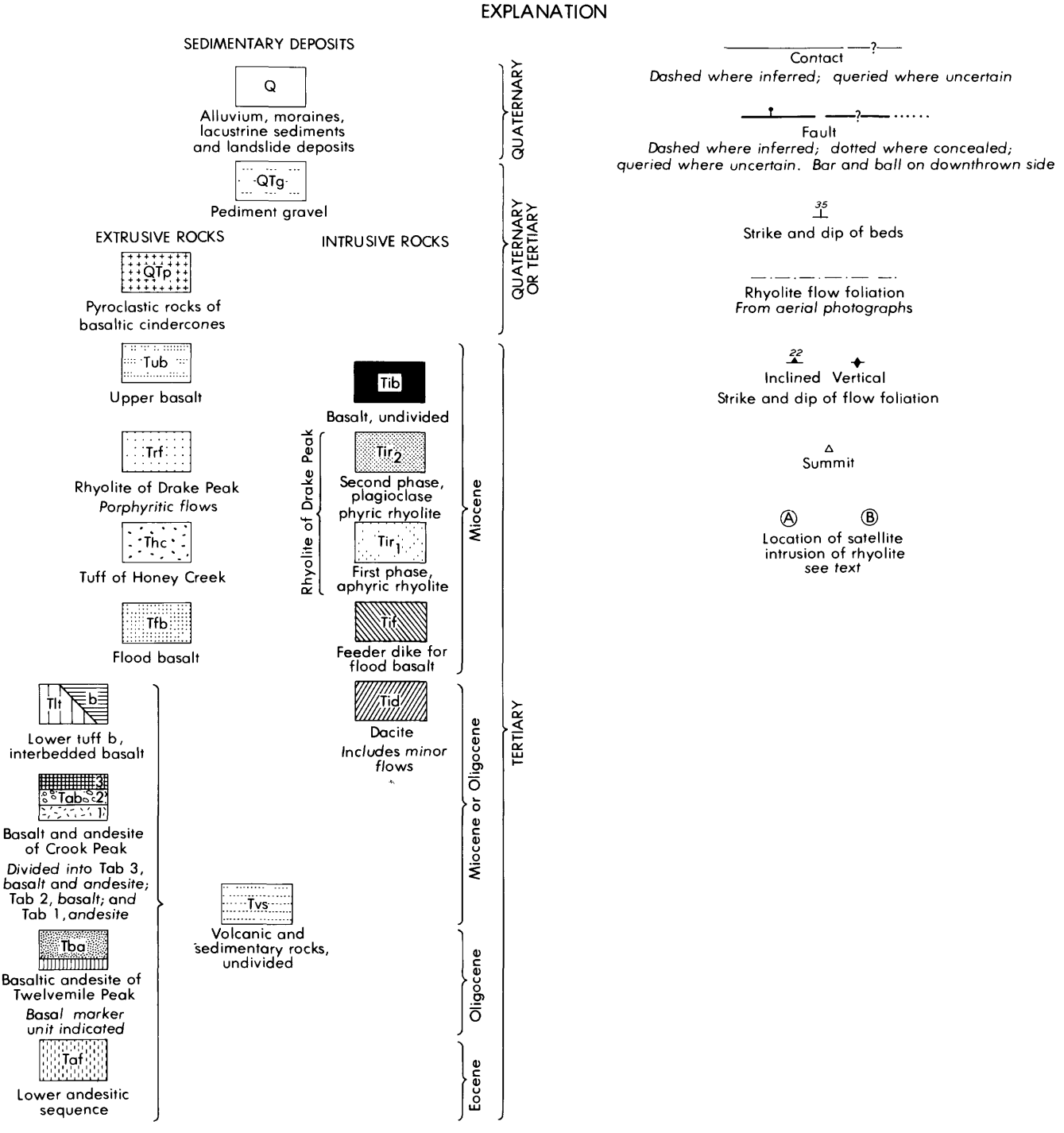

FIGURE 3.—Continued.

LOWER ANDESITIC SEQUENCE

The lower andesitic sequence consists of andesite flows, flow breccia, mudflows, ash-flow tuff, fluvial tuff, conglomeratic sandstone, and minor basalt flows. It crops out over a wide area in the middle of the Drake Peak volcanic center, where 650 m is exposed in the lowest parts of the eroded updomed blocks surrounding the central ring intrusion. Its base is nowhere exposed, so its total thickness is not known. The oldest exposed strata are probably the conglomeratic volcanic arkose and lithic sandstone that crop out along the east flank of the amphitheater inside the central ring intrusion. They are generally very coarse grained and consist of variable

amounts of labradorite, andesitic rock fragments, amphibole, and clinopyroxene and lesser amounts of microcline, muscovite, and polycrystalline quartz. The conglomerate lenses contain well-rounded cobbles of andesite, basalt, and quartzite.

The sedimentary rocks interfinger upsection with hornblende and pyroxene andesite flows and lahars. Andesitic flow breccias and thin basalt flows are sporadically interbedded with the lahars. Fine- to coarse-grained epiclastic tuffs and ash-flow tuffs that crop out near the base of Crook, McDowell, and Twelvemile Peaks form the upper part of the sequence.

A K-Ar age of 40.2±4 m.y. was determined for a hornblende andesite near the base of the exposed sequence (table 1). This age is compatible with those obtained on other older andesitic sequences in the region. A sequence similar to that of the Drake Peak area crops out in the Warner Mountains 90 km to the south in California (Russell, 1928). Axelrod (1966) reports an age of 40 m.y. on an andesite flow low in the central Warner Mountains section, and Duffield and McKee (1974) reported an age of 32 m.y. on andesitic ash-flow tuffs about 450 m above the base of the exposed section in the south Warner Mountains. An older andesitic sequence of similar character exposed in the Paisley Hills 34 km northwest of Drake Peak is intruded by a 33-m.y.-old granodiorite plug (Peterson and McIntyre, 1970). The lower andesitic sequence correlates in part with the Clarno Formation of central Oregon (see K-Ar ages in Enlows and Parker, 1972).

TABLE 1.—*Potassium-argon age determinations from the Drake Peak area, Oregon*

[Potassium-argon dates by E.H. McKee]

Unit and Mineral dated	Hornblende andesite, lower andesite sequence (hornblende)	Rhyolite of Drake Peak; flow (plagioclase)
Field no.	DP-154	DP-108
Latitude	42°20'54"N	42°18'30"N
Longitude	120°07'12"W	120°08'50"W
K_2O (wt. percent)	0.363	0.871 0.910
Radiogenic ^{40}Ar (moles/g)	2.1804×10^{-11}	1.8898×10^{-11}
Percent ^{40}Ar	17.3	15.96
Age (m.y.)	40.2±4	14.3±2

BASALTIC ANDESITE OF TWELVEMILE PEAK

A distinctive basaltic andesite overlies the lower andesitic sequence and forms a thick lenticular accumulation that is well exposed in the upturned blocks of the Drake Peak volcanic center. The unit is about 1000 m thick along the east face of Twelvemile Peak and thins northeastward to about 310 m on the Fort Creek–McDowell Creek divide. Flow units consist of flow breccia and range from 3 to 13 m in thickness. Discontinuous zones of massive lava are common within the flows, and baked soil horizons are found between some flows. Tabular units of black unaltered nonvesicular holocrystalline basalt occur sporadically throughout the unit and probably represent sills intruded into the volcanic pile. Also found are lesser amounts of hornblende andesite and locally thick accumulations of zeolitized red volcanic breccia. The andesite is highly vesicular and porphyritic, averaging 46-percent phenocrysts of milky white plagioclase ($\sim An_{50}$), black clinopyroxene, and red altered olivine. The rocks are pervasively altered, and vesicles and fractures are filled with green clay, calcite, and zeolites.

No similar rocks are exposed on any of the major fault scarps in the vicinity. The absence of exposures outside the complex, even in the deeply incised Crooked Creek canyon only 4 km to the west, suggests that the basaltic andesite is a localized accumulation. The lenticular outcrop pattern and the onlapping of overlying units to the south indicate a possible vent center near Twelvemile Peak.

The age of the basaltic andesite is uncertain. It overlies strata of late Eocene age and is in turn overlain by a varied volcanic sequence over 1000 m thick that separates it from overlying tuffs of middle to late Miocene age.

BASALT AND ANDESITE OF CROOK PEAK

The basalt and andesite of Crook Peak is exposed above the basaltic andesite on Crook and McDowell Peaks. About 530 m is exposed on Crook Peak, and, toward the northeast, the sequence thickens to 720 m. Three subdivisions of nearly equal thickness have been made in the sequence. The lowermost unit consists of red-brown hornblende andesite, gray pyroxene andesite, and reddish-gray olivine basalt flows. Black to greenish-black aphyric (nonporphyritic) basalt making up the middle unit weathers to a distinctive orange, and it is generally without vesicles or flow structures. Gray to purplish-gray aphanitic basalt and olivine basalt form the upper part of the group. Most flows in the upper unit are quite vesicular and display well-developed platy jointing along the flow tops.

A few similar flows are interbedded in the upper Oligocene or lower Miocene lower tuff along the western margin of the area, and the upper part of

the lower tuff overlies the upper andesitic sequence in the upturned blocks of the structural dome. The basalt and andesite of Crook Peak is therefore considered to be of late Oligocene or early Miocene age.

LOWER TUFF

The lower tuff is a widespread composite unit consisting of ash-flow tuff, tuffaceous sediment, and interbedded basalt that is widely exposed west of the Drake Peak volcanic center. The upper 300 m of the lower tuff crops out in the canyons of Crooked Creek and its tributaries. The thickness of the unit decreases eastward, where in the upturned blocks of the dome it is represented by less than 30 m of strata.

The lower tuff is composed primarily of intermediate to silicic ash-flow tuff units. The lower part of the section in Crooked Creek Canyon consists of light-brown lithic tuff, pink crystal-rich welded tuff, and pale-gray vitric welded tuff. They are overlain by several unwelded massive buff to light-brown pumice lapilli ash-flow tuffs at least 65 m thick.

The base of the lower tuff is not exposed in the west half of the study area, but in the east half, where the unit is much thinner, it rests on the basalt and andesite of Crook Peak and possibly also on the basaltic andesite of Twelvemile Peak. The variation in thickness of the unit from west to east suggests that it laps onto the preexisting high of basaltic andesite. Basalt similar to that in the basalt and andesite of Crook Peak is interbedded in the lower tuff in the west part of the study area, which, along with the rapid east-to-west facies change, suggests that the lower tuff may be in part equivalent in age to the basalt and andesite of Crook Peak and somewhat younger than the basaltic andesite of Twelvemile Peak. Plant remains found 2 km west of the study area indicate a late Oligocene or early Miocene age for the lower tuff (Walker, 1960). This tuff unit probably correlates in part with the John Day Formation of central Oregon (Swanson, 1969).

MIDDLE(?) MIOCENE AND YOUNGER VOLCANIC ROCKS

MIOCENE FLOOD BASALT

The most widely distributed unit in the Drake Peak area is a flood basalt sequence similar in appearance and stratigraphic position to the Steens Basalt (Fuller, 1931; Piper and others, 1939) exposed on Steens Mountain, 110 km to the east. This well-exposed flow sequence, up to 600 m thick, caps the tilted blocks of the Drake Peak dome and forms the inner canyon walls along Honey and Little Honey Creeks, north of the volcanic center. The flows are typically less than 6 m thick, and many are 2 to 3 m. The absence of tuffaceous interbeds, soil horizons, and top and bottom flow breccias suggests that the basalt was very fluid and that the flows were erupted in rapid succession. Light-gray ophitic diktytaxitic (crystal-bounded vesicles) olivine basalt is the most common type in the Drake Peak area. Some flows are coarsely porphyritic and contain plagioclase phenocrysts up to 20 mm long. The plagioclase content varies regularly within a flow sequence; coarsely porphyritic flows are overlain by successive flows in which plagioclase becomes less abundant.

The thickness of the flood basalt sequence varies widely within the Drake Peak area. A 610-m section on the east flank of the complex thins and disappears to the southwest, suggesting that the basalt flowed over a surface of considerable relief. The basalt unconformably overlies the basaltic andesite of Twelvemile Peak, lower tuff, and basalt and andesite of Crook Peak.

The geomagnetic polarities of the flood basalt were determined with a portable fluxgate magnetometer. Sections of five to seven flows on McDowell Peak, in Honey and Little Honey Creek canyons, and on the basalt ridge on the east flank of the complex are all reversely polarized. Reversely polarized flow sequences can be traced west to the Abert Rim escarpment, where they presumably correlate in part with a reversely polarized section of 16 flows, described by Watkins (1965). The Steens Basalt, however, exhibits a polarity transition from reversed to normal upsection that has been dated at 15.1 ± 0.3 m.y. (Baksi and others, 1967). The flood basalt of the Drake Peak area is roughly correlative with the Steens Basalt, as it is onlapped by tuffaceous sediments containing a Barstovian (middle Miocene) fauna in Honey Creek canyon (Walker, 1960) and is underlain by the upper Oligocene or lower Miocene lower tuff. It may or may not be of the same reversed-polarity epoch as the lower Steens Mountain section.

RHYOLITE OF DRAKE PEAK

The rhyolite of Drake Peak consists of a differentiated suite of rhyolite intrusions and flows that were emplaced into or erupted from the Drake Peak volcanic center.

FLOWS

The flows consist mostly of massive or flow-foliated light-gray to black porphyritic vitrophyre and stony rhyolite containing plagioclase, biotite, and hypersthene phenocrysts. Potassium-argon dating of plagioclase from a flow sample gives an age of 14.3± 2 m.y. (table 1). The flows form a massive apron or wedge of coalescing lobes that cover about 29 km^2 on the southern flank of the structural dome. Erosion has extensively modified the shape of the flow mass, but several flow lobes still persist. The main rhyolite body rests on the upthrown blocks of the foundation volcanic sequence and has 750 m of relief from base to top. The average thickness of the main body is difficult to determine because of the irregularities of the underlying topography, but rough estimates on the large southeastern lobe suggest a thickness there of approximately 300 m. The absence of visible stratigraphic breaks in the main rhyolite mass suggest that it is the product of a single eruption or a rapid series of eruptions.

Outliers of rhyolite on the west flank of the dome are erosional remnants of a formerly larger body that covered the west slope of the structural dome. The largest detached mass, about 100 m thick, caps Twelvemile Peak. Two other lobate masses, about 30 m thick, lie about 2 km northwest of Twelvemile Peak. A separate flow covering about 2.6 km^2 lies slightly east of the main rhyolite edifice and apparently originated from a separate vent. On the northeast side of the dome are two small flow remnants associated with small silicic intrusions.

The rhyolites unconformably overlie the structurally domed foundation and were erupted after doming occurred. The base of the rhyolite is at widely different elevations around the rim of the outer ring, indicating that the rhyolite flowed over a terrain of differentially uplifted (or eroded) blocks having considerable relief.

Viscous flow has produced a variety of internal structures. Flow layering is conspicuous and generally occurs throughout the flow mass except where obscured by later devitrification. A thick weathered zone obscures much of the flow geometry on the west slope of the dome, but on the east slope it is well exposed and suggests a flow direction south and east away from Drake Peak. Moderate- to steep-dipping ramp structures are well exposed on the distal parts of the flow lobes. On Light Peak, large east-west-trending synformal flow folds, over 100 m wide, suggest channelized flow, possibly through gaps between tilted blocks of the structural dome. A source east of Light Peak and north of Drake Peak is suggested by the progressive steepening of flow layering to vertical in that area.

The cooling zones in a rhyolite flow described by Christiansen and Lipman (1966) are also developed in the Drake Peak flows. Ideally, the zones include a surface layer of pumiceous breccia and flow-layered pumice, an envelope of massive flow-layered vitrophyre, a core of massive flow-layered devitrified rhyolite, and a basal flow breccia of vitrophyric and pumiceous blocks. Erosion has stripped the pumiceous surface layer from the flows, exposing the thick envelope of massive vitrophyre. Extensive erosion between Light and Drake Peaks has exposed the devitrified rhyolite core. A basal flow breccia consisting of about 35 m of flow-banded cobbles and boulders imbedded in a fine-grained white matrix is exposed on the ridge north of Light Peak where the flow inclines steeply upward. The contact of the breccia and the underlying flood basalt is also exposed there. Other breccia zones have been observed in the flows, but they differ from the basal breccia and were not formed by successive eruptions of rhyolite onto previously cooled flows. The most common intraflow breccia contains distorted augenlike rhyolite clasts in a red glassy matrix and is probably the result of reincorporation of solid fragments into the hot flow interior. Vertical breccia dikes about 15 m thick on the north face of Drake Peak just below the summit consist of flow-banded fragments up to 150 mm across embedded in a finely divided white glassy matrix. The dikes are near a probable vent and may have been created by violent degassing through the rhyolite pile.

INTRUSIONS

At least 13 separate rhyolite intrusions are exposed within the Drake Peak volcanic center; the largest is the felsitic ring intrusion exposed in its eroded core. The semicircular ring has an east-west diameter of 3 km and a north-south diameter of 3.3 km. Remnants of the intruded lower andesitic sequence still cling to the flanks of the intrusion resulting in an irregular contact. The rhyolite is not well exposed; extensive jointing produces widespread talus that effectively obscures outcrops. The few good exposures consist of sugary light-gray to white aphyric felsite. In some areas, flow banding is well developed, and, where exposed in outcrop, it is generally vertical. Several smaller intrusions of identical aphyric felsite in the interior of the complex are probably attached to the main felsite mass of the ring intrusion. The felsite consists of a spherulitic interlocking mat of quartz and alkali

feldspar lightly dusted with clay alteration products; it is texturally and mineralogically quite different from the flows that cover the flanks of the structural dome.

Intrusions west and south of the ring intrusion are similar to the flows. They contain phenocrysts of plagioclase, hypersthene, and biotite in a devitrified microlitic matrix. The intrusion at the base of Twelvemile Peak has a breccia zone along its contact with the ring intrusion that incorporates rhyolite fragments similar to those of the ring.

Small intrusions on the northeast and southeast flanks of the main structural dome fill the source vents for small flows isolated from the main rhyolite mass. The northeast intrusions are plagioclase-oxyhornblende(?) dacites that have deformed the surrounding country rock. Onlapping of the Miocene flood basalts onto the deformed rocks indicates that the dacites are older than the rhyolite.

TUFF OF HONEY CREEK

The tuff of Honey Creek is named for outcrops along Honey Creek from Sherman Valley east to its confluence with Snyder Creek, about 7 km northeast of the Drake Peak volcanic center. It consists of silicic tuffaceous sediments, welded tuff, and a few intercalated basalt flows that surround and apparently lap against the Drake Peak structural dome. The tuff of Honey Creek overlies the Miocene flood basalts with a slight angular unconformity and is in turn overlain by several widespread basalt flows. Near the volcanic center the tuffaceous rocks are very coarse grained crudely stratified sandstone containing fragments of flow-banded vitrophyre, felsite, and diktytaxitic ophitic basalt in a matrix of silicic glass shards. In places, the tuff contains large boulders of basalt apparently derived from the uplifted Miocene flood basalts of the structural dome.

Welded tuff occurs at several localities, the most prominent being an extensive rimrock exposure 5 km northeast of the complex on the south side of Honey Creek. Isolated outcrops also occur at the 2200-m level on the north shoulder of Twelvemile Peak and on either side of Honey Creek about 2 km east of Sherman Valley. All are eutaxitic vitrophyre containing partially collapsed pumice fragments and phenocrysts of sanidine, plagioclase, or anorthoclase, and amphibole. The welded tuff units are thin (less than 6 m) and mineralogically unlike the rhyolite of Drake Peak, indicating they originated outside the Drake Peak area.

At greater distances from the volcanic center, thin-bedded pumicite and friable fine-grained tuff rich in plant fragments suggest lacustrine or floodplain deposition. The coarse debris forming an apron around the Drake Peak center was derived from erosion of the structural dome and is younger than the intrusive activity in the dome. However, the welded tuff remnant high on Twelvemile Peak must have been uplifted by the doming, indicating that part of the tuff of Honey Creek predates the Drake Peak volcanic center. Vertebrate remains collected near the confluence of Honey and Snyder Creeks indicate a Barstovian (middle Miocene) age for the tuff of Honey Creek (Walker, 1960).

UPPER BASALT

Remnants of an extensive sheet of rim-capping basalt, termed the upper basalt in this report, are widely exposed on the upland surfaces surrounding the Drake Peak volcanic center. The unit is from 3 to 60 m thick, with individual flows averaging about 3 m. Most flows are highly vesicular and range from light-gray diktytaxitic olivine basalt to platy black aphanitic basalt. The upper basalt overlies the tuff of Honey Creek and the Miocene flood basalts with a slight angular unconformity, and in sections where the intervening tuff is not exposed, the two basalts are virtually indistinguishable. Paleomagnetic studies by Larson (1965) suggest that in the areas north and east of the Drake Peak dome, the upper basalt may be distinguished from the reversed Miocene flood basalts by its normal polarity. Field polarity checks of the upper basalt at several localities (Mud Creek Campground, the Drake Peak Lookout Road, isolated exposures south of Sherman Valley, exposures north and south of Honey Creek, and rimrock north of Vee Lake) all indicate the basalt is normally polarized.

The upper basalt is in part equivalent to the "vesicular basalt flows" and "basalt," as mapped by Walker (1963) in the Klamath Falls quadrangle, for widespread rim-forming basalt generally having dips of less than 5°. It is also equivalent to Larson's (1965) upper basalt and young upper basalt, which he correlated eastward as far as the Plush escarpment.

The upper basalt in the Drake Peak area overlies the middle or upper Miocene tuff of Honey Creek and forms the uppermost volcanic unit in the section. It apparently flowed around the high ground of the Drake Peak volcanic center along its northern and southern margins and consequently is younger than the rhyolite of Drake Peak. About 5 km northeast

of the Drake Peak area, a welded ash-flow tuff correlated by Larson (1965) with the Danforth Formation of Piper, Robinson, and Park (1939) overlies the upper basalt. Several ash-flow tuff units recognized within the Danforth Formation range in age from 9.2 to 6.8 m.y., and the tuff of Double O Ranch (6.8 m.y.) is the most likely candidate for correlation with Larson's (1965) ash-flow tuff (Greene and others, 1972; Greene, 1973). The upper basalt must then be of middle or late Miocene age.

TERTIARY BASALT INTRUSIVE ROCKS

Basaltic dikes are locally abundant along the western margin of the map area. Medium- to fine-grained olivine-plagioclase-phyric (porphyritic) dikes, up to 50 m thick, intrude the tuff of Honey Creek and probably represent feeders for the rim-capping middle or late Miocene upper basalt. A complex of dikes and sills of probable middle Miocene age crops out along Crooked Creek and along Abert Rim, 2 km west of the map area. A differentiated sill, at least 70 m thick, occupies the bottom of the canyon, and a large olivine-phyric ophitic dike connected to the sill cuts through the lower tuff but does not cut the tuff of Honey Creek. These large intrusions are petrographically similar to the middle Miocene flood basalts and probably represent feeders for the flows.

SURFICIAL DEPOSITS

A variety of surficial deposits occur in the Drake Peak area, but they are not discussed in any detail in this report. They include the following: Pliocene or Pleistocene pediment gravel veneering a high-level erosion surface east of the dome; Pleistocene glacial moraines on the north side of Drake Peak; lacustrine deposits in unusual rimmed basins formed on flood basalt; large Pleistocene(?) landslide deposits, especially along Crooked Creek; and Holocene sediments forming alluvial flats where local base levels have been maintained by resistant basaltic units.

PETROGRAPHY AND PETROCHEMISTRY OF THE RHYOLITE OF DRAKE PEAK

PETROGRAPHY

The rhyolite flows contain 10 to 23 percent phenocrysts of plagioclase, hypersthene, and biotite and minor amounts of quartz, amphibole, clinopyroxene, and opaque minerals in a microlitic or vitrophyric matrix. The modal composition of 27 samples is 83 percent groundmass, 13 percent plagioclase, 1 percent each of biotite and hypersthene, 0.7 percent opaque minerals, and less than 0.2 percent each of quartz, amphibole, and clinopyroxene. Zoned plagioclase, An_{38-50}, is ubiquitous and forms isolated euhedral laths and glomeroporphyritic clots up to 10 mm across, with common honeycomb resorption in the more calcic zones. Both normal and oscillatory zoning are common. Hypersthene forms strongly pleochroic subhedral to euhedral prisms up to 1 mm long and also occurs as microlites in the groundmass of some samples. Biotite occurs in nearly all samples as isolated plates up to 1 mm across. Commonly it is strongly resorbed and rimmed or completely replaced by granular iron oxides. Quartz occurs as rare, strongly resorbed, spherical grains in a few samples. Sparse phenocrysts of light-green clinopyroxene, green euhedral amphibole, and opaque minerals occur in a few samples. Glomeroporphyritic clots of plagioclase, hypersthene, clinopyroxene, and opaque minerals are common. Groundmass textures are hyalopilitic to trachytic, with oligoclase microlites typically forming 50 percent of the groundmass.

The mafic mineral assemblages vary among the rhyolite flows and intrusions. The major part of the main flow mass is hypersthene+biotite rhyolite, as are several of the intrusions south and west of the ring intrusion. The two detached flow lobes on the northwest side of the volcanic center are hypersthene rhyolite containing little or no biotite. In contrast, the isolated flow on the southeast flank consists of biotite rhyolite containing no hypersthene. A small intrusion just east of the glacial moraine is also composed of biotite rhyolite with minor amphibole. The central ring and associated intrusions contain no mafic phases. The differences in the mafic phenocryst assemblage may be controlled by variations in partial pressure of H_2O or by the temperature of the magma. The sequence of eruption, determined from field relations, suggests that the aphyric rhyolite was erupted first and was followed by the biotite±amphibole rhyolite and finally by the hypersthene+biotite rhyolite. This seems consistent with the successive tapping of hotter magmas, perhaps representing deeper levels of a vertically zoned magma chamber.

PETROCHEMISTRY

Thirteen samples representing a variety of rhyolite types were analyzed for major and selected trace elements (table 2). The rhyolite flows and intrusions are peraluminous and have K_2O in excess of Na_2O. The major-element chemistry is comparable to some of the older domes (5–10 m.y.) described by MacLeod, Walker, and McKee (1975) in southeastern Oregon, although Ti, Ca, and Mg are somewhat more

TABLE 2.—*Major-element and normative compositions, in percent, of the rhyolite of Drake Peak*

[Chemical analyses by x-ray fluorescence methods of Norrish and Hutton (1969); Na_2O by INAA methods of Gordon and others (1968). Analyst: R.E. Wells]

Sample no.	83	103	103A	109	112	122	125	131	134	139	144	141	149	205
Major oxides (weight percent)														
SiO_2	71.6	72.2	72.3	69.3	69.6	70.6	70.2	72.1	74.6	73.6	75.5	72.3	76.5	-
Al_2O_3	15.2	14.7	14.6	14.3	14.4	14.6	14.8	14.4	13.4	13.7	13.4	14.1	13.6	-
[1]Fe_2O_3	2.3	2.6	2.2	2.5	2.4	2.1	2.5	2.3	1.6	1.7	.51	2.2	.38	-
MgO	1.2	.90	.74	.88	.79	.57	.60	.40	.52	.53	.29	.8	.21	-
CaO	1.8	1.9	1.8	1.9	1.9	1.8	1.9	1.6	1.2	1.3	.85	1.8	.81	-
Na_2O	3.7	3.8	4.0	3.8	3.7	4.1	4.0	3.8	3.5	3.7	3.9	3.6	3.9	-
K_2O	4.6	4.4	4.6	4.6	4.7	4.5	4.6	4.7	4.9	4.7	4.6	4.5	4.7	-
TiO_2	.41	.40	.40	.40	.40	.39	.42	.38	.28	.28	.08	.36	.10	-
MnO	.05	.05	.06	.07	.06	.06	.06	.05	.05	.03	.02	.06	.04	-
P_2O_5	.20	.14	.18	.13	.13	.11	..14	.11	.08	.07	.03	.13	.00	-
[2]Loss	.54	.65	.85	2.2	1.9	.53	.56	.57	.52	.61	.56	.99	.56	-
Total	101.60	101.74	101.73	100.05	99.90	99.36	99.78	100.41	100.65	100.22	99.74	100.84	100.80	-
Catanorms[3]														
q	24.4	24.8	24.4	23.9	23.3	23.3	22.9	26.0	29.2	28.3	30.8	27.0	31.2	-
or	27.0	26.1	27.2	28.0	28.7	27.1	27.4	27.8	29.3	28.1	27.7	27.0	27.8	-
ab	32.9	34.1	35.3	34.0	34.0	37.0	36.0	34.5	32.0	33.6	35.4	33.0	35.2	
an	7.8	8.8	8.0	8.7	8.6	8.3	8.5	7.3	5.7	6.2	4.1	8.0	4.0	-
cor	1.6	.5	.3	.3	.2	.7	.3	.5	.3	.3	.6	.5	.6	-
en	3.3	2.4	2.0	2.0	2.2	1.6	1.7	1.1	1.5	1.5	.9	2.1	.6	-
fs	1.4	1.6	1.3	1.5	1.5	1.2	1.5	1.4	1.0	1.0	.3	1.4	.2	-
hy	4.7	4.0	3.3	3.5	3.7	2.8	3.2	2.5	2.5	2.5	1.1	3.5	.8	-
mt	.7	.8	.7	.7	.7	.6	.8	.7	.5	.5	.2	.7	.1	
il	.6	.6	.5	.6	.6	.6	.6	.5	.4	.4	.1	.5	.1	-
ap	.4	.3	.4	.3	.3	.21	.3	.2	.1	.1	.04	.3	-	-
[4]Diff. Index	84.3	85.0	86.9	85.5	86.0	87.4	86.4	88.3	90.5	90.0	93.8	86.6	94.3	
Trace elements (parts per million)														
Rb	53	-	68	55	60	61	-	62	70	72	99	61	100	100
Sr	216	-	176	273	278	268	-	252	165	167	25	270	56	50
Zr	133	-	105	154	160	162	-	160	85	90	36	160	60	60
Y	10	-	15	14	18	16	-	17	-	-	-	19	18	18
Nb	7	-	8	7	9	8	-	9	-	-	-	11	7	10

[1]All iron as Fe_2O_3.
[2]Loss on Ignition.
[3]Fe^{3+}/Fe^{2+} set at 0.4 for normative calculations.
[4]D.I. of Thornton and Tuttle (1960).

Sample	Sample localities:	Quadrangle:
83	42°18'00"N;120°07'10"W	Drake Peak 7½'
103	42°20'10"N;120°08'23"W	Crook Peak 7½'
103A	42°20'10"N;120°08'25"W	do.
109	42°18'30"N;120°08'50"W	do.
112	42°18'50"N;120°09'00"W	do.
122	42°18'10"N;120°07'23"W	Drake Peak 7½'
125	42°18'18"N;120°07'22"W	do.
131	42°18'46"N;120°05'54"W	Drake Peak 7½'
134	42°19'02"N;120°06'45"W	do.
139	42°19'50"N;120°05'00"W	do.
144	42°19'16"N;120°07'30"W	Crook Peak 7½'
141	42°18'46"N;120°07'54"W	do.
149	42°19'40"N;120°06'56"W	Drake Peak 7½'
205	42°21'36"N;120°06'45"W	do.

abundant for a given SiO_2 content in the rhyolite of Drake Peak.

The absence of potassium feldspar and the general paucity of quartz result from the relatively high calcium content of the magma. The normative bulk compositions of the rhyolite are plotted in the Q–Ab–An–Or system in figure 4. The samples contain approximately 5 to 10 percent normative An and plot in the plagioclase field well above the two-feldspar surface. The rare, strongly resorbed quartz phenocrysts indicate that initial crystallization began at moderate crustal depths and higher water pressures, as inferred from Tuttle and Bowen's (1958) studies in the Q–Ab–Or–H_2O system. Resorption of quartz occurred when pressure was released, probably during the rise of the magma to shallower crustal levels.

When weight-percent oxides of the rhyolite of Drake Peak are plotted against the Thornton-Tuttle Differentiation Index (D.I.) (Thornton and Tuttle, 1960) (fig. 5), the compositions fall into three groups that are consistent with groupings defined in the field. The most differentiated rhyolites (D.I. ~94) are those of the central ring intrusion, which on the basis of field evidence were the first to be emplaced. The two samples with intermediate indices (D.I. ~90) are from a peripheral intrusion southeast of the main structural dome and a small isolated intrusion south of the central ring. The direction of the flow from the southeast intrusion suggests that it was emplaced after the formation of the main structural dome. Those samples with indices of 84 to 88 are from the main flow mass on the south side of the volcanic center, which was probably the last rhyolite body to be erupted.

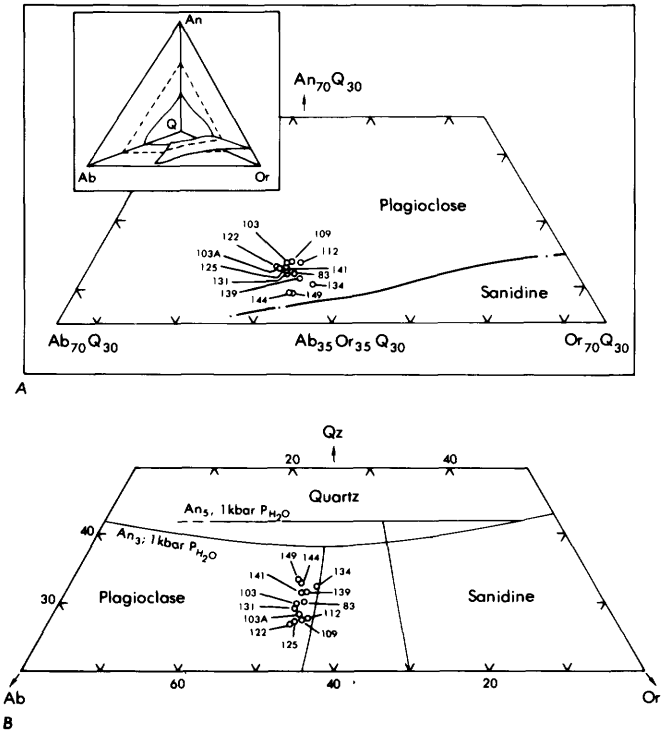

FIGURE 4.—Normative compositions of rhyolite of Drake Peak plotted in Q–Ab–An–Or system. *A*, Compositions of rhyolite of Drake Peak plotted on Q_{30} plane in Q–Ab–An–Or system at $P_{H_2O}=P_{total}=1$ kbar. Position of plagioclase-sanidine cotectic is from James and Hamilton (1969). Schematic Q–Ab–An–Or system (after Carmichael and others, 1974) shown in inset, with dotted line indicating plane of projection. *B*, Rhyolite compositions plotted on base of Q–Ab–An–Or system; conditions as in *A*. Cotectics for systems with 3 and 5 percent An component from James and Hamilton (1969). Compositional trend follows isobaric fractionation path as inferred from Tuttle and Bowen (1958).

The regular variation in major-element chemistry is complemented by a smooth variation in abundances of selected trace elements with D.I. (fig. 5*B*). Strontium is relatively abundant, and Rb/Sr increases with D.I. from about 0.2 to 4. This ratio is an order of magnitude less than in some other high-silica rhyolites from the Basin and Range Province (Noble and others, 1972) and indicates that the rhyolite of Drake Peak has not undergone extreme fractionation. The major- and trace-element compositions correlate directly with an observed phenocryst assemblage of plagioclase, pyroxene, biotite, opaque minerals, and zircon that constitutes up to 23 percent of the later rhyolite flows. The eruption of progressively less differentiated rhyolite with increasing crystal content is comparable to the inverted compositional zonation commonly observed in ash-flow sheets (Lipman, 1966).

Although the mineralogical and chemical variations at Drake Peak are qualitatively consistent with differentiation by crystal fractionation, other processes may be responsible for the compositional zonation of the magma chamber. Hildreth (1976) demonstrated compositional zonation in the Bishop Tuff (from the Long Valley caldera in eastern California) that cannot be explained by crystal fractionation models. He postulated a process of thermogravitational diffusion to account for observed compositional gradients in large rhyolite magma bodies.

Structural relations in the Drake Peak volcanic center require the existence of a large magma body beneath it. The chemical variation in the rhyolite probably resulted from differentiation within a simple magma chamber rather than from the production of several physically and chemically discrete magmas from separate sources.

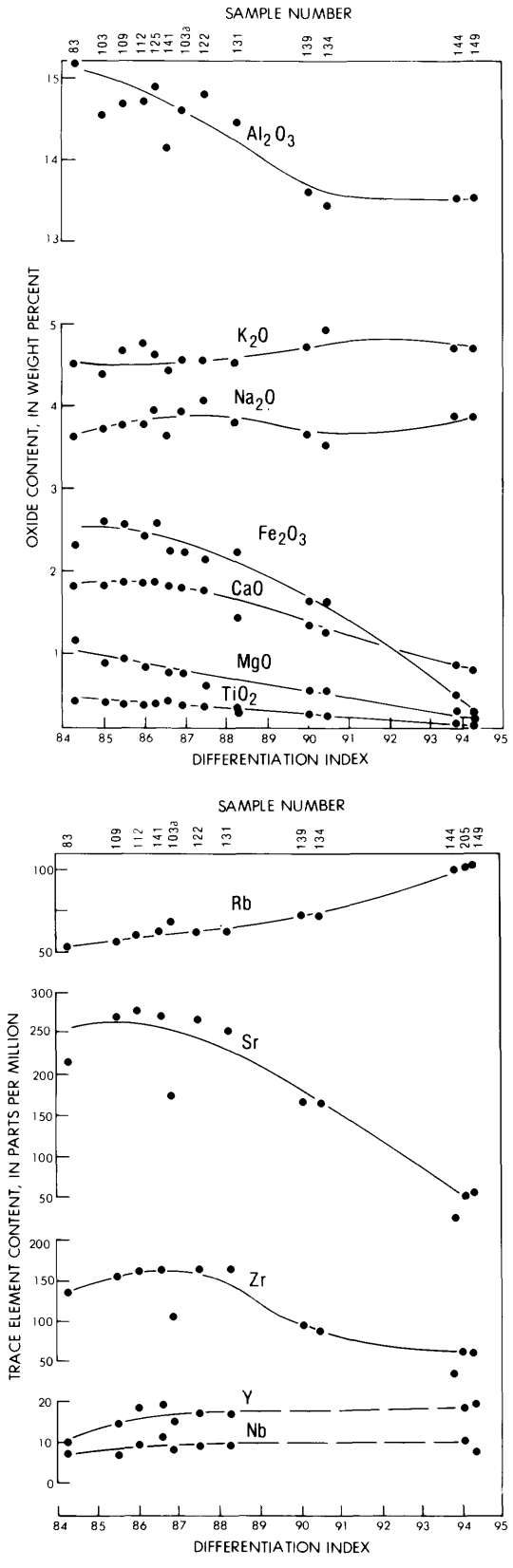

STRUCTURE OF THE DRAKE PEAK VOLCANIC CENTER

DRAKE PEAK DOME

The largest of the three structural domes in the Drake Peak volcanic center is about 9 km across at its base, and the felsitic ring intrusion is exposed in its deeply eroded core. About 1600 m of strata has been stripped from the domal core, and remnant blocks of the foundation volcanic rocks form a ring of hills with quaquaversal dip slopes. Radial faults have broken the dome into several structural blocks. McDowell Peak, Crook Peak, and smaller blocks east of Crook Peak are bounded by radial faults, and McDowell Creek, Fort Creek, and Twelvemile Creek follow radial fault zones for long distances. Displacements observed across the faults indicate dip-slip and rotational movement. Radial faults such as those bounding McDowell Peak are normal faults having a small component of rotational movement away from the center of the dome. Others like the McDowell Creek fault and the east bounding fault of the Crook Peak block have a large component of rotational movement, and adjacent blocks commonly dip between 60° and 80° away from the center of the dome. In the core of the dome, a compound graben formed by closely spaced block faults has been complicated by the intrusion of the rhyolite ring.

The fault pattern of the Drake Peak dome is the result of extensional failure of the foundation rocks during their doming and stretching by the vertically rising rhyolite magma. The fault pattern is analogous to the pattern over salt domes, where extensive radial and normal faulting occurs in response to the diapiric rise of salt. Although tensional stresses dominated the early stages of dome formation, the eventual rise of magma into the dome displaced the overlying blocks upward and outward from the intrusive body. The rotational displacement of the foundation volcanic sequence to nearly vertical attitudes and the incremental outward and upward displacement of units adjacent to the intrusion are the result of forceful intrusion of magma rather than the tensional collapse across the domal crest. The

FIGURE 5.—Major and trace element compositions of rhyolite of Drake Peak plotted against Differentiation Index (Thornton and Tuttle, 1960). *A*, Weight percent major-element oxides of rhyolite of Drake Peak plotted against Differentiation Index. *B*, Trace-element concentrations of rhyolite of Drake Peak plotted against Differentiation Index.

limited, nearly circular region of doming is consistent with rise of a roughly cylindrical magma body rather than a body of broadly conical shape.

OTHER DOMAL STRUCTURES IN THE DRAKE PEAK AREA

An intrusion of dacitic magma 4 km northeast of the Drake Peak dome (location A on fig. 3) has deformed the older Tertiary volcanic rocks but apparently has not deformed the Miocene flood basalts. The flood basalt unconformably overlies strata that strike parallel to the intrusive contacts and dip more than 30°. Also unconformably overlying pre-middle Miocene strata are remnants of dacite flows presumably erupted from one of the small plugs in the area.

On the southeast flank of the Drake Peak dome, a satellite intrusion of rhyolite (location B on fig. 3) has updomed the foundation volcanic rocks in an unusual manner. A block of the overlying strata has been moderately tilted to the east where it meets steeply east-dipping strata along a hinge line concavely curved towards the intrusion. The structure is interpreted as a monoclinal flexure, with the uplifted block analogous to a trapdoor hinged along the flexure and open to the west. The rhyolite that erupted onto the surface preferentially flowed southeast, suggesting that the southeast dome may have formed on the flank of the preexisting Drake Peak dome.

ORIGIN OF THE CENTRAL RING INTRUSION

The ring intrusion is 3 km in diameter and consists of a uniform felsitic rhyolite having vertical or nearly vertical flow foliation in all observed outcrops. The intrusive contact is not well exposed, but the inner contact apparently dips toward the center and the outer contact away from the center of the ring. The ring intrusion itself does not seem large enough to account for the observed scale of doming. The large-scale deformation accompanying the intrusion suggests that the rhyolite ring and associated intrusions of similar composition are part of a larger buried mass. The block-faulted country rock in the center of the dome is thus interpreted as a relatively thin roof covering the core of the intrusion.

The structural setting of the ring intrusion is somewhat different from those of ring intrusions in large central igneous complexes. Most ring dikes are associated with cauldron subsidence of several thousand meters (Billings, 1945; Smith and Bailey, 1968; Roberts, 1970), but in the Drake Peak center there is no evidence for extensive cauldron subsidence in connection with the ring intrusion. The structural doming argues for the forceful emplacement of the intrusion under excess magma pressure, with tensional failure along arcuate, inward-dipping fractures occurring above the intrusive mass. The rising magma invaded the tensional fracture zones and probably enlarged them by explosively venting to the surface. Piecemeal stoping apparently was not an important intrusive mechanism, judging from the absence of xenolithic material in the rhyolite. Minor subsidence in the center of the dome may also have contributed to the formation of the ring dike. Venting to the surface and the resultant reduction of magma volume may have allowed the center of the dome to sag into the magma, leaving an annular ridge of magma between the subsiding central blocks and the periphery of the magma chamber (see Smith and Bailey, 1968, p. 656).

BASIN-AND-RANGE STRUCTURE IN THE DRAKE PEAK AREA

Two sets of normal faults of moderate displacement occur in the area; the dominant set trends N. 15°–45° W., and a subordinate set trends N. 10–45° E. Most faults offset the upper Miocene upper basalt, but some earlier faults in Honey Creek Valley displace rocks no younger than the middle Miocene flood basalts. North of the volcanic center the middle Miocene flood basalts dip 3° E., and the upper basalt dips 1.5°. The intervening tuff of Honey Creek thins to the west against the tilted Miocene flood basalts, indicating some of the displacement on the faults is at least as old as middle Miocene. Throughgoing regional faults are absent in the Drake Peak volcanic center, although it is somewhat older than most of the regional faulting. It is possible that most of the regional stress was taken up in readjustments along the many preexisting faults in the volcanic center. The apparent faulting of the upper basalt northwest of McDowell Peak may be the result of reactivation of the radial faults bounding McDowell Peak. Reactivation of faults along Fort and McDowell Creeks may also explain the radial faults that extend as much as 8 km from the volcanic center.

SUMMARY

The Drake Peak volcanic center is a structurally unusual vent complex that has undergone several periods of shallow intrusive activity, structural doming, and eruption of rhyolite flows. Exposed in its eroded domal core is a 2000-m section of upper

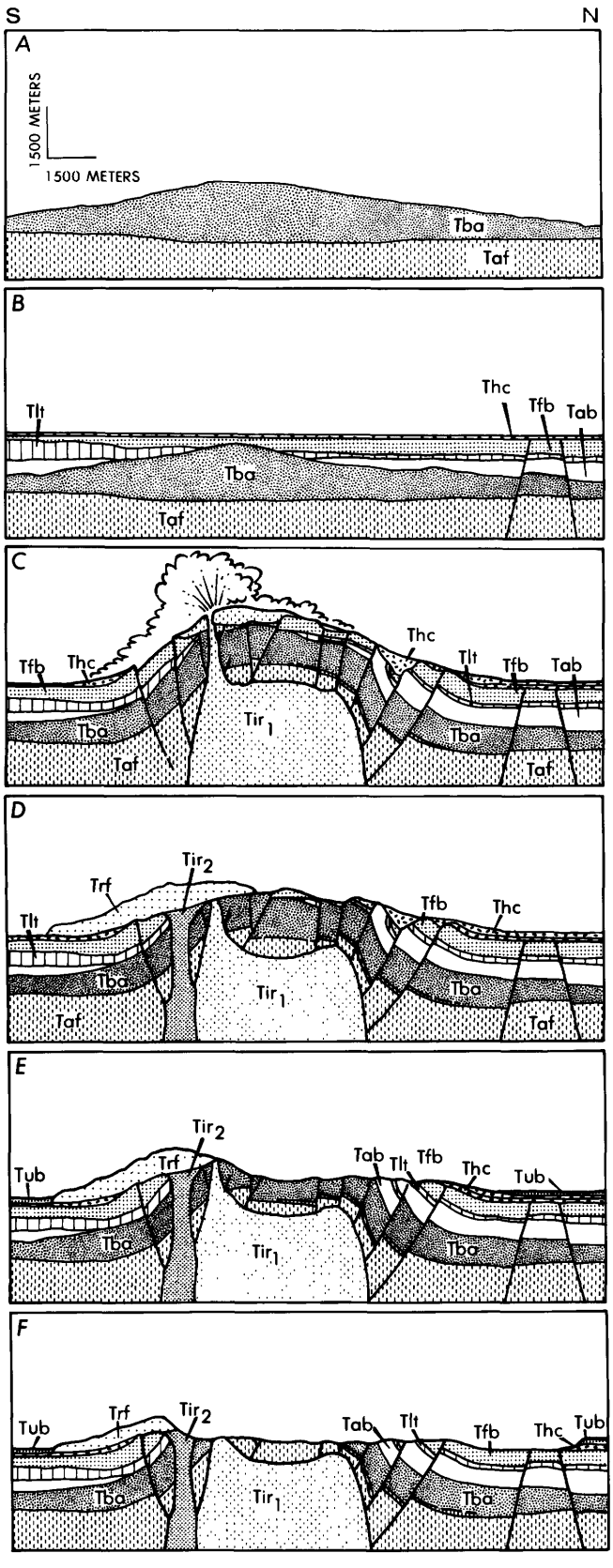

Eocene to middle Miocene volcanic rocks that records the early volcanic history of the area. An interpretation of the volcanic and structural history of the Drake Peak center is shown diagrammatically in figure 6.

A variety of plagioclase-phyric and aphyric rhyolites ranging from 69 to 76 percent SiO_2 were intruded into or erupted from the vent complex. They form a differentiated sequence in which the last flows to be erupted have the most crystals and are the least differentiated. The rhyolites were probably erupted from a compositionally zoned magma chamber.

REFERENCES CITED

Axelrod, D. I., 1966, Potassium-argon ages of some western Tertiary floras: Am. Jour. Sci., v. 264, p. 487–506.

Bailey, R. A., Dalrymple, G. B., and Lanphere, M. A., 1976, Volcanism, structure and geochronology of Long Valley caldera, Mono County, California: Jour. Geophys. Research, v. 81, no. 5, p. 725–744.

Baksi, A. K., York, Derek, and Watkins, N. D., 1967, The age of the Steens Mountain geomagnetic polarity transition: Jour. Geophys. Research, v. 72, p. 6299–6308.

Berggren, W. A., 1972, A Cenozoic time-scale—Some implications for regional geology and paleobiogeography: Lethaia, v. 5, no. 2, p. 195–215.

Billings, M. P., 1945, Mechanics of igneous intrusion in New Hampshire: Am. Jour. Sci., v. 243A, p. 41.

Carmichael, I. S. E., Turner, F. J., and Verhoogen, J., Jr., 1974, Igneous petrology: New York, McGraw-Hill, 739 p.

Christiansen, R. L., and Lipman, P. W., 1966, Emplacement and thermal history of a rhyolite lava flow near Forty-

FIGURE 6.—North-south cross sections through Drake Peak volcanic center at various stages in its evolution. *A*, Latest Eocene (~40 m.y.) and Oligocene: deposition of andesitic sandstone and quartzitic conglomerate, andesitic lahars, andesite and basalt flows, and ash-flow and stratified silicic tuff of lower andesitic sequence (Taf); eruption of flow breccia and highly vesicular basaltic andesite of Twelvemile Peak (Tba). *B*, Late(?) Oligocene through early middle Miocene: successive onlapping of basalt and andesite of Crook Peak (Tab), silicic ash-flow and stratified tuff of the lower tuff (Tlt), middle Miocene flood basalt (Tmb), and ash-flow of lower part of tuff of Honey Creek (Thc) onto basaltic andesite of Twelvemile Peak. Beginning of basin-and-range faulting. *C*, Middle Miocene I: structural doming by intrusion of aphyric felsite phase of rhyolite of Drake Peak (Tir_1); probable eruptions of aphyric rhyolite followed by collapse of domal core; deposition of parts of tuff of Honey Creek (Thc). *D*, Middle Miocene II: eruption of plagioclase-phyric rhyolite (Trf) onto flank of structural dome; some additional doming; deposition of upper part of tuff of Honey Creek (Thc). *E*, Late Miocene: erosion of the dome and flows; eruption of the upper basalt (Tub). *F*, Latest Miocene to Holocene: continued erosion of dome; exposure of ring intrusion; glaciation above 2000 m during Pleistocene.

mile Canyon, southern Nevada: Geol. Soc. America Bull., v. 77, p. 671–684.

Duffield, W. A., and McKee, E. H., 1974, Tertiary stratigraphy and timing of Basin and Range faulting of the Warner Mountains, northeast California [abs.]: Geol. Soc. America Abs. with Programs, v. 6, no. 3, p. 168.

Enlows, H. E., and Parker, D. J., 1972, Geochronology of the Clarno igneous activity in the Mitchell quadrangle, Wheeler County, Oregon: Ore Bin, v. 34, p. 104–110.

Evernden, J. F., Savage, D. E., Curtis, G. H., and James, C. T., 1964, Potassium-argon dates and the Cenozoic mammalian chronology of North America: Am Jour. Sci., v. 262, p. 145–198.

Fuller, R. E., 1931, The geomorphology and volcanic sequence of Steens Mountain in southeastern Oregon: Seattle, Washington Univ. Pub. Geology, v. 3, p. 1–130.

Gordon, G. E., Randle, K., Goles, G. G., Corliss, J., Beeson, M. H., and Oxley, S. S., 1968, Instrumental neutron activation analysis of standard rocks with high resolution γ-ray detectors: Geochim. et Cosmochim. Acta, v. 32, p. 369–396.

Greene, R. C., 1973, Petrology of the welded tuff of Devine Canyon, southeastern Oregon: U.S. Geol. Survey Prof. Paper 797, 26 p.

Greene, R. C., Walker, G. W., and Corcoran, R. E., 1972, Geologic map of the Burns (AMS) quadrangle, Oregon: U.S. Geol. Survey Misc. Geol. Inv. Map I–680, scale 1:250,000.

Hildreth, W., 1976, The Bishop Tuff: Compositional zonation in a silicic magma chamber without crystal setting [abs.]: Geol. Soc. American Abs. with Programs, v. 8, no. 6, p. 918.

James, R. S., and Hamilton, D. L., 1969, Phase relations in the system $NaAlSi_3O_8$–$KAlSi_3O_8$–$CaAl_2Si_2O_8$–SiO_2 at 1 kilobar water vapor pressure: Contr. Mineralogy and Petrology, v. 21, p. 111–141.

Larson, E. E., 1965, The structure, stratigraphy, and paleomagnetics of the Plush area, southeastern Lake County, Oregon: Boulder, Colorado Univ., Ph. D. thesis, 166 p.

Lipman, P. W., 1966, Water pressures during differentiation and crystallization of some ash-flow magmas from southern Nevada: Am. Jour. Sci., v. 264, p. 810–826.

MacLeod, N. S., Walker, G. W., and McKee, E. H., 1975, Geothermal significance of eastward increase in age of upper Cenozoic rhyolitic domes in southeastern Oregon: U.S. Survey Open-File Rept. 75–348, 21 p.

Noble, D. C., Korringa, M. K., Hedge, C. E., and Riddle, G. O., 1972, Highly differentiated subalkaline rhyolite from Glass Mountain, Mono County, California: Geol. Soc. America Bull., v. 83, p. 1179–1184.

Norrish, K., and Hutton, J. T., 1969, An accurate X-ray spectrographic method for the analysis of a wide range of geological samples: Geochim. et Cosmochim. Acta, v. 33, p. 431–453.

Peterson, N. V., and McIntyre, J. R., 1970, Reconnaissance geology and mineral resources of eastern Klamath County and western Lake County, Oregon: Oregon Dept. Geology and Mineral Industries Bull. 66, 70 p.

Piper, A. M., Robinson, T. W., and Park, C. F., 1939, Geology and ground-water resources of the Harney Basin, Oregon: U.S. Geol. Survey Water-Supply Paper 841, 189 p.

Roberts, J. L., 1970, The intrusion of magma into brittle rocks, *in* Newell, G., and Rast, N., eds., Mechanisms of igneous intrusion: Liverpool, Gallery Press, p. 287–338.

Russell, R. J., 1928, Basin and Range structure and stratigraphy of the Warner Range, northeastern California: California Univ. Dept. Geol. Sci. Bull., v. 17, no. 11, p. 387–496.

Smith, R. L., and Bailey, R. A., 1968, Resurgent cauldrons, *in* Studies in volcanology—A memoir in honor of Howel Williams: Geol. Soc. America Mem. 116, p. 613–662.

Swanson, D. A., 1969, Reconnaissance geologic map of the the east half of the Bend quadrangle, Crook, Wheeler, Jefferson, Wasco, and Deschutes Counties, Oregon: U.S. Geol. Survey Misc. Geol. Inv. Map I–568, scale 1:250,000.

Thornton, C. P., and Tuttle, O. F., 1960, Chemistry of igneous rocks, pt. 1, Differentiation index: Am. Jour. Sci., v. 258, p. 664–684.

Tuttle, O. F., and Bowen, N. L., 1958, The origin of granite in light of experimental studies in the system $NaAlSi_3O_8$–$KAlSi_3O_8$–SiO_2–H_2O: Geol. Soc. America Mem. 74, 153 p.

Walker, G. W., 1960, Age and correlation of some unnamed volcanic rocks in south-central Oregon: U.S. Geol. Survey Prof. Paper 400–B, p. B293–B300.

———1963, Reconnaissance geologic map of the eastern half of the Klamath Falls (AMS) quadrangle, Lake and Klamath Counties, Oregon: U.S. Geol. Survey Mineral Inv. Field Studies Map MF–260, scale 1:250,000.

———1973, Preliminary geologic and tectonic maps of Oregon east of the 121st meridian: U.S. Geol. Survey Misc. Field Studies Map MF–495, scale 1:500,000.

Walker, G. W., and King, P. B., 1969, Geologic map of Oregon: U.S. Geol. Survey Misc. Geol. Inv. Map I–595, scale 1:2,000,000.

Walker, G. W., Peterson, N. V., and Greene, R. C., 1967, Reconnaissance geologic map of the east half of the Crescent quadrangle, Lake, Deschutes, and Crook Counties, Oregon: U.S. Geol. Survey Misc. Geol. Inv. Map I–493, scale 1:250,000.

Walker, G. W., and Repenning, C. A., 1965, Reconnaissance geologic map of the Adel (AMS) quadrangle, Lake Harney, and Malheur Counties, Oregon: U.S. Geol. Survey Misc. Geol. Inv. Map I–446, scale 1:250,000.

———1966, Reconnaissance geologic map of the west half of the Jordan Valley quadrangle, Malheur County, Oregon: U.S. Geol. Survey Misc. Geol. Inv. Map I–457, scale 1:250,000.

Watkins, N. D., 1965, A paleomagnetic observation of Miocene geomagnetic secular variation in Oregon: Nature, v. 206, no. 4987, p. 879–882.

Palladium, Platinum, and Rhodium Concentrations in Mafic and Ultramafic Rocks from the Zhob Valley and Dargai Complexes, Pakistan

By NORMAN J. PAGE, JOSEPH HAFFTY, *and* ZAKI AHMAD

SHORTER CONTRIBUTIONS TO MINERALOGY AND PETROLOGY, 1979

GEOLOGICAL SURVEY PROFESSIONAL PAPER 1124-F

CONTENTS

ILLUSTRATIONS

TABLES

PALLADIUM, PLATINUM, AND RHODIUM CONCENTRATIONS IN MAFIC AND ULTRAMAFIC ROCKS FROM THE ZHOB VALLEY AND DARGAI COMPLEXES, PAKISTAN

By NORMAN J PAGE, JOSEPH HAFFTY, and ZAKI AHMAD

ABSTRACT

The Zhob Valley and Dargai complexes, Pakistan, consist of harzburgite and dunite tectonites containing chromite deposits, pyroxenite, wehrlite, and gabbro. Both are ophiolite complexes. Palladium, platinum, and rhodium were found in concentrations of up to 170, 200, and 22 parts per billion, respectively. Average concentrations for both complexs and all rock types collected are 28 ppb palladium, 33 ppb platinum, and 9 ppb rhodium. The Pt:Pt+Pd ranges from 0.41 to 0.67 and averages 0.57. The concentration levels and ratios of these metals are similar to other alpine ultramafic bodies that have been analyzed by modern techniques.

INTRODUCTION

Inasmuch as alpine ultramafic bodies, interpreted to be parts of ophiolitic complexes, are thought to represent parts of the oceanic crust and upper mantle, examination of the concentrations of platinum-group elements in these rocks could provide data to determine the sources, concentration processes, and models for the derivation of these elements in other magmatic rocks or within alpine complexes themselves. As part of a survey of the platinum-group elements in alpine rocks, two areas in Pakistan were sampled in 1974 during the field excursions of the CENTO (Central Treaty Organization) Working Group on Volcanic and Intrusive Rocks and Their Associated Ore Deposits. The two areas are the Zhob Valley complex northeast of Quetta and the Dargai complex northeast of Peshawar (fig .1).

The geologic framework of both areas is briefly described here as a background for interpretation of the platinum, palladium, and rhodium concentrations in ultramafic, mafic, and chromite-bearing rocks. Data from these rocks are compared with rocks from other similar environments on which modern analytical techniques for the determination of these platinum-group elements have been applied.

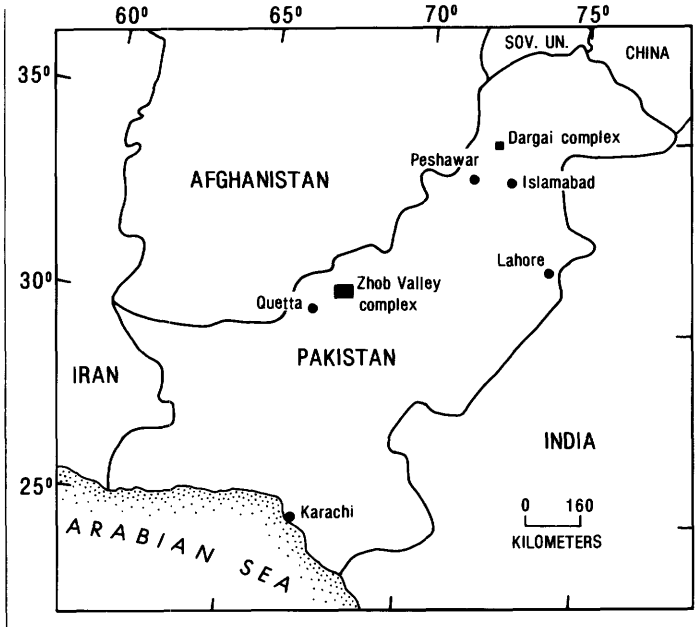

FIGURE 1.—Location of Zhob Valley and Dargai complexes in Pakistan.

GEOLOGIC SETTING OF AREAS

The Zhob Valley igneous complex (Bilgrami and Ingamells, 1960; Bilgrami 1961, 1963), consisting of ultramafic and mafic rocks, was emplaced in Late Cretaceous to Paleocene time by major thrust faulting along the central axial tectonic belt of Pakistan (Rossman and others, 1971; D. L. Rossman, Z. Ahmad, and H. Rahman, unpub. data, 1970). Figure 2 shows the major subdivisions of the complex and

[1] Geological Survey of Pakistan, Islamabad, Pakistan.

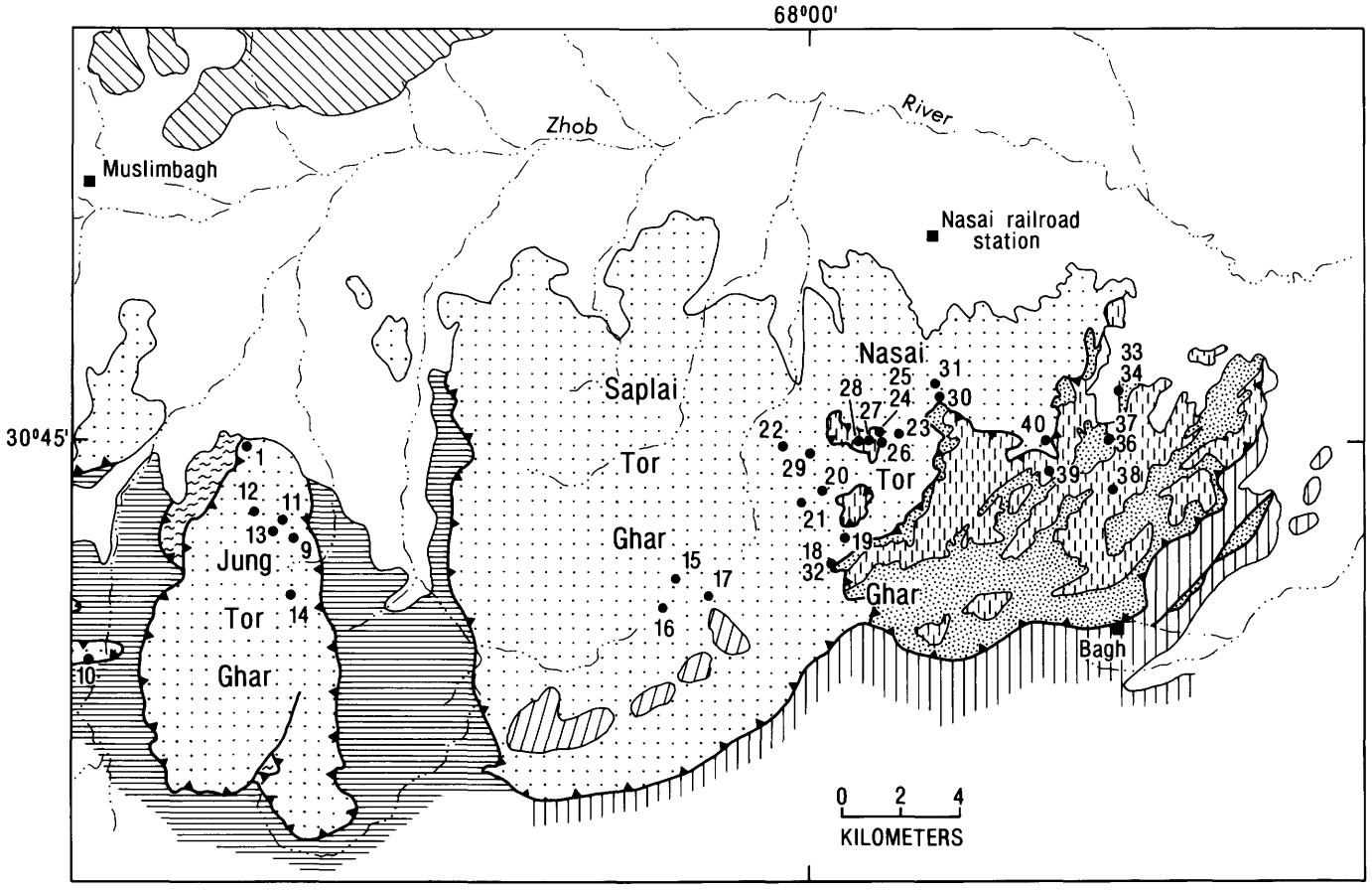

UNCONSOLIDATED AND CEMENTED GRAVELS (Pleistocene and Holocene)

SHAIGALU LIMESTONE (Oligocene and Miocene)

NASAI LIMESTONE (Eocene)

ZHOB VALLEY IGNEOUS COMPLEX—Emplaced Late Cretaceous and Paleocene

HARZBURGITE AND DUNITE TECTONITE

PYROXENITE AND WEHRLITE

GABBRO

PARH GROUP (Cretaceous)

ALOZAI GROUP, LORALAI LIMESTONE, AND PARH GROUP (Triassic and Cretaceous)

AMPHIBOLITE

Contact, approximately located

Fault, approximately located

Thrust fault, approximately located—Sawteeth on upper plate

Sample location—See table 1 for analysis

FIGURE 2.—Geologic sketch map of Zhob Valley complex, Pakistan, showing location of analyzed samples.

its tectonic setting as compiled by the Photographic Survey of Corporation, Ltd. (1958a, b), detailed mapping by Rossman, Ahmad, and Rahman (1971) and by D. L. Rossman, Z. Ahmad and G. Abbas (unpub. data, 1970). Some of the structural interpretations and rock relations shown in the figure are based on field examinations made during the CENTO field excursion.

The Zhob Valley igneous complex overlies sedimentary rocks of Triassic to Cretaceous age and was extensively eroded and deeply weathered, and a laterite developed by mid-Eocene time. Locally, the

Nasai–Saplai Tor Ghar mass is overlain disconformably by remnants of shale and limestone of Eocene age.

The Zhob Valley igneous complex occurs in two detached masses. One, the Jung Tor Ghar mass, consists predominantly of harzburgite and dunite tectonites; the other, the Nasai–Saplai Tor Ghar mass, consists of harzburgite and dunite tectonites, pyroxenite, wehrlite, and gabbro. In both masses, podiform chromite deposits occur within the harzburgite and dunite tectonites.

The pyroxenite and wehrlite unit in the Nasai–Saplai Tor Ghar mass contains repetitive sequences of rocks consisting of olivine, clinopyroxene, and olivine plus clinopyroxene. Textures of the rocks suggest that these sequences were formed by cumulate processes. All the petrologic features of the Zhob Valley igneous complex are those of an ophiolite complex, which probably represents part of the oceanic crust and upper mantle.

Descriptions of the analyzed samples from the Zhob Valley complex and their locations are given in table 1, and their locations are shown on figure 2. All the samples are grab samples weighing 1–2 kg.

The Dargai complex, which extends for 26 km from east to west and about 6 km from north to south, consists of ultramafic and mafic rocks that are separated from country rocks by faults. The complex probably was emplaced along a major east-west-striking thrust fault whose trace parallels the front of the Himalaya Mountains.

The country rocks are chlorite, mica, and graphite schist, and marbles of an undetermined age; the south side of the complex is overlapped by sedimentary rocks and gravel of Pleistocene and Holocene age.

The complex contains predominately harzburgite and dunite with minor wehrlite and has a small amount of leuco- and melanogabbroic rocks exposed on its northern margin. The harzburgite and dunite are interlayered on the scale of centimeters to hundreds of meters. Crests of folds can be observed locally in the layered ultramafic rocks, the associated chromitite occurrences, and the gabbroic rocks. Most of the ultramafic part of the complex is tectonite similar to the harzburgite and dunite tectonite of the Zhob Valley complex. Although there are apparently more clinopyroxene-bearing rocks (lherzolite and wehrlite) interlayered with the dunite and harzburgite in the Dargai complex than in the Zhob Valley complex, the Dargai complex also probably represents part of an ophiolite complex and could be interpreted as a piece of the upper oceanic mantle. Samples from the Dargai complex are described and their locations given in table 1.

PALLADIUM, PLATINUM, AND RHODIUM ANALYSES

The analyses of rocks from the Zhob Valley and Dargai complexes given in table 1 were performed by the method of Haffty and Riley (1968). Of the samples analyzed, 73 percent contain detectable rhodium, 35 percent contain detectable palladium, and 33 percent contain detectable platium. Palladium concentrations range from <4 to 170 ppb and average 27 ppb for samples in which it was detected; platinum concentrations range from <10 to 200 ppb and average 46 ppb; and rhodium concentrations range from <5 to 22 ppb and average 10 ppb. The average Pt:Pt+Pd is 0.57 and ranges from 0.41 to 0.67. Significant characteristics of the distribution of the three metals in both complexes (table 1) are as follows:

1. Of 25 samples of the chromitites, 16 contain more than 7 ppb rhodium; no mafic or ultramafic rocks contain rhodium above the limit of determination (5 ppb or greater).
2. Of 11 samples of the mafic and ultramafic rocks, 9 contain 4 ppb or more palladium; palladium was detected and determined in only 4 of 25 samples of the chromitites.
3. Of 11 samples of the mafic and ultramafic rocks, 7 contain more than 10 ppb platinum; no chromitites contain platinum at or above this level of concentration.

The data on platinum, palladium, and rhodium from the Zhob Valley and Dargai complexes can be compared with results from analyses of ultramafic and mafic rocks from (1) southwestern Oregon, (2) Red Mountain, Calif., (3) Burro Mountain, Calif., (4) the Eagle quadrangle, Alaska, (5) Eklutna complex, Alaska, (6) the Urals and other parts of the U.S.S.R., and (7) Mount Albert complex, Quebec. All seven areas contain alpine ultramafic rocks similar to those from Pakistan. Table 2 lists average concentrations for samples with palladium, platinum, and rhodium above detection limits from the above seven areas for comparison with data from the Zhob Valley and Dargai complexes. The values listed contain a strong bias toward high values because palladium, platinum, and rhodium were not detected in about half of the rocks analyzed from California, Oregon, the Eagle quadrangle, and Pakistan. Comparison of the average values in table 2 for the Zhob Valley and Dargai complexes with

TABLE 1.—*Palladium, platinum, and rhodium analyses, sample descriptions, and locations of rock samples from the Zhob Valley ultramafic complex and the Dargai ultramafic complex, Pakistan*

[Rock classification after Streckeisen (1976). <, not detected at that level; Tr., trace. In calculations, "traces" of Pd, Pt, and Rh were assigned values of 2, 7, and 3 parts per billion, respectively. Analysts: Joseph Haffty and A. W. Haubert]

Sample number	Pd	Pt	Rh	ΣPt+Pd+Rh	Sample description and location
	(parts per billion)				
					ZHOB VALLEY COMPLEX
1JG74	14	24	<5	38	Foliated dunite, mylonitized olivine, northwest end of Jung Tor Gar.
9JG74	<4	<10	14	14	Layered chromitite in dunite, north of Mine 213.
10JG74	<4	<10	5	5	Layered chromitite.
11JG74	<4	<10	12	12	Chromitite, Mine 166.
12AJG74	7	<10	<5	7	Serpentinized harzburgite, near Mine 166.
12JG74	<4	<10	13	13	Massive chromitite, Mine 166.
13JG74	<4	<10	14	14	Massive chromitite.
14JG74	<4	<10	20	20	Massive chromitite from mine dump.
15JG74	<4	<10	9	9	Disseminated chromitite, from dump of 7ML mine.
16JG74	<4	<10	11	11	Massive chromitite, from ore pile of 4ML mine.
17JG74	<4	<10	22	22	Massive chromitite, from ore pile of 9ML mine.
18JG74	<4	<10	13	13	Massive chromitite, from ore pile of 8ML mine.
19JG74	<4	<10	9	9	Massive chromitite, from ore pile of 5CPL mine.
20JG74	<4	<10	12	12	Massive chromitite, from ore pile of Mine 81, Shinakhowra mines.
21JG74	<4	<10	5	5	Layered chromitite, from ore pile of Mine 604, Shinakhowra mines.
22JG74	<4	<10	11	11	Massive chromitite, from ore pile of Mine 41, Shinakhowra mines.
23JG74	Tr.	<10	5	7	Massive chromitite, from dump of Mine 153.
24JG74	<4	<10	<5		Wehrlite, relict cumulate textures.
25JG74	6	12	<5	18	Clinopyroxenite.
26JG74	<4	Tr.	9	16	Massive chromitite from mine dump.
27JG74	27	54	<5	81	Foliated melanogabbro.
28JG74	20	36	<5	56	Do.
29JG74	62	<10	5	67	Massive chromitite, from pillar in Mine PCM41.
30JG74	<4	<10	16	16	Friable chromitite, from ore pile Mine 8ML/2.
31JG74	<4	<10	Tr.	3	Massive chromitite from Mine 8ML/1.
32JG74	<4	<10	Tr.	3	Massive chromitite from Mine 5CPL.
34JG74	20	19	<5	39	Foliated leucograbbro.
36JG74	170	200	5	375	Interlayered melanograbbro and anorthosite.
37JG74	9	11	<5	20	Foliated leucogabbro.
40JG74	4	Tr.	7	18	Layered chromitite.
					DARGAI COMPLEX, PESHAWAR DIVISION
1DG74	9	Tr.	Tr.	19	Harzburgite, adjacent to Heru Shah Chrome mine.
2DG74	<4	<10	5	5	Massive chromitite, Heru Shah Chrome mine.
3DG74	<4	<10	<5		Dunite, near Heru Shah Chrome mine.
5DG74	<4	<10	8	8	Massive chromitite, Landiraudi Chrome prospect.
6DG74	10	Tr.	6	25	Concentrate of chromite nodules, Landiraudi Chrome prospect.
7DG74	<4	Tr.	8	15	Massive chromitite, from ore pile, Qila mine.

those of the other complexes suggests that, except for a few anomalously high individual concentrations in rocks not included in the averages, there is not much difference in concentration of palladium, platinum, and rhodium in the rock types of alpine complexes studied to date. Pt:Pt+Pd ranges from 0.23 to 0.81 when calculated with average concentrations for the alpine ultramafic rocks. Most of the Pt:Pt+Pd for the various areas studied are greater than 0.58.

INTERPRETATION AND CONCLUSIONS

If the Zhob Valley and Dargai complexes are interpreted as parts of the oceanic crust and upper

TABLE 2.—*Comparison of average palladium, platinum. and rhodium contents of Zhob Valley and Dargai rocks with average contents from other alpine ultramafic localities*

[<, less than; --, not detected; number in parentheses is number of samples with detectable concentrations]

Description, location, and reference	Average (parts per billion) Pd	Pt	Rh	Sum of average Pd+Pt+Rh	Pt/Pd+Pt (percent)
CHROMITITE					
Zhob Valley and Dargai, Pakistan (this report)	20 (4)	7 (4)	10.3(25)	37	25.9
Southwestern Oregon (Page and others, 1975)	7.5(10)	[1]26.3 (8)	25.4(23)	59.2	77.8
Red Mountain, California (Page, 1969)	10 (2)	36 (2)	9.5 (2)	55.5	78.3
Weighted average	11 (16)	22.2(14)	17 (50)	50	66.7
DUNITE, PERIDOTITE, AND SERPENTINIZED EQUIVALENT					
Zhob Valley and Dargai, Pakistan	10 (3)	16 (2)	<3 (1)	29	61.5
Harzburgite, southwestern Oregon (Page and others, 1975)	8.4 (5)	8.3 (6)	<5	16.7	49.7
Dunite and harzburgite, Burro Mountain, California (Loney and others, 1971).	3.7(18)	12.8(18)	<5	16.5	77.6
Serpentinized ultramafic rocks, Eagle quadrangle, Alaska (Keith and Foster, 1973).	[2]7.5(16)	[2]11.3 (8)	2 (1)	20.8	60.1
Ultramafic rocks, Eklutna, Alaska (Clark and Greenwood, 1972).	140 (12)	42 (12)	--	182.0	23.1
Dunite and peridotite, Urals, Russia (Fominykh and Khvostova, 1970).	18 (8)	73 (8)	1.99(8)	92.99	80.2
Dunite and peridotite, Mount Albert, Quebec (Crocket and Chyi, 1972).	9.4(13)	--	--		
Weighted average	29 (75)	28 (54)	2 (10)	59	49.1
PYROXENITE AND GABBROIC ROCKS					
Zhob Valley and Dargai, Pakistan (this report)	42 (6)	48 (7)	5 (1)	90.7	53.7
Pyroxenite, southwestern Oregon (Page and others, 1975)	2.0 (1)	7.0 (1)	<5	9.0	77.8
Weighted average	36 (7)	43 (8)	<5 (1)	84	54.4

[1]Average does not include two samples containing 450 and 850 ppb Pt.

[2]Average does not include one sample containing 300 ppb Pt and 200 ppb Pd.

mantle, as is implied by the ophiolite model, what do the concentrations of palladium, platinum, and rhodium indicate about the composition of the upper mantle? A decision must be made as to whether these rocks represent mantle that has been depleted or partly depleted in platinum-group elements or mantle that could be a source rock for magmas that could have generated platinum-enriched deposits. Naldrett and Cabri (1976) assumed that they represented the source rocks, but the fact that there are scattered anomalously high values (4–20 times greater than average values) in some samples from each complex suggests to us that these rocks may instead represent a mantle depleted or partially depleted in platinum-group metals. In addition, the large number of rocks that contain concentrations below the limits of determination suggests that the mantle or depleted mantle has a much lower average platinum, palladium, and rhodium content than reflected by values in table 2.

Although the highest platinum plus palladium plus rhodium content found is 375 ppb (0.012 oz/ton), which is not of economic grade, the possibility of discovering concentrations of platinum-group metals in the gabbroic part of the Nasai Tor Ghar area should not be overlooked. In order to evaluate this possibility more extensive sampling should be done there.

REFERENCES CITED

Bilgrami, S. A., 1961, Distribution of Cu, Ni, Co, V, and Cr in rocks of the Hindubagh igneous complex, Zhob Valley, West Pakistan: Geol. Soc. America Bull., v. 72, p. 1729–1738.

——— 1963, Further data on the chemical composition of Zhob Valley chromites: Am. Mineralogist, v. 48, p. 573–577.

Bilgrami, S. A., and Ingamells, C. O., 1960, Chemical composition of the Zhob Valley chromites, West Pakistan: Am. Mineralogist, v. 45, p. 576–585.

Clark, A. L., and Greenwood, W. R., 1972, Geochemistry and distribution of platinum-group metals in mafic to ultramafic complexes of southern and southeastern Alaska, *in* Geological Survey research, 1972: U.S. Geol. Survey Prof. Paper 800–C, p. C157–C160.

Crocket, J. H., and Chyi, L. L., 1972, Abundances of Pd, Ir, Os, and Au in an alpine ultramafic pluton: Internat. Geol. Cong., 24th, Montreal, Canada, 1972, Sec. 10, p. 202–209.

Fominykh, V. G., and Khvostova, V. P., 1970, Distribution of platinum metals in rock-forming minerals of the Gusevogorskoye deposit: Akad. Nauk SSSR Doklady, v. 200, p. 182–183.

Haffty, Joseph, and Riley, L. B., 1968, Determination of palladium, platinum, and rhodium in geologic materials by fire assay and emmission spectrography: Talanta, v. 15, p. 111–117.

Keith, T. E. C., and Foster, H. L., 1973, Basic data on the ultramafic rocks of the Eagle quadrangle, east-central Alaska: U.S. Geol. Survey open-file rept. 4 sheets.

Loney, R. A., Himmelberg, G. R., and Coleman, R. G., 1971, Structure and petrology of the alpine-type peridotite at Burro Mountain, California, U.S.A.: Jour. Petrology, v. 12, p. 245–309.

Naldrett, A. J., and Cabri, L. J., 1976, Ultramafic and related mafic rocks—Their classification and genesis with special reference to the concentration of nickel sulfides and platinum-group elements: Econ. Geology, v. 71, p. 1131–1158.

Page, N. J, 1969, Platinum content of ultramafic rocks, *in* U.S. Geological Survey heavy metals program progress report 1968—Topical studies: U.S. Geol. Survey Circ. 622, p. 5.

Page, N. J, Johnson, M. G., Haffty, Joseph, and Ramp, Len, 1975, Occurrence of platinum-group metals in ultramafic rocks of the Medford-Coos Bay 2° quadrangle, southwestern Oregon: U.S. Geol. Survey Misc. Field Studies Map MF–694, scale 1:250 000.

Photographic Survey of Corporation, Ltd., 1958a, Reconnaissance geology of part of west Pakistan: Toronto, Canada, Photographic Survey Corp. Ltd., in cooperation with Geol. Survey Pakistan, Geol. Map 26, Quetta 34 J–F, scale 1:253 440.

——— 1958b, Reconnaissance geology part of west Pakistan: Toronto, Canada, Photographic Survey Corp. Ltd., in cooperation with Geol. Survey Pakistan, Geol. Map 27, Loralai 39 B–F, scale 1:243 000.

Rossman, D. L., Ahmad, Zaki, and Rahman, Hamidur, 1971, Geology and economic potential for chromite in Zhob Valley ultramafic rock complex, Hindubagh, Quetta Division, West Pakistan: (Project rep. (IR) PK–50) U.S. Geological Survey open-file rept, 63 p.

Streckeisen, Albert, 1976, To each plutonic rock its proper name: Earth Sci. Rev., v. 12, p. 1–33.

☆U.S. GOVERNMENT PRINTING OFFICE: 1979 O— 311-344/138